17716

NATIONAL LIBRARY
OTTAWA

CANADA

BIBLIOTHÈQUE NATIONALE
OTTAWA

NAME OF AUTHOR...SHAPOUR VOSSOUGHI.........

TITLE OF THESIS...Non-Newtonian Flow Distribution In a Porous Bed...............

UNIVERSITY...University of Alberta...........

DEGREE FOR WHICH THESIS WAS PRESENTED.....M.Sc..........

YEAR THIS DEGREE GRANTED....1973......................

Permission is hereby granted to THE NATIONAL LIBRARY OF CANADA to microfilm this thesis and to lend or sell copies of the film.

The author reserves other publication rights, and neither the thesis nor extensive extracts from it may be printed or otherwise reproduced without the author's written permission.

(Signed)..S. Vossoughi......

PERMANENT ADDRESS:

C/o. Dept. of. Chem. Eng
Univ. of. Alberta.
Edmonton 7, Alta. CANADA

DATED. Oct. 5, ...1973

NL-91 (10-68)

THE UNIVERSITY OF ALBERTA

NON-NEWTONIAN FLOW DISTRIBUTION IN A POROUS BED

by

Ⓒ SHAPOUR VOSSOUGHI

A THESIS
SUBMITTED TO THE FACULTY OF GRADUATE STUDIES AND RESEARCH IN
PARTIAL FULFILMENT OF THE REQUIREMENTS FOR THE DEGREE OF
MASTER OF SCIENCE

in

CHEMICAL ENGINEERING

DEPARTMENT OF CHEMICAL ENGINEERING

EDMONTON, ALBERTA
FALL, 1973

UNIVERSITY OF ALBERTA

FACULTY OF GRADUATE STUDIES AND RESEARCH

The undersigned certify that they have read, and recommend to the Faculty of Graduate Studies and Research for acceptance a thesis entitled "Non-Newtonian Flow Distribution in a Porous Bed," submitted by Shapour Vossoughi in partial fulfilment of the requirements for the degree of Master of Science in Chemical Engineering.

........F A Seyer........
Supervisor

....

....

Date ....Sep't 27/73......

To *Ziba*

whom I love most

ABSTRACT

Fluid flow of both Newtonian and viscoelastic fluid was studied in a model porous medium composed of a matrix of small glass cylinders. Local velocity profiles and flow distribution were determined by a streak photomicrography technique. Measurements were obtained for average interstitial velocities of the bed ranging from $V/\varepsilon = 0.0568$ cm/sec to 0.568 cm/sec. The major effect focused on was the variation in flow between pores owing to small inhomogeneities in the bed.

Compared to the Newtonian fluid, the effect of viscoelastic fluid was found to be a suppression of the velocity and also flow distribution variations with pore opening. The effect of elasticity on flow distribution was observed to occur before its influence in pressure drop measurement.

Qualitative visual observations also revealed that the number of dead zones, or nearly dead zones and recirculation regions for viscoelastic fluid were reduced relative to the Newtonian case.

ACKNOWLEDGEMENTS

In compiling the present thesis the author wishes to acknowledge the aid and assistance given by the following:

Dr. F. A. Seyer, research supervisor, for his generous help and constructive criticism.

The staff of the Workshop and the Instrument Shop for their assistance in building the equipment.

The Petroleum Aid to Education fund which provided partial support for the research.

Dow Chemical Co. who donated the Polymer used in the research, and

Mrs. Beth Scott who typed the manuscript.

TABLE OF CONTENTS

Chapter Page

I. INTRODUCTION AND BACKGROUND 1
  I.1 General. 1
  I.2 Mobility Ratio Concept 4
  I.3 Polymer Flooding 9
II. THEORY. 19
  II.1 Introduction 19
  II.2 Parallel-Plates Capillary Model--Pressure Drop. 20
  II.3 Power-Law Model. 27
  II.4 Modified Friction Factor and Reynolds Number. 28
  II.5 Application of Theory. 28
III. EXPERIMENTAL EQUIPMENT AND PROCEDURE. 30
  III.1 Multi-Cylinder Matrix. 30
  III.2 Experimental Fluids. 35
  III.3 Pumping. 36
  III.4 Streak Photography Technique 37
    III.4-1 Optical System. 37
      a. Light Source 37
      b. Chopper Disk 39
      c. Photomicrography Assembly. 40
    III.4-2 Measurement of the Streak Length 40

Chapter | Page

III.5 Pressure Drop Measurement 44

IV. RESULTS. 45

IV.1 Pressure Drop 45

IV.2 Streamlines. 49

IV.3 Local Velocity Profiles 49

V. DISCUSSION OF THE RESULTS. 65

V.1 Pressure Drop 65

V.2 Streamlines 72

V.3 Visual Observation. 75

V.4 Local Velocity Profiles and Flow Distribution. 76

IV. CONCLUSION AND RECOMMENDATIONS 100

VI.1 Conclusions 100

VI.2 Recommendations 101

BIBLIOGRAPHY 102

APPENDIX A RHEOLOGICAL PROPERTIES OF THE SOLUTIONS 107

I. Rheogoniometer Parameters 108

II. Evaporation Correction. 111

APPENDIX B PRESSURE DROP AND RELATED CORRELATIONS. 123

APPENDIX C CONSTRUCTION OF VELOCITY PROFILE FROM STREAK LENGTH. 139

APPENDIX D FLOW THROUGH PARALLEL PLATES-- POWER LAW MODEL 144

Chapter Page

APPENDIX E EXPERIMENTAL DATA POINTS 147

LIST OF TABLES

Table Page

V-1 FLOW PARAMETERS OF 0.2% SEPARAN SOLUTION 70

V-2 MAXIMUM VELOCITIES AT CENTER LINE OPENING 82

V-3 CORRECTED FRACTIONAL FLOW RATES. 91

A-1 CALIBRATION OF NORMAL FORCE TRANSDUCER 116

A-2 VISCOMETRIC MEASUREMENTS FOR STANDARD OIL, GLYCEROL, AND POLYMER SOLUTION 116

B-1 FLOW BEHAVIOR PARAMETERS OF 96% GLYCEROL SOLUTION. 131

B-2 FLOW BEHAVIOR PARAMETERS OF 0.2% SEPARAN 135

B-3 PREDICTED PRESSURE DROPS BY BERGELIN'S CORRELATION--0.2% SEPARAN. 137

C-1 OPENINGS, d, AREA UNDER THE DIMENSIONLESS VELOCITY PROFILES A_i, AND FRACTIONAL FLOW RATES, q%. 142

E-1 STREAK LENGTH DATA OF GLYCEROL 149

E-2 STREAK LENGTH DATA OF SEPARAN. 167

LIST OF FIGURES

Figure		Page
II-1	PARALLEL-PLATE CAPILLARY MODEL	21
II-2	RECTILINEAR FLOW THROUGH PARALLEL PLATES	22
III-1	TRIANGULAR-PITCH ISOCELL	31
III-2	MULTI-CYLINDER MATRIX.	31
III-3	TOP VIEW OF GLASS RODS	34
III-4	SCHEMATIC PLAN VIEW OF OPTICAL SYSTEM	38
III-5	PHOTOMICROGRAPHY ASSEMBLY.	41
IV-1	PRESSURE DROP V.S. FLOW RATE-- GLYCEROL	46
IV-2	PRESSURE DROP V.S. FLOW RATE-- SEPARAN.	47
IV-3	FRICTION FACTOR V.S. REYNOLDS NUMBER	48
IV-4	PHOTOGRAPH NO. 1: FLOW PAST SINGLE CYLINDER	50
IV-5	PHOTOGRAPHS NO.'S 2, 3, 4: NEWTONIAN FLOW PAST MULTI CYLINDERS.	51
IV-6	PHOTOGRAPHS NO.'s 5, 6, 7: VISCO-ELASTIC FLOW PAST MULTI CYLINDERS. . . .	52
IV-7	LOCAL VELOCITY PROFILES OF POSITION NO. 2--GLYCEROL.	55
IV-8	LOCAL VELOCITY PROFILES OF POSITION NO. 2--SEPARAN	56
IV-9	LOCAL VELOCITY PROFILES OF POSITION NO. 17--GLYCEROL	57

Figure Page

IV-10 LOCAL VELOCITY PROFILES OF POSITION NO. 17--SEPARAN 58

IV-11 LOCAL VELOCITY PROFILES OF POSITION NO. 27--GLYCEROL. 59

IV-12 LOCAL VELOCITY PROFILES OF POSITION NO. 27--SEPARAN 60

IV-13 CENTERLINE VELOCITY PROFILE 64

V-1 ESTIMATION OF ELONGATIONAL RATE 69

V-2 DEPENDENCE OF ELASTICITY EFFECT UPON THE DEBORAH NUMBER OF THE FLOW PROCESS. 73

V-3 VISUAL OBSERVATION--GLYCEROL. 78

V-4 VISUAL OBSERVATION--SEPARAN 80

V-5 MAXIMUM CENTER LINE VELOCITIES--ROW NO. 20. 84

V-6 MAXIMUM CENTER LINE VELOCITIES--ROW NO. 21. 85

V-7 MAXIMUM CENTER LINE VELOCITIES--ROW NO. 22. 86

V-8 RESULTANT OF MAXIMUM CENTER LINE VELOCITIES OF THREE ROWS--GLYCEROL. 88

V-9 RESULTANT OF MAXIMUM CENTER LINE VELOCITIES OF THREE ROWS--SEPARAN 89

V-10 FLOW DISTRIBUTION WITH OPENING--GLYCEROL. 94

V-11 FLOW DISTRIBUTION WITH OPENING--SEPARAN 95

V-12 FLOW DISTRIBUTION WITH OPENING--GLYCEROL. 96

V-13 FLOW DISTRIBUTION WITH OPENING--SEPARAN 97

Figure Page

A-1 NORMAL FORCE TRANSDUCER CALIBRATION 112

A-2 VISCOMETRIC BEHAVIOR OF NEWTONIAN FLUIDS. 113

A-3 VISCOMETRIC BEHAVIOR OF SEPARAN AP-273, 0.2% (BY WEIGHT). 114

A-4 RELAXATION TIME OF SEPARAN AP-273, 0.2% (BY WEIGHT). 115

E-1 DIRECTION OF X AND THE ORIGIN WITH RESPECT TO THE LIGHT AND FLOW DIRECTION. 148

NOMENCLATURE

A	Cross-sectional area of the bed, cm^2
A_i	Area under the dimensionless velocity profile, cm.
A_v	Area under the velocity profiles, cm^2/sec.
b_1	Constant, cm.
C	Solute concentration, gr/cm^3
$C_1 - C_6$	Constants
C_D	Dispersion coefficient, cm^2/sec.
d	Minimum opening between two adjacent cylinders of the same row, cm.
d_M	Minimum opening between two adjacent cylinders of the same row, in.
d_c	Diameter of the constriction, cm.
d_{Pl}	Diameter of the platen, cm.
D	Diameter of the cylinders, cm.
D_P	Diameter of the particles, cm.
f	Corrected fractional flow rate, dimensionless.
f_B	Friction factor defined by Eq. (B-6), dimensionless.
f_K	Friction factor defined by Eq. (II-38), dimensionless.
F	Normal force, dyne
$F(\ )$	Function of.

g	Acceleration of gravity, cm/sec^2.
H	Viscosity parameter defined by Equation (I-5), grcm^{-n} sec^{n-2}.
K	Effective permeability, cm^2
K_1	Constant, defined by Equation B-3, dimensionless.
K_t	Torsion bar constant, dyne/micron
ℓ	Exposed length of the cylinders, cm.
L	Length of the bed, cm
L'	Tortuous length of particle path, cm.
m	Mobility ratio, dimensionless
m_1	Power-law parameter, gr cm^{-1} sec^{n-2}.
n	Power-law parameter, dimensionless.
N	Number of major restrictions encountered in flow through the bank.
N_{Deb}	Deborah number defined by Equation (I-12), dimensionless.
N_m	Number of the minimum openings in one row.
N_{Re}	Reynolds number defined by Equation (II-40), dimensionless.
N_T	Total number of cylinders, dimensionless.
N_{We}	Weissenberg number defined by Equation (I-11), dimensionless.
P	Pressure, dyne/cm^2
P_t	Pitch ratio, dimensionless.
$P_{11} - P_{22}$	Primary normal stress difference, dyne/cm^2

q	Total volumetric flow rate, cm^3/sec.
q_i	volumetric flow rate passing through each opening, cm^3/sec.
R	One half the gap between two parallel plates, cm.
Re_C	Reynolds number defined by Equation (V-9), dimensionless.
Re_t	Reynolds number defined by Equation (B-4), dimensionless.
R_g	Gas constant, gr cm^2/sec^2 g-mole oK
R_H	Hydraulic radius, cm.
R_{Pl}	Radius of the platen, cm.
RPM	Revolutions per minute.
s	length of the streaks, cm.
S	Length of the streaks, in.
S_1	Sensitivity of the torque transducer, micron/volt.
S_2	Sensitivity of the normal force transducer, gr/volt.
S_B	Minimum free flow area, cm^2.
S_L	Longitudinal pitch, cm.
S_s	Specific surface, cm^{-1}.
S_T	Transverse pitch, cm.
S_v	Wetted surface per volume of bed, cm^{-1}.
t	Duration of one revolution, second/rev
Δt	Movement of torsion head transducer, volt.

T	Absolute temperature; oK
t_P	Time of period of opening or closing the light, sec.
T_r	Torque, dyne cm.
u	Interstitial velocity, cm/sec.
U	Ap[illegible]ach velocity, cm/sec.
u_m	Average interstitial velocity from center line openings, cm/sec.
$\bar{u}_{max}$	Average value of the maximum velocities at center line openings of two consecutive rows, cm/sec.
u_z	velocity in the z-direction, cm/sec
V	Superficial velocity, cm/sec.
$\bar{V}$	Average velocity of the flow through parallel plates, cm/sec.
V_C	Volume occupied by cylinders, cm^3.
v_t	Output of transducer, volt.
V_T	Total volume, cm^3.
V_v	Void volume, cm^3.
V_w	Volume of the water, cm^3.
W_B	Mass flow rate, gr/sec.
x	x-coordinate, cm.
X	X-coordinate, in.
y	y-coordinate, cm.
z	z-coordinate, cm.

Greek Symbols

α	Angle of cone, degrees
β	Angular rotation of the platen, rad./sec.
∇	Delta operator.
ε	Volumetric porosity, dimensionless.
ε_s	Surface porosity, dimensionless.
Γ	Average nominal shear rate, sec^{-1}.
λ	Mobility, cm^3 sec/gr
μ	Viscosity, poise.
μ_o	Limiting viscosity at low shear rate, poise.
μ_s	Viscosity of the solvent, poise.
ρ	Density, gr/cm^3.
τ	Shear stress, $dyne/cm^2$
Θ_o	Limit of the relaxation time at low shear rate, sec.
Θ_f	Relaxation time of fluid, sec.
Θ_{pr}	Duration of a process, sec.
σ	Shear rate, sec^{-1}.

Subscripts

B	indicate an ideal bundle of tubes.
e	elastic
G	Glycerol
o	oil
S	Separan
w	water
W	wall
ε	modified for the porous bed.

CHAPTER I

INTRODUCTION AND BACKGROUND

I.1 General

Increasing demands for petroleum supply and the limited number of the oil reservoirs make it inevitable not only to use the produced oil efficiently but also to increase the ultimate recovery of reservoirs. Investigation of the many fields revealed (1) that more than 50 per cent and in the case of heavy oil reservoir, even 80 per cent of the original oil in the reservoir remained unrecovered after primary recovery; i.e., when the production rate became so low as to make economical operation impracticable.

Oil production requires energy to expell the oil trapped in the interstices of the porous rock into the production well. This energy may be available in the reservoir initially in different forms. The major forms of natural energy in the oil reservoirs are:

1. Compression energy of the oil or water within the field or contiguous to the oil-bearing rock.
2. Compression energy of the gas dissolved in the oil or free-gas zones overlying the oil layer.
3. Gravitational energy due to the difference in hydrostatic level of producing well and upper part of the

reservoir.

If no natural energy is available in the reservoir or if the existing energy is not sufficient, the external energy should be applied to exceed the economical rate of production. Even in the case of high pressure reservoirs, the initial content of energy would be depleted after a long period of production and, therefore, external energy would be required.

Fluid injection as an external energy supply to the reservoir may be applied for two different purposes; (a) during the period of the operation of the well to compensate for the pressure decline created due to the oil withdrawals from the space voidage. The fluid injection will help to keep the rate of production almost constant and above the limit of economical rate, (b) after the production well reaches a state of substantially complete depletion of its initial content of energy. In reservoir engineering terminology the former is called "Pressure Maintenance" or "Pressure Regulation" and the latter "Secondary Recovery." In secondary recovery operations the pressure required for the fluid injection is often lower than that which would be required for injection under primary pressure maintenance.

Fluid injection as a method of oil recovery is indeed more than one century old. The first accidental or perhaps intentional water flooding occurred in 1865 in the Pithole City of Pennsylvania.(2) Since then a great variety of fluids such as gas, liquids, even slurries, and also different additives to the fluids to achieve better performance have been tried.

Of the different methods of the secondary oil recovery, water flooding is the most advanced method. Gas-injection operations, usually termed "gas repressuring," are less common than water flooding. Secondary recovery by water flooding has been carried on, as a common practice, in regular patterns. Historically, the first type of regular network was the alternating-line-drive pattern(3). Next followed the five-spot pattern which is most commonly employed. The mechanisms of the fluid displacement for various patterns of injection and production wells have been extensively investigated (4-12). The injected water pushes the oil in a somehow piston-like behavior from the vicinity of the injection wells and ahead of the advancing water, a zone of high oil saturation is formed which moves toward the producing well. The clean oil is produced until the oil-water bank reaches the producing well at which point breakthrough occurs. After breakthrough, increasing amounts of water are produced with the oil.

Development of the oil bank and its stability governs the success of the operation. In some projects the high oil saturation zone does not develop at all and breakthrough takes place from the start. The rate of the production of water may reach a limit such that the production of oil becomes too low to support continued operation.

It is intuitively understood that if the conditions at the start of the flood are such that the water can move more readily than oil, the displacement front will spread into the oil and early breakthrough occurs. Water intrusion into the frontal oil bank is termed "fingering."

I. 2 Mobility Ratio Concept

Whether or not a stable oil bank develops depends largely on the relative permeability characteristics of the formation, on the viscosity of the displacing and displaced fluids, on the saturations of water and oil at the time the water injection is started and also on the inhomogeneities of the rock itself. The first two conditions can be regrouped in mobility ratio (13) which is defined as the ratio between the mobilities of the displacing and displaced fluids, where

$$m = \frac{\lambda_w}{\lambda_o} , \qquad \text{(I-1)}$$

m represents mobility ratio and λ_w and λ_o are mobilities of water and oil respectively.

Definition of the mobility is better understood by studying Darcy's law. The theory of flow through porous media originated by Darcy's experiment in 1856 (14a). Darcy found that the flow rate is proportional to the pressure drop along the bed, or in terms of superficial velocity,

$$V = \lambda \frac{\Delta P}{L}, \qquad \text{(I-2)}$$

where V is superficial velocity, ΔP, pressure drop, L, length of the porous medium and λ, constant which by definition is the mobility of the fluid. Later, in 1930, Nutting elucidated (14a) the physical significance of λ and stated that,

$$\lambda = \frac{K}{\mu}, \qquad \text{(I-3)}$$

where μ is the viscosity of the fluid and K the specific permeability of the porous medium. Substituting (I-3) into (I-2), one obtains,

$$V = \frac{K}{\mu} \frac{\Delta P}{L} \qquad \text{(I-4)}$$

Equation (I-4) is known as Darcy's law which holds for the laminar flow of Newtonian fluids through homogeneous porous media.

Darcy's law was modified by Christopher, et al. (15) for the flow of power-law model fluids through porous media. Using a modified Blake-Kozeny equation, they obtained,

$$V = \left(\frac{K}{H} \frac{\Delta P}{L}\right)^{1/n}, \qquad \text{(I-5)}$$

where n is power-law parameter and H, viscosity level parameter, a factor which accounts for the additional dependence of V on K and porosity due to non-Newtonian behavior.

The first theoretical attempt to show the role of the mobility ratio in fluid displacement was carried on by Leverett, who published his fractional flow formula in 1940. On neglecting capillary pressure gradient and gravity effects his equation takes on the following simple form (16a)

$$f_w = \frac{1}{1 + \frac{K_o \mu_w}{K_w \mu_o}} , \qquad \text{(I-6)}$$

or, using the mobilities of two fluids,

$$f_w = \frac{1}{1 + \frac{\lambda_o}{\lambda_w}} , \qquad \text{(I-7)}$$

where,

$$f_w = \frac{q_w}{q_w + q_o} , \qquad \text{(I-8)}$$

q_w and q_o are volumetric flow rates of water and oil respectively. In an attempt to calculate the oil recovery, Welge (17), Aronofsky (4,5) and other investigators (8,12,18) also recognized that through decreased mobility ratio an improvement in displacement efficiency could be obtained. Mungan (19) amongst others showed qualitatively the conditions of stability at a displacement front in a simplified model. He considered the incompressible horizontal linear displacement of oil by water in a piston-like manner and neglected capillary effects. In a system of length L the displacement front is at position x where $x < L$. Writing Darcy's law for the positions filled with water and oil,

$$\frac{q}{A} = -\lambda_w \frac{P_i - P_x}{x} , \qquad \text{(I-8)}$$

$$\frac{q}{A} = -\lambda_o \frac{P_x - P_L}{L - x} \qquad \text{(I-9)}$$

where q is volumetric flow rate, A, cross-sectional area, $\frac{q}{A}$, velocity of the displacement front, P_i, P_x, P_L, pressure at inlet, displacement front and outlet respectively. Eliminating P_x between Equations (I-8, 9),

$$\frac{q}{A} = (P_i - P_L)\ \lambda_o\ \lambda_w \frac{1}{L\lambda_w + x(\lambda_o - \lambda_w)} \cdot \qquad \text{(I-10)}$$

The Equation (I-10) shows, qualitatively, the role of the mobility ratio in stability of oil sweeping. When $\lambda_o/\lambda_w > 1$, i.e. $\lambda_o > \lambda_w$, for any increment increase of x, say dx, which physically is indicated by forming a tiny finger or kink of water into the oil-filled segment the velocity of displacement front, i.e. q/A, will decrease. Therefore, the finger or kink of water can not proceed into the oil-filled segment. That is the tendency for early breakthrough will be suppressed. For the case when $\lambda_o/\lambda_w < 1$, i.e. $\lambda_o < \lambda_w$, any incremental increase of x will increase the velocity of the displacement front which leads eventually to complete breakthrough.

Slobod, et al (10, 11) studied fingering in miscible-phase displacement by an X-ray shadowgraph technique. Their photographs showed that at high flow rate (i.e. 29 ft/day) a large number of very thin fingers was developed; whereas, the slow flowrate (i.e. 1.6 ft/day) showed a gradual blending of fluids with no fingering. Both had an unfavorable mobility ratio of 3. Photographs taken for mobility ratio of unity revealed no fingering. One interesting effect was the complete elimination of fingering when they used a continuous gradation in viscosity of flooding fluid. It is worthwhile to note that the overall viscosity ratio had the unfavorable value of $\mu_o/\mu_w = 3$. This can well be in support of Mungan's modification in polymer slug process (20).

Since the mobility of the oil is a fixed parameter--depending on the kind of reservoir and oil--the only possibility to maintain stability in water flooding is to reduce the water mobility.

An improved mobility ratio would also increase recovery efficiency by correcting permeability distribution problems as discussed by Stiles (21), Dyskstra, et al. (22), and Pye (23).

Mobility reduction may be achieved by one or a combination of the following two ways:

1. Permeability reduction of the porous media.
2. Increasing the viscosity of the injected water.

Materials such as Glycerol, sugar, starch, etc. have been used to increase the water viscosity. However, due to the large amount of the materials to be used, the method is not economically feasible. The concept of using natural high molecular weight polymers to increase the water viscosity is not new. The first patent appeared in 1944 by Detting (Shell Development Co.). The reader is referred to 27 different patents mentioned in reference (1). These patents were granted during 1944 to 1961.

I. 3 Polymer Flooding

The use of synthetic polymers in the injected water of the water flood, as compared to the former mentioned additives, is a fairly new technique. Polyacrylamide was first introduced in 1964 by Pye (23) and Sandiford (1). Their experiments showed that the presence of this kind of polymer in dilute concentrations decreases the water mobility 5 to 20 times more than would be expected from measurement of the solution viscosity. Since then it has become of increasing interest to study and investigate the flow behavior and mechanism of polymer flooding and recovery (20, 24-28). In addition to the laboratory experiments, the polymer water flood has also been successful in the majority of the small or even large scale field projects where it has been employed (29-33).

In polymer water flooding a water-soluble high molecular weight polymer which is partially hydrolyzed is desirable. The polymer solutions, at the concentrations generally used in polymer floods, are non-Newtonian and show pseudoplastic behavior in viscosity measurement and elastic effects in normal force measurement. The pseudoplasticity is suppressed greatly in the presence of the strong electrolytes (20, 24, 34).

The main preference of the polymer water flooding over the conventional method is that a greater fraction of the reservoir volume may be swept at water breakthrough. In other words, the sweep efficiency increases by introducing a small amount of polymer into the injected water. In addition to the increased macroscopic sweep efficiency, improved microscopic displacement at a given amount of fluid injected has also been observed (1), i.e. the residual oil saturation would be less in swept areas compared with that of conventional flooding. The surprising ability of the polymer to lower the mobility of flooding water may be attributed to the adsorption of the polymer molecules on the pore surface, to the plugging of the very fine pores by polymers, to the viscoelastic effect of the polymer solution, or to a combination of all of these.

Lee, et al. (27) studied the behavior of the polymer solution in oil recovery by looking at pseudoplasticity effect. They concluded that provided the polymer concentration in the flood water is such that the average mobility ratio is favorable or unfavorable, the oil-water contact may exhibit a stable or unstable situation during the course of the flood. Their visual study on a Hele-Shaw model verified their qualitative prediction of the fingering based on pseudoplasticity effect. However, there is considerable evidence to doubt that the power-law model is sufficient to predict the flow behavior of polymer solution in real porous media under all conditions of interest.

Burcik (35-38) attributed the mobility control of the polymer solution not only to the viscosity improvement but also to the reduction of the effective permeability due to adsorption of polymer molecules on the surface of pores. He observed dilatant behavior of polymer solution flow through a disc of Berea Sandstone which, presumably, was a result of the bound polymer molecules within the pore structure reducing the effective permeability. To distinguish this behavior from true dilatancy, the author suggested that the phenomenon observed be designated as pseudo-dilatancy. Plugging effects, as well as adsorption have also been noticed by other investigators (20, 24, 28, 29, 31). In another paper, Burcik and Walrond (39) proposed that small particles of microgel might be primarily responsible for the permeability reduction; however, Lynch and MacWilliams (40) in response to Burcik's claim showed that gel particles need not be present to have polymer units of the order of one micron and single polymer molecules of that size can be reasonably expected in the ranges of 3 million molecular weight. Patton, etal. (41) revealed that the polymers with less adsorption affinity on the pore surface are more effective at the flood front and also on the oil recovery. They found that the quantity of adsorption varied widely from one polymer to another. For one specific kind of polymer the adsorption varied from one type of mineral surface to another and increased with salt concentration (28). Reduction in relative permeability observed by Patton, et al. (41) was attributed largely to the tight connate water-saturated pores. These colloidal particles could physically block the smaller capillaries and inhibit the displacement of the connate water.

The relative permeability becomes insensitive to the concentration of the polymer solution above a minimum value of concentration. The dependency of the relative permeability on the polymer concentration has been discussed by Jennings, et al. (34).

At this stage it is felt fruitful to define two factors namely "Resistance Factor" and "Residual Resistance Factor." Both are descriptive of polymer behavior but in different situations. Resistance factor, as defined by Pye (23), is the ratio of the brine mobility to the polymer solution mobility. Resistance factor is indeed a measure of adsorption together with entrapment of the large molecules in the small size pores and also elasticity which mostly has been ignored. Jennings, et al. (34) showed that resistance factor decreases as K/ε increases; where K is permeability and ε, the porosity of bed. Residual Resistance Factor called "Permeability Reduction" by Smith (28) is defined as the ratio of the brine mobility in a rock, not previously contacted by polymer, to the brine mobility in the same rock after being swept by polymer solution. Smith (28) pointed out that permeability reduction is due to the immobile polymer retained within the porous medium. It is greater in less permeable rocks and increases with the polymer molecular weight and also with the flow rate. According to Jewett, et al. (32), the oil recovery increases with both factors which is inconsistent with Patton, et al. (41).

In flows which are non-steady from a Lagrangian point of view, the flow behavior of polymer solutions is often surprisingly different from that of Newtonian fluids and is very dependent upon exact details of velocity field; e.g. flow around submerged objects or flow in converging-diverging channels. Ultman, et al. (42), studied the flow of polymer solution around a submerged single cylinder and sphere using Polyacrylamide and high molecular weight Cellulose Gum as polymers. They introduced Weissenberg number and studied the effect of the magnitude of the Weissenberg number on the effect of viscoelasticity. Weissenberg number was defined (42) as,

$$N_{we} = \frac{\Theta_0 U}{D}, \qquad \text{(I-11)}$$

where Θ_0 is the limit of relaxation time at low shear rate, U, the approach velocity, and D, diameter of the cylinder or sphere. They noticed a significant difference in the shape of the streamlines. For instance the streamlines of the flow of viscoelastic fluid across a submerged cylinder responded to the presence of the cylinder earlier than those of the Newtonian fluids and returned to the undisturbed motion sooner. The position of the separation point at the aft portion of the cylinder was noticed to be dependent upon the magnitude of the Weissenberg number.

The effects of elasticity of polymer solutions in porous media have been completely or partially ignored in a great number of papers published in this field. Some authors such as Jennings, et al. (34), Smith (38), and Harvey (43) believed that the effect of elasticity of the low polymer concentrations of polymer solutions in porous media is insignificant. Sadowski and Bird (44), to justify their capillary-hydraulic radius model based on three-parameter Ellis model which suffered from lack of the time-dependent elastic phenomena, reasoned that no significant elastic effect would be observed provided the fluid relaxation time is small with respect to the transit time.

By the same reasoning one can conclude that the effect of elasticity could be significant if the geometry of the media is such that the transit time of the fluid flow through a contraction or expansion in a tortuous channel is comparable with the relaxation time of the fluid. This expectation has been theoretically shown and experimentally verified by Marshall and Metzner (45). They gave a correlation of the effect with Deborah number for Polyisobutylene and partially hydrolyzed Polyacrylamide solutions. Deborah number was defined as,

$$N_{Deb} = \frac{\theta_f}{\theta_{Pr}}, \qquad \text{(I-12)}$$

where θ_f is the relaxation time of the fluid, and θ_{Pr}, the duration of a process which represents either the duration of a given deformation state or, equivalently, the reciprocal of the rate at which the deformation process changes (46, 47). In their analysis, Marshall and Metzner (45) used the convected Maxwell model to approximate the behavior of the viscoelastic fluid and thus could estimate the fluid relaxation time from steady shear flow measurements of the normal stresses. By assuming the porous media to be a series of converging sections in the flow direction Z, they showed that the appropriate measure of the process time in a packed bed of spheres is the reciprocal of the deformation or stretch rate in the flow direction, i.e. $(\frac{\partial u_z}{\partial z})^{-1}$ which in turn is approximately D_p/u_m where u_m is average interstitial velocity and D_p the particle diameter. With this choice of θ_{Pr}, Equation (I-12) becomes,

$$N_{Deb} = \theta_f \frac{\partial u_z}{\partial z} \approx \theta_f \frac{u_m}{D_p} \tag{I-13}$$

The quantity u_m/D_p may also be viewed as a measure of the deformation rate or so called elongation rate in the flow direction. In pure steady elongation flows, the Maxwell model they used predicts infinite stresses must occur when the N_{Deb}, defined by (I-13), approaches 1/4. Intuitively then, they suggested that the pressure drop required to pump a viscoelastic fluid through porous medium would rise to infinity as N_{Deb} defined by (I-13) approaches a value of 1/4. The experimental pressure drop measurements presented by Marshall and Metzner indicated that appreciable influences of the fluid elasticity were felt when N_{Deb}, as defined by Equation (I-13), was approximately 0.05-0.06 and at the very low values of the Deborah number the effect of elasticity were negligible. It is worthwhile to mention that some investigators (15, 48) have failed to see the viscoelastic deviation in friction factor--Reynolds number plot even at higher values of Deborah number than that from Marshal and Metzner (45) or Sadowski (44).

Elasticity has no effect on flow behavior in Lagrangian steady flows. Therefore, the increase in pressure drop due to elasticity can only be observed in an elongational flow experiment; i.e. a converging-diverging strata which is very much likely to appear in porous media. The failure of the capillary tube model of porous media to predict this phenomenon is, therefore, evident.

Pye (23) seems to be the first one who observed the increase in resistance factor with advance rate which appeared to be noticeable only in tortuous passages not straight capillaries. Similar observations and statements have been brought up by Gogarty (24), Dauben and Menzie (25), Smith (28), Jennings, et al. (34) and Harrington, et al. (49). It is interesting to mention that Jones and Maddock (50) observed this behavior of viscoelastic fluid in porous media, but they considered it disadvantageous rather than advantageous for oil displacement.

The effect of elasticity of the viscoelastic fluids, contrary to what Jennings, et al. (34) stated, need not, necessarily, be expected to happen only at high flow rates. Jennings, et al. (34) tried to include the relaxation time into the flow resistance correlation. They considered the total pressure drop, P, across a system to be the sum of the viscous, kinetic energy, and an elastic term, ΔP_e, i.e.

$$\Delta P = C_1 \mu L u_m + C_2 \rho u_m^2 + \Delta P_e, \qquad \text{(I-14)}$$

where C_1 and C_2 are constants and ρ, density. They made a further assumption that the elastic pressure drop be proportional to the normal stress difference. The final correlation appeared to be,

$$\frac{\Delta P}{u_m} = C_1 \mu L + C_2 \rho u_m + C_3 \mu \theta_f \frac{u_m}{d_c^2}, \qquad \text{(I-15)}$$

where, C_3 is constant and d_c, the diameter of the constriction. They plotted $\frac{\Delta P}{u_m}$ v.s. u_m for two different molecular weight polymer solutions passing through a core specimen of rock and noticed a significant difference in the slope which was presumed to be due to the sensitivity of θ_f--not viscosity--with molecular weight, and quantitative justification was avoided.

To conclude, this entire section can be summarized as follows. Addition of polymers to water has been shown to be effective in enhancing behavior of water floods in porous media. The mechanism and therefore controlling factors, however, are poorly understood. In a number of experiments increases in pressure drop, much above what would be expected from a consideration of viscosity, have been observed. This effect has been variously attributed to pore blockage, adsorption and viscoelasticity. In the case of viscoelasticity, theoretical considerations, although only semi quantitative, suggest significant changes can occur in flow distribution and in pressure drop. It is significant that the predictions and resultant dimensionless groups are very dependent on the velocity field of the fluid. As pointed out, in steady flow in a capillary tube, elasticity has nothing to do with either pressure drop or velocity distribution.

Since experimental data and an analysis are available for flow around a single cylinder, it was decided appropriate to study the flow of a viscoelastic fluid in a porous bed composed of closely spaced cylinders. The scale of the experiments is such that any effects of blockage, etc. can be safely ignored and attention can be focused on any changes in flow field that might occur as a result of continuum properties of the polymer.

CHAPTER II

THEORY

II. 1 Introduction

Solving the equations of change to predict the velocity field and pressure drop with the exact boundary conditions of the present model would be extremely tedious--if at all possible. However, as a first approximation, for slow flow the opening between two parallel cylinders--especially when the gap between is small compared to the diameter--can be simulated by two parallel plates with an unknown equivalent length. The unknown equivalent length for the entire bed can be obtained experimentally by experiments with a Newtonian fluid. The procedure would be the same as for the capillary tube model commonly used in porous media.

The capillary tube model, in spite of its lack of ability to portray time-dependency, has been successfully applied in porous media to predict the pressure drop or friction factor--Reynolds number relation of purely viscous flow (15, 51). The model is based on cylindrical Poiseuille flow using hydraulic radius of the medium instead of radius of the cylinder. Then, a correction factor due to the tortuousity of the bed is considered. A similar approach but with parallel-plates approximating the capillary pores will be followed for the present bed. It is worthwhile to mention that the pores of the present bed are actually rectangular channels with dimensions d and ℓ, where d is the opening between two rods and ℓ, the exposed length of rods. However, since ℓ >> d the channel can be fairly taken as a two infinite parallel plates.

To achieve a more comprehensive feeling concerning the above approach, consider the plane perpendicular to the paper along the line A-A in Figure (II-1). The space between the glass rods along the line A-A are simulated as parallel plates and at the rear side of the rods, say along the line B-B, the plates are discontinued. Since the gaps are very small most of the pressure drop will result from the flow between adjacent cylinders in a given row rather than flow from one row to the next.

The shape of the intersticial velocity profiles of the assumed model is the same as that of flow through parallel plates. The equations of the velocity profiles for the flow of Newtonian and power-law model fluids through parallel plates, which can be found elsewhere (52a, 53) and are presented in Appendix D, will not be discussed in this chapter.

II. 2 Parallel-Plates Capillary Model--Pressure Drop

Consider the flow of a fluid through two parallel plates in the z-direction as shown in Figure (II-2). One can write,

$$q_i = 2 \int_0^{\ell} \int_0^{R} u_z \, dy \, dx, \qquad \text{(II-1)}$$

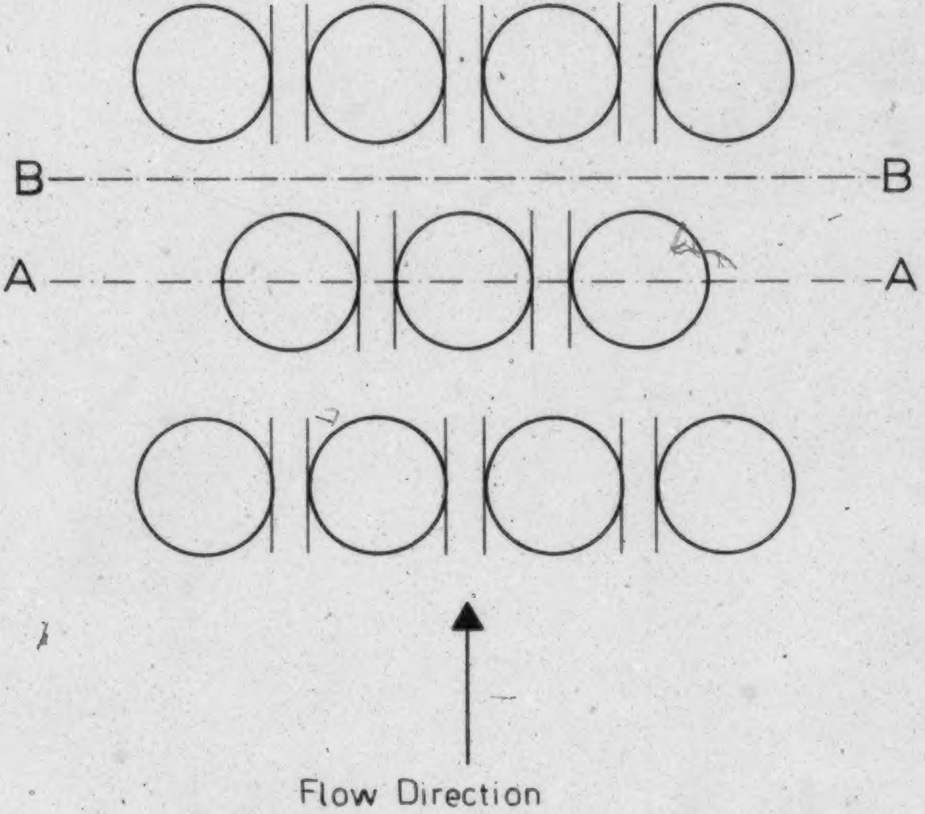
B
B
A
A
Flow Direction

FIGURE II-1 PARALLEL-PLATE
CAPILLARY MODEL

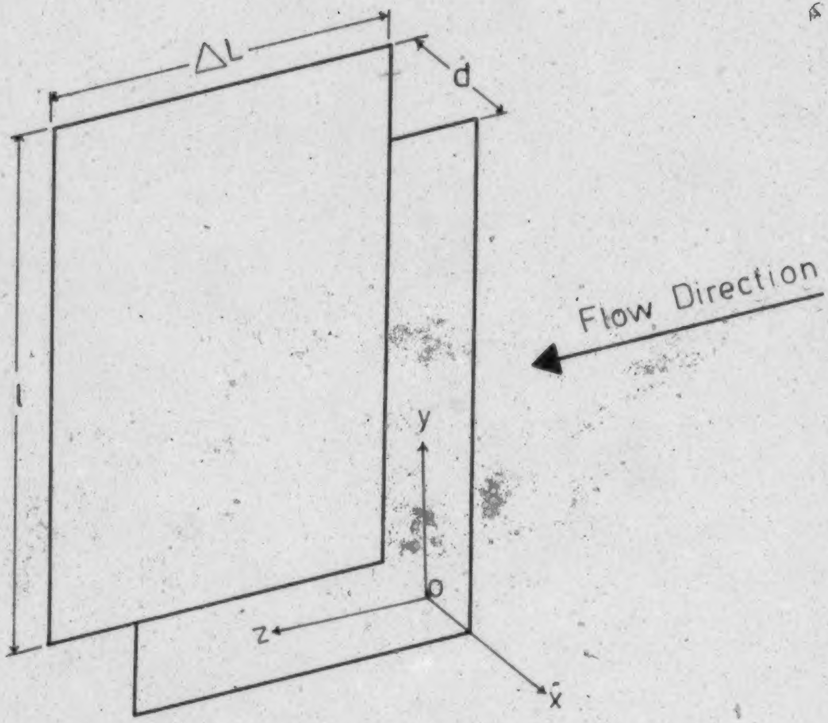
ΔL
d
l
Flow Direction
y
o
z
x

FIGURE II-2 RECTILINEAR FLOW THROUGH PARALLEL PLATES

where, q_i is volumetric flow rate, u_z, velocity in the z-direction, ℓ, the length of the channel in transverse direction and R, half the gap between the plates, i.e.,

$$R = d/2. \qquad \text{(II-2)}$$

Since flow is assumed rectilinear, u_z is a function of x only, i.e.

$$\frac{q_i}{2\ell} = \int_0^R u_z \, dx. \qquad \text{(II-3)}$$

Integrating Equation (II-3) by parts,

$$\int_0^R u_z \, dx = u_z \, x \Big/_0^R - \int_0^R x \, du_z. \qquad \text{(II-4)}$$

Assuming no slip at the wall,

$$u_z \, x \Big/_0^R = 0. \qquad \text{(II-5)}$$

From Equation (II-4) and (II-5), Equation (II-3) can be written,

$$\frac{q_i}{2\ell} = -\int_0^R x \, du_z, \qquad \text{(II-6)}$$

or,

$$\frac{q_i}{2\ell} = -\int_0^R x \left(\frac{du_z}{dx}\right) dx. \qquad \text{(II-7)}$$

The equation of motion (52b) for the laminar flow of Figure (II-2) takes the following simple form,

$$\underset{\sim}{\nabla} P = - \nabla . \underset{\approx}{\tau}, \qquad \text{(II-8)}$$

where P is pressure and $\underset{\approx}{\tau}$, stress tensor. Integrating Equation (II-8) for the present case,

$$\tau = \left(\frac{P_i - P_L}{\Delta L}\right) x = \frac{\Delta P}{\Delta L} x. \qquad \text{(II-9)}$$

τ represents τ_{xz}. From Equation (II-9) the wall shear stress, τ_W, is obtained,

$$\tau_W = \frac{\Delta P}{\Delta L} R. \qquad \text{(II-10)}$$

Dividing Equation (II-9) by (II-10) and solving for x,

$$x = \frac{R}{\tau_W} \tau, \qquad \text{(II-11)}$$

and,

$$dx = \frac{R}{\tau_W} d\tau, \qquad \text{(II-12)}$$

If we substitute (II-11, 12) into (II-7), we get,

$$\frac{q_i}{2\ell} = - \frac{R^2}{\tau_W^2} \int_0^{\tau_W} \tau \left(\frac{du_z}{dx}\right) d\tau, \qquad \text{(II-13)}$$

or,

$$\frac{q_i}{2\ell R} = u_m = - \frac{R}{\tau_W^2} \int_0^{\tau_W} \tau \left(\frac{du_z}{dx}\right) d\tau, \qquad \text{(II-14)}$$

where u_m is average velocity and du_z/dx is shear rate and will be designated by σ, so that,

$$u_m = - \frac{R}{\tau_W^2} \int_0^{\tau_W} \tau \sigma \, d\tau . \qquad \text{(II-15)}$$

For the assumed steady flow σ is a function only of τ. For Newtonian fluids,

$$\sigma = -\frac{\tau}{\mu}, \tag{II-16}$$

and for a fluid approximated by the power-law model,

$$\tau = m_1|\sigma|^n, \tag{II-17}$$

where $|\sigma|$ is the absolute value of σ, m_1 and n are rheological parameters. By defining Γ as an average nominal Shear rate,

$$\Gamma = \frac{u_m}{R}, \tag{II-18}$$

Equation (II-15) can be written in the following form,

$$\Gamma = -\frac{1}{\tau_W^2}\int_0^{\tau_W} \tau\,\sigma\,d\tau. \tag{II-19}$$

To modify Equation (II-19) for the multicylinder box, it is sufficient to introduce V/ε_s in place of u_m, i.e.

$$u_m \equiv \frac{V}{\varepsilon_s}, \tag{II-20}$$

where ε_s is surface porosity. Surface porosity is calculated as follows,

$$\varepsilon_s = \frac{\Sigma d}{\Sigma d + \Sigma D} \tag{II-21}$$

Therefore, Equations (II-18) and (II-19) become,

$$\Gamma_\varepsilon = \frac{V}{\varepsilon_s R} = -\frac{1}{\tau_\varepsilon^2}\int_0^{\tau_\varepsilon} \tau\,\sigma\,d\tau \tag{II-22}$$

where the subscript ε indicates that the equation has been modified for the porous bed. Also, Equation (II-10) can be modified for the porous bed as follows,

$$\tau_\varepsilon = \frac{\Delta P}{L'} R, \tag{II-23}$$

where L' is written instead of L, the length of the bed, to include tortuousity, i.e.

$$L' = C_4 L. \tag{II-24}$$

C_4 is geometric constant which accounts for tortuousity of the path of the fluid particles. The magnitude of C_4 is estimated from Figure (II-1) to be approximately equal to,

$$C_4 \simeq \frac{(\pi D/2)\ N}{L} = 1.5, \tag{II-25}$$

where $(\pi D/2)$ is half the circumference of the cylinder and N the number of rows. A more accurate value of C_4 which will be presented later, should be determined experimentally. Substituting (II-24) into (II-23),

$$\tau_\varepsilon = \frac{\Delta P}{C_4 L} R. \tag{II-26}$$

For a Newtonian fluid, Equation (II-22) by using Equation (II-16) becomes,

$$\Gamma_\varepsilon = \frac{\tau_\varepsilon}{3\mu} \tag{II-27}$$

Solving for μ,

$$\mu = \frac{\tau_\varepsilon}{3\Gamma_\varepsilon}. \tag{II-28}$$

The expression found for μ is defined as Darcy's viscosity. Substituting (II-22, 26) into (II-28),

$$\mu = \frac{\varepsilon_s R^2}{3C_4} \frac{\Delta P}{LV} \tag{II-29}$$

By comparing Equation (II-29) with Darcy's law, Equation (I-4), the expression for the permeability of a Newtonian fluid in the parallel-plates capillary model bed is obtained as,

$$K = \frac{\varepsilon_s R^2}{3C_4}, \tag{II-30}$$

in which C_4, as stated earlier, has to be evaluated experimentally.

II. 3 Power-Law Model

Assuming fluid flow is purely viscous, the power-law model can be used to approximate the properties of the polymer solution. Solving for σ from Equation (II-17),

$$\sigma = -\left(\frac{\tau}{m_1}\right)^{1/n}, \tag{II-31}$$

where the minus sign is chosen because of the choice of coordinates. Substituting (II-31) into (II-22) and integrating,

$$\Gamma_\varepsilon = \frac{n}{1+2n}\left(\frac{\tau_\varepsilon}{m_1}\right)^{1/n}, \tag{II-32}$$

or,

$$\tau_\varepsilon = m_1\left[\frac{1+2n}{n}\Gamma_\varepsilon\right]^n. \tag{II-33}$$

Further, we write τ_ε and Γ_ε in terms of K and C_4 using Equations (II-22, 26, 30),

$$\tau_\varepsilon = \sqrt{3K/C_4\varepsilon_s}\,\frac{\Delta P}{L}, \tag{II-34}$$

$$\Gamma_\varepsilon = V/\sqrt{3C_4K\varepsilon_s}. \tag{II-35}$$

If we substitute (II-34, 35) into (II-33) and solve for V^n,

$$V^n \doteq \frac{(3K/C_4\varepsilon_s)^{1/n}\,(3C_4K\varepsilon_s)^{n/2}}{m_1\left(\frac{1+n}{n}\right)^n}\,\frac{\Delta P}{L}. \tag{II-36}$$

Comparing Equation (II-36) with the modified Darcy's law, i.e. Equation (I-5), H can be obtained,

$$H = \frac{m_1}{3} \left(\frac{1+2n}{n}\right)^n (3C_4 K \varepsilon_s)^{(1-n)/2} . \qquad \text{(II-37)}$$

From (II-37), it is evident that $H = m = \mu$ when $n = 1$ as for a Newtonian fluid.

II. 4 Modified Friction Factor and Reynolds Number

If we use Ergun's definition of the friction factor (54), we obtain,

$$f_K = \frac{2d\, \varepsilon_s^2\, \Delta P}{\rho\, V^2\, L} . \qquad \text{(II-38)}$$

The Reynolds number is arbitrarily defined so that,

$$f_K = 1/N_{Re} . \qquad \text{(II-39)}$$

After straight forward algebraic manipulation, it follows from Equations (II-2, 30, 38) and (I-5),

$$N_{Re} = \frac{\rho\, d\, V^{2-n}}{24\, C_4\, \varepsilon_s\, H} . \qquad \text{(II-40)}$$

For a Newtonian fluid, we set $n = 1$ and therefore,

$$N_{Re} = \frac{\rho\, d\, V}{24\, C_4\, \varepsilon_s\, \mu} . \qquad \text{(II-41)}$$

II. 5 Application of Theory

The permeability, K, of the bed can be determined from Equation (I-4) by a Newtonian fluid flow experiment. Then, from Equation (II-30) the tortuousity factor, C_4, can be predicted. Therefore, H from Equation (II-37), and consequently, ΔP from Equation (I-5) for the polymer solution runs are calculated.

Equation (I-5) predicts that a plot of ΔP v.s. V on log-log scale is a straight line with slope n in the absence of inertia and elastic effects. Upward deviation of experimental points from this straight line might be due to the inertia effect, elastic effect or both. Effect of elasticity would be confirmed by showing the absence of inertia effect with a Newtonian fluid of similar viscosity. An equivalent verification can be obtained by plotting friction factor v.s. Reynolds number which according to (II-39) would give a straight line with slope -1 on log-log scale.

CHAPTER III

EXPERIMENTAL EQUIPMENT AND PROCEDURE

III. 1 Multi-Cylinder Matrix

To simulate flow in porous media a regularly spaced matrix of 6mm diameter glass rods in a triangular arrangement was used. Figure (III-1) illustrates a unit cell of triangular pitch. The cylinders were contained in a rectangular channel of inside cross section 5.2 cm x 6.5 cm--Figure (III-2). The top and side walls of the channel were made of 1/2" Plexiglass sheets and the bottom, inlet and outlet, of stainless steel. On the bottom plate a 1mm brass sheet was set to keep the cylinders fixed in their positions. The inside surface of the rear side wall was painted black by "Wrought Iron Black" paint to eliminate reflection. The front side of the box (i.e. the side facing the light source) was covered with a black hard paper which had an approximately 1mm horizontal slit at the middle to provide a narrow slit of light from the broader slit coming from the light source.

To minimize the inlet and outlet disturbances, two distributors, 26 cm apart, were used; one before the first row and the other after the last row. The distance between the distributors and the inlet/outlet plates was 1.5 cm. The length of the model was 40 rows of of cylinders, each

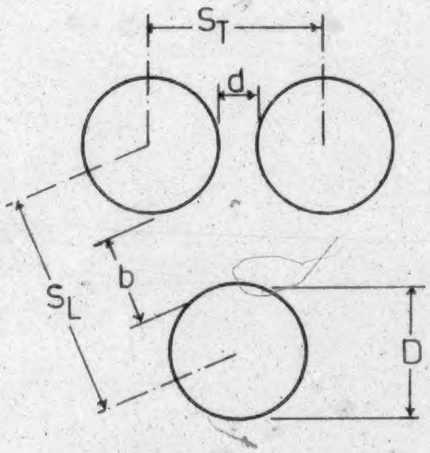

FIGURE III-1 TRIANGULAR-PITCH ISOCELL

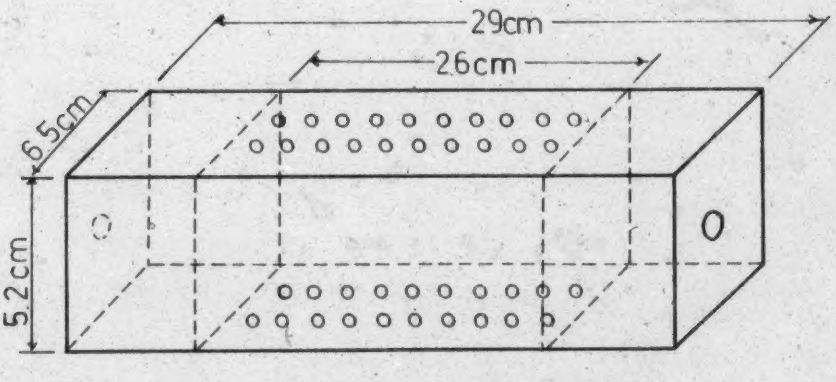
29cm
26cm
6.5cm
5.2cm

FIGURE III-2 MULTI-CYLINDER MATRIX

row alternatively 9 or 10 cylinders across. The minimum and maximum pore openings, shown as d and b in Figure III-1, were approximately 0.5 and 1mm, respectively. The volumetric porosity, ε, of the bed was 0.357. Measurement of ε was performed by measuring the void volumes, V_v. The box was filled with water, then the volume of the water, V_w, was measured. Knowing the total volume of the box, V_T, porosity was obtained by,

$$\varepsilon = \frac{V_v}{V_T} = \frac{V_w}{V_T} . \qquad \text{(III-1)}$$

Void volume can also be approximated by,

$$V_v = V_T - V_C , \qquad \text{(III-2)}$$

where V_C is the volume occupied by cylinders and is equal to,

$$V_C = \frac{\pi D^2}{4} \ \ell \ N_T , \qquad \text{(III-3)}$$

where N_T is the total number of cylinders.

A similar model with cylinders of shorter length and larger diameter was used by Kyle, et al. (55). A smaller diameter was chosen for the present study to achieve larger elongational rates (i.e. $\partial u_z/\partial z$ in Equation V-3) which is required to observe any significant elastic effect.

The model was constructed to represent a uniform homogeneous bed, but it was found that some inhomogeneity in the microscopic scale existed. Specifically, the minimum opening, which was nominally to be 0.5mm, varied between 0.46 to 0.787mm--excluding the openings next to the walls. These openings are given in Table (C-1) for three rows. And the diameter of rods which were nominally 6mm circular cross-section varied from 5.9 to 6.2mm. The cylinders were not perfectly circular and the maximum to minimum diameter ratio was as large as 1.03.

The twentieth, twenty first and twenty second rows--numbered from the inlet--were chosen to represent the bed. The positions are numbered from 1 to 32 as shown, schematically, in Figure (III-3). A complete map of these rows, measured at a total magnification 100 was prepared to define the spacings of the cylinders. This was performed by projecting the pictures taken of the different positions which covered the whole area of interest.

An attempt was made to obtain velocity profiles at the minimum openings, where the maximum pressure drop and the maximum deformation rates occur. These positions are along the line A-A in Figure (III-3). However, due to the difficulties involved in photography--e.g. not having enough light at some center line positions--it was not possible to have photographs of usable quality at these positions for all the 32 openings. As a result of this the complete distribution of the flow across a row had to be determined indirectly. Thus some of the pictures had to be taken from the positions below or above the line A-A, say B-B. The center line openings (i.e. the openings along the line A-A such as

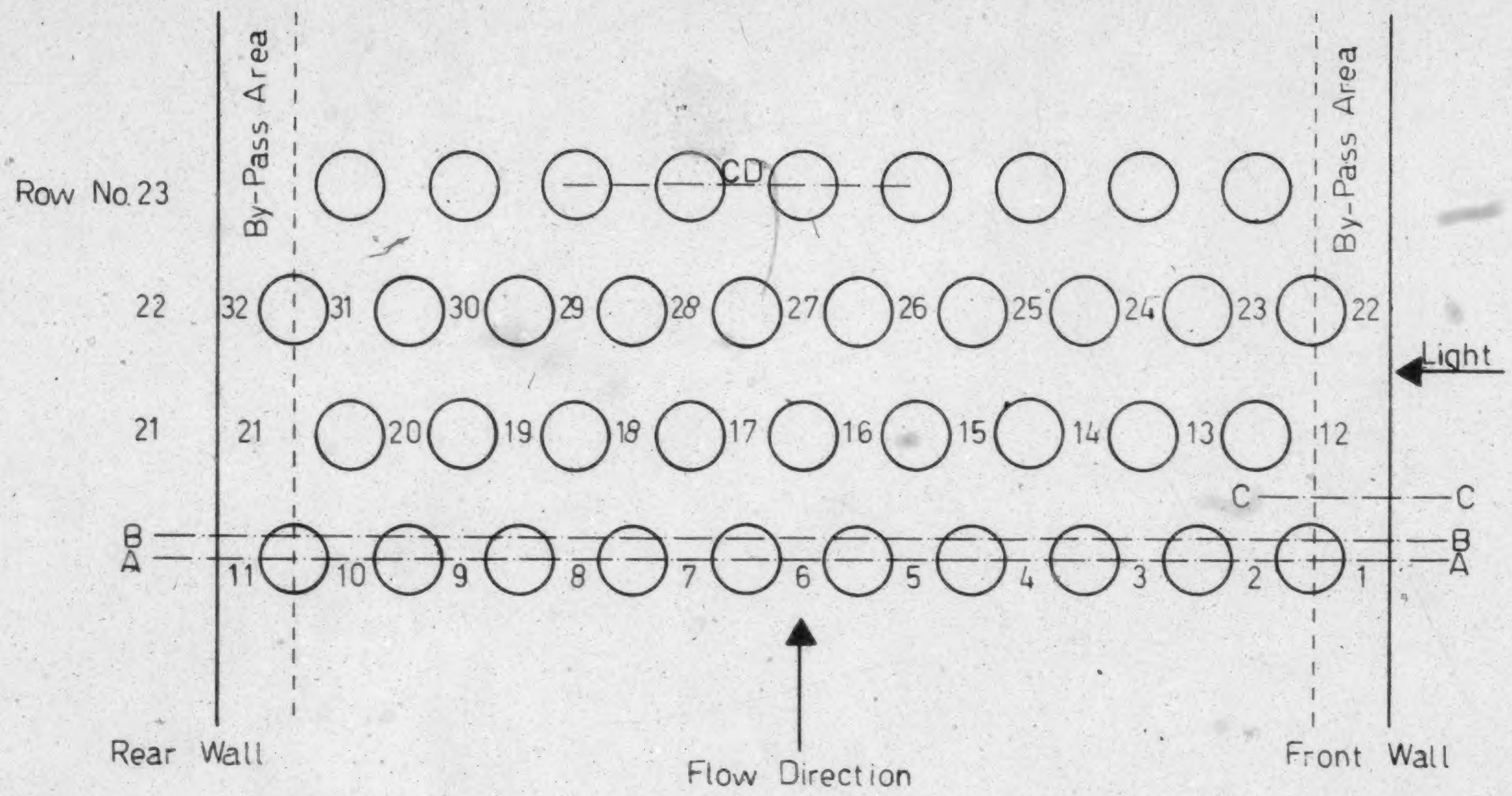
Row No.23
22
21
By-Pass Area
By-Pass Area
CD
32
31
30
29
28
27
26
25
24
23
22
21
21
20
19
18
17
16
15
14
13
12
Light
C
C
B
A
B
A
11
10
9
8
7
6
5
4
3
2
1
Rear Wall
Flow Direction
Front Wall

FIGURE III-3 TOP VIEW OF GLASS RODS

CD in Figure III-3 are designated by d; and the openings above or below A-A are called NCL, implying "Not Center Line." The relative magnitude of NCL with respect to d is an indication of the relative position of the line B-B with respect to the line A-A. In the case of NCL, the orthogonal component of the streaks length was taken; but for the center line openings this need not be considered, because all the streaks are perpendicular to A-A. For the positions 1, 11, 22, and 3 2 the "Not Center Line," NCL, was taken even farther than B-B, say C-C, and those streamlines, crossing C-C, which passed through these positions were chosen.

Every alternate row of the matrix had two large openings next to walls. These openings were in the order of magnitude of the radius of cylinders, i.e. 3mm, while the minimum openings between two cylinders as was already mentioned, were designed to be 0.5mm. These large openings caused by-pass channels near the walls. That is a larger fraction of fluid passed from the openings next to walls. The by-pass area is shown in Figure (III-3) by dashed-line.

III. 2 Experimental Fluids

A partially hydrolized Polyacrylamide product of Dow Chemical Co., trade name SEPARAN AP-273 was used as polymer. This white granular powder is soluble in water and has a molecular weight of approximately three million. Its solution in water shows effects of elasticity and the rheological properties of 0.2% (by weight) solution, which was used for the entire experiment, are given in Appendix A. Domestic tap water was used for preparation of polymer solutions and care was taken to avoid mechanical degredation of the polymer molecules by stirring the solution very gently during preparation. The solutions were protected from bacterial degredation by approximately 1cc of Sodium Benzoate powder in 10^6cc solution. The specific gravity of the polymer solutions, determined for every new solution, was 0.9965 gr/cc.

To provide a wide range of friction-factor Reynolds number for Newtonian fluids, Glycerol solutions ranging from 96 to 58% Glycerol by volume in tap water were used.

Aluminum metal dust, manufactured by J. T. Baker Chemical Co., Lot No. 2347, was used to visualize the flow pattern. The volumetric concentration of Aluminum dust was approximately 2cc of the bulk dust in 10^6cc solution.

III. 3 Pumping

Fluid flow at a desired rate was obtained by a ZENITH gear pump driven by a variable speed transmission. For low flow rates (i.e. 0.685 to 6.85 cc/sec) one pump was used but for higher flow rates, which were required to increase the range of flow rate for pressure drop measurement, two pumps were used. The pumps were calibrated by weighing the polymer solution collected over a known period of time. Since the Glycerol solutions (i.e. more than 85% Glycerol by volume) are highly hygroscopic a complete closed recycle system was used. For the polymer solution, to avoid degradation of the polymer molecules, recycling was avoided. Rheological properties were measured before and after running and consistency was checked to assure absence of any degradation.

III. 4 Streak Photography Technique

Streak photography not only gives the streamlines but also the velocity profile can be established by measuring the length of the streaks of known duration. These were provided by placing a chopping disk perpendicular to the light beam to interrupt the light for known duration of time. In the present work the streak photography using a photomicrography technique was applied to obtain the local velocity profile.

III. 4-1 Optical System

The main features of the optical system are shown in Figure (III-4) which are briefly reviewed below.

a. Light Source

The light source used in the present study was the same as the one used by Rollin (56) and Catania (57). It was a CHRISTIE Xenon arc-lamp which operated from a three phase CHRISTIE transformer of D.C. maximum output of 3300 Watts at 100 amps. The necessary optical alignment and adjustments of the lamphouse No. BSF 50 were made to achieve the maximum brightness and light uniformity. Immediately in front of the lamphouse lens an adjustable horizontal slit, then a converging lens were placed. Therefore a narrow beam

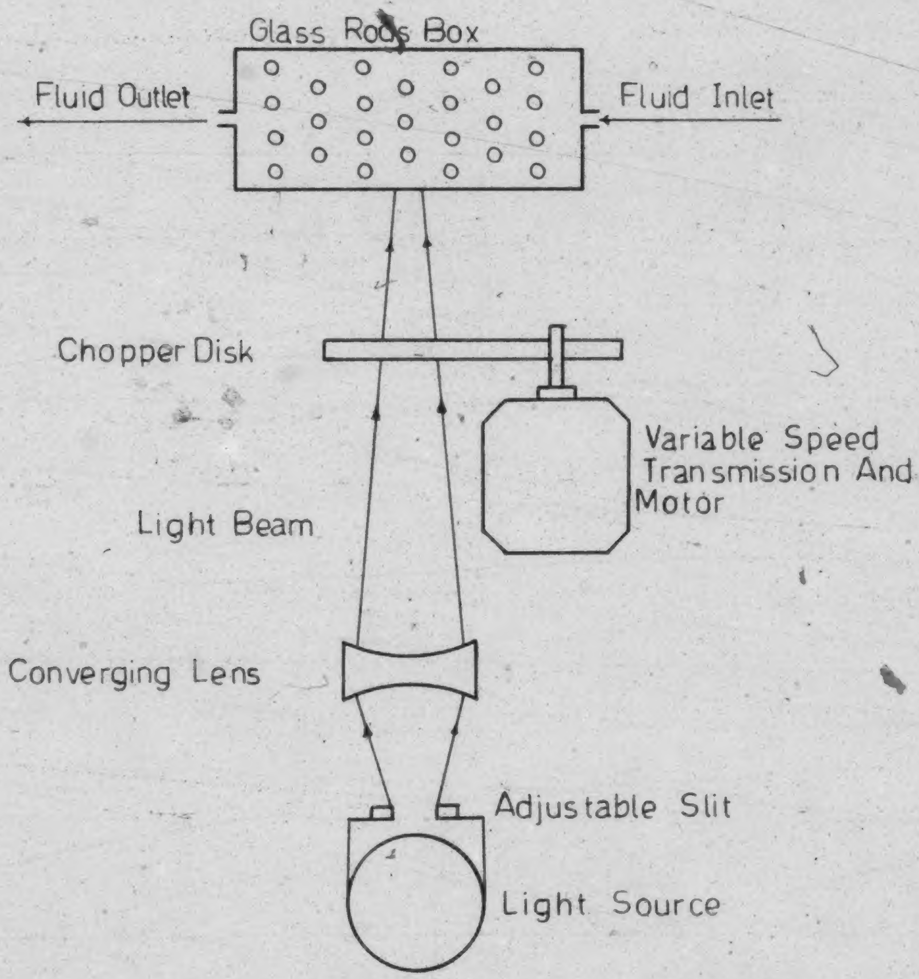
Glass Rods Box
Fluid Outlet
Fluid Inlet
Chopper Disk
Variable Speed Transmission And Motor
Light Beam
Converging Lens
Adjustable Slit
Light Source

FIGURE III-4 SCHEMATIC PLAN VIEW OF OPTICAL SYSTEM

to a thickness of, approximately, 2mm, less than the slits on the chopper disk but broader than the slit on the box was produced. The light slit was set horizontal so that the plane of light beam was perpendicular to the rods.

b. Chopper Disk

Two transparent lucite disks were assembled on a variable speed transmission through a pulley connection with a ratio of diameter of disk pulley to transmission pulley 2.7:1. In order to interrupt the light and provide streaks of known duration, a paper wheel with 8 equal radial slits and spokes was placed between the lucite disks and fastened together. The chopper disk was placed perpendicular to the light beam with the axis of rotation in the plane of the light slit.

The rotational speed of the motor was set in order to obtain reasonable length of streaks. In an accelerating flow long streaks are not representative of the local velocity; on the other hand, uncertainty in the length measurement of very short streaks is more than that of longer ones. It is evident that higher flow rates require higher rotational speed. The rotational speed of the chopper above 100 RPM was measured by a Stroboscope Type 1531-A STROBOTAC. Below 100 RPM, speed was determined using a stop watch.

After the experiment was finished a disagreement was noticed between the actual and experimental total flow rates. The actual total flow rate was measured by the formerly calibrated pump, while the experimental flow rate was calculated from the area under the velocity profiles. This disagreement appeared only for the two high flow rates where the rotational speed of the chopper was above 100 RPM. By checking the stroboscope, it was found that the stroboscope was not calibrated and the measured RPM's were 10.4 per cent less than the actual RPM's which was indeed equal to the inconsistency of the flow rates.

C. Photomicrography Assembly

As illustrated in Figure (III-5), a Miranda 35mm camera was positioned at the top of a phototube of a Wild M5 microscope. The phototube was perpendicular to the light and the camera film parallel. Magnification on the microscope was 12X, but the real magnification on the film was 4X. Thirty-five mm Tri-X film with ASA speed of 400 was used. The exposure times were determined after a set of trials and were approximately 15 to 20 seconds. The exposure times were different according to the brightness of the position. For the positions where the light was not sufficient the exposure time was extended even to one minute in order to increase the probability of having a bright particle passing that position.

III. 4-2 Measurement of the Streak Length

A Bell & Howell projector was used to project the negatives on a large sheet of graph paper. Total magnification of the streaks on the graph paper was 100 in all cases. The distance between the projector and graph paper was adjusted so as to obtain the final magnification of 100. The graph

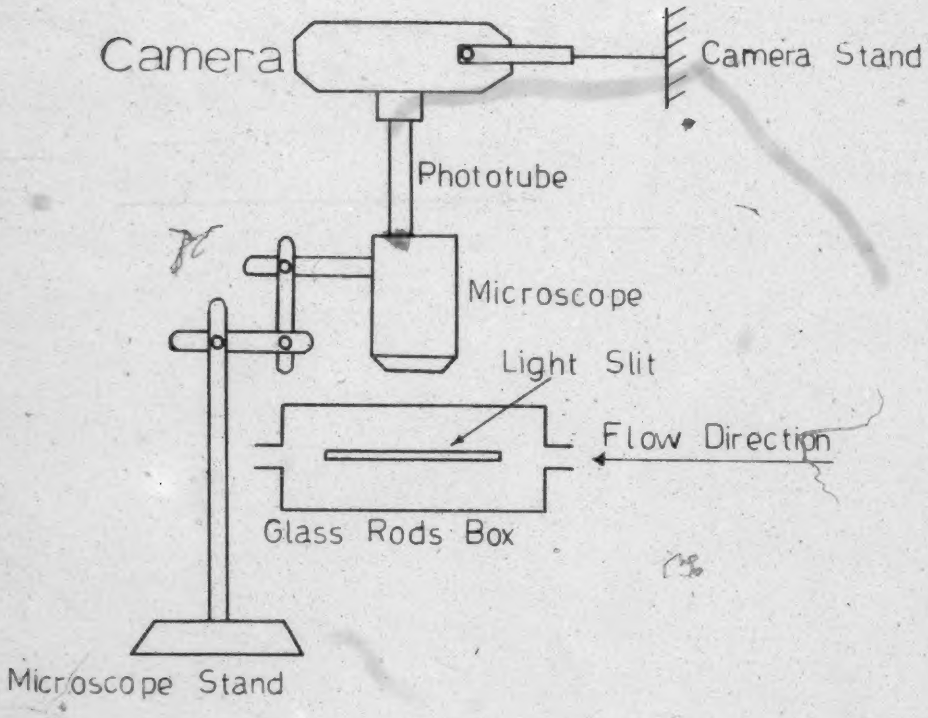
Camera
Camera Stand
Phototube
Microscope
Light Slit
Flow Direction
Glass Rods Box
Microscope Stand

FIGURE III-5 PHOTOMICROGRAPHY ASSEMBLY

paper had 0.1" divisions and the length of the streaks were read directly from the graph paper at the total magnification of 100. Therefore all the reported lengths in Tables (E-1, 2) are in units of 10^{-3} inches.

The system was calibrated by projecting photographs of a precision steel ruler with 0.5mm division.

To eliminate the error due to the half-shadow at the beginning and the end of every light period of the chopper's opening, all measurements of streak length were performed on head-to-head or tail-to-tail basis. That is the length 'a' was measured not 'b'.

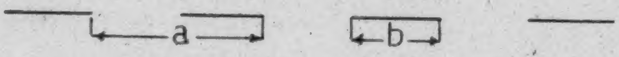

Some typical photographs are given for Glycerol and Separan in Figures (IV-5, 6).

Two major sources of error which caused the data points to be scattered in Figures (IV-7 to 12) or (IV-13) are how accurately the streaks could be located with respect to the edge of the rods and the hazy beginning and end of the streaks.

By observing several photographs, points on the circumference of the rods were located and the cross sections of the rods were drawn onto the graph paper. In pictures which did not provide sharp edges, uncertainty in determining the points on the circumference is in the range of a few tenths of an inch in the magnified scale. This uncertainty is, approximately, 10 per cent the nominal center line opening, d = 0.5mm. Noting that the slope of the local velocity profiles near the walls is high, the uncertainty in the location of the streaks causes significant scattering. For instance, the velocity profile of position No. 13 of Separan in Figure (IV-13) is a good example. In this profile, two groups of data points which belonged to two different photographs are observed at the left side of the mid-point of the opening. By shifting the upper group 0.05mm to the right, the scattering could be minimized significantly. This effect is more severe near the cylinders where the slope of the velocity profiles is high, but is zero at the mid-point of the opening where the slope is almost zero.

The formerly mentioned second source of error is the measurement of the length of the streaks which is due to the hazy beginning and end of the streaks. This could reach two-tenths of an inch in the magnified scale for good pictures. The percentage contribution of this error is negligible for long streaks, say 3 inches in magnified scale, but is significant for the short ones which are near the cylinders; e.g. for a 0.4 inches long streak in magnified scale, the percentage of the error in measurement is 50 per cent. Position No. 13 of Glycerol in Figure IV-13 is a good example of this kind of scattering. For the pictures of poor quality, the hazy part of streaks was much larger than what was reported above. This could reach to even half an inch in magnified scale. Some of the data points of positions No. 15 and 16 of Separan in Figure (IV-13) belong to this kind of picture.

The "Not Center Line" positions were chosen so that both of these two sources of error were minimized. That is, they were chosen along a line where sharp image of the cylinder allowed accurate positioning and also where sharp streaks images occurred.

III. 5 Pressure Drop Measurement

Mercury and also two colored manometer liquids, MERIAN No. D-2883 and D-8325 with specific gravity of 2.95 and 1.75 respectively, were used to measure the pressure drop. Pressure taps were located on the rear side of the box, 22.2 cm apart, between row No. 3 and row No. 38. Pressure drop was measured for pure, 96% (by volume), 81% (by volume), 58% (by volume) Glycerol, tap water, and 0.2% (by weight) Separan solutions. The range of flow rates for the different fluids is given below,

Fluid	Range of Flow Rates
Pure Glycerol	0.431 - 3.42 cc/sec
96% Glycerol	0.835 - 17.06 cc/sec
81% Glycerol	0.835 - 10.76 cc/sec
58% Glycerol	2.13 - 34.35 cc/sec
tap water	10.76 - 34.35 cc/sec
0.2% Separan	0.431 - 34.35 cc/sec

CHAPTER IV

RESULTS

IV. 1 Pressure Drop

Figure (IV-1) is a plot of the measured pressure drop v.s. superficial velocity for the several Newtonian fluids. In this plot the empirical correlation of Bergelin, et al. (58) for the flow across banks of cylinders has been shown. This empirical correlation is discussed in Appendix B. The data points of this plot, together with the calculated permeability, are recorded in Table (B-1). The permeability of the bed has been calculated for individual runs using Darcy's law, i.e. Equation (I-4). The arithmetic average permeability of the runs number 1 to 41 in Table (B-1) has been chosen to approximate the permeability of the bed, i.e.

$$K = 1.3 \times 10^{-4} \text{ cm}^2 \qquad \text{(IV-1)}$$

Figure (IV-2) shows the pressure drop measurement v.s. superficial velocity for polymer solution. In this plot the predicted curve of pressure drop by Equation (I-5) based on the parallel-plate capillary model is presented. The empirical correlation of Bergelin which gave a good prediction for Glycerol solutions was modified for the polymer solution and the predicted curve is also given in Figure (IV-2).

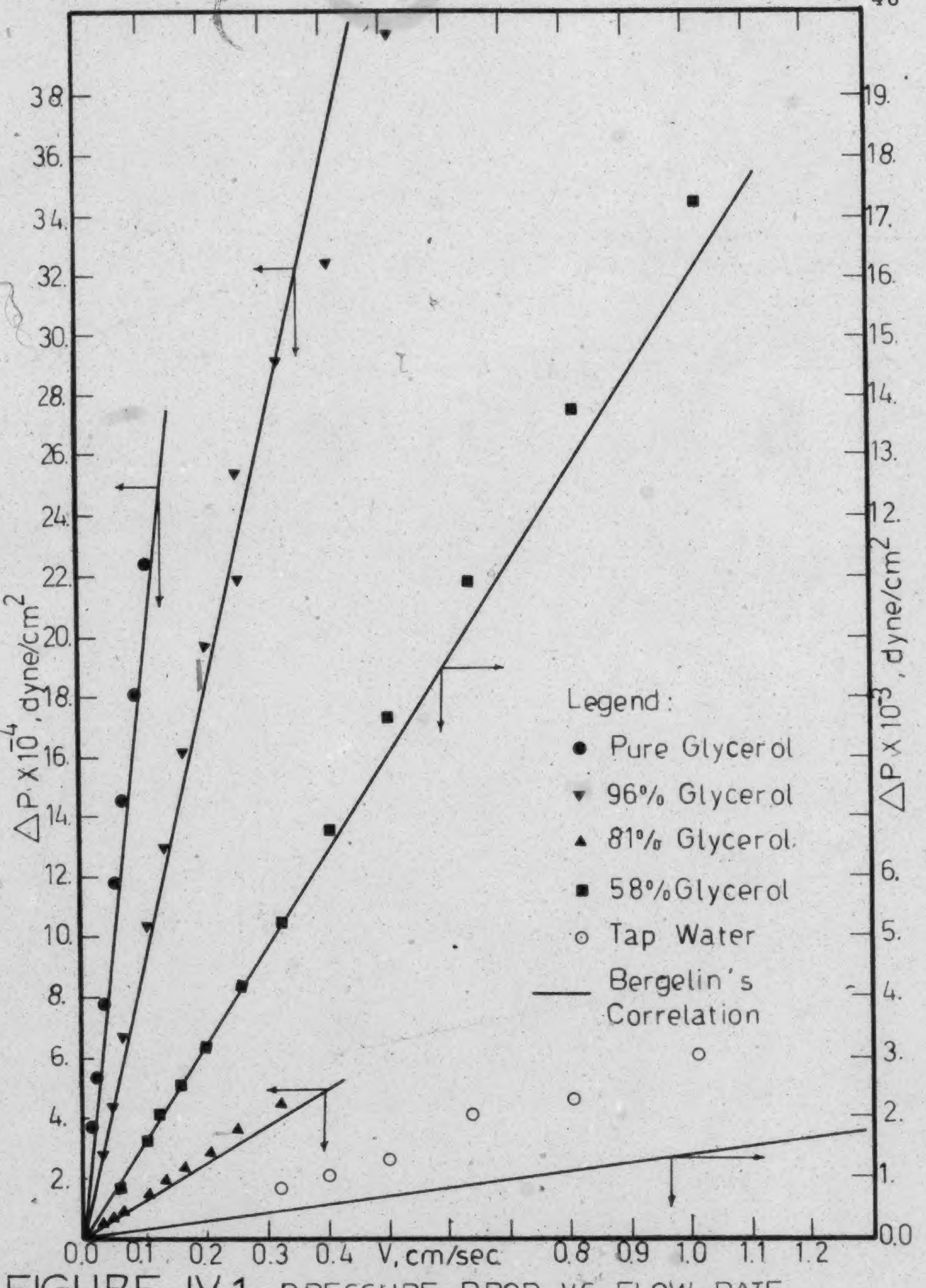

FIGURE IV-1 PRESSURE DROP V.S. FLOW RATE GLYCEROL

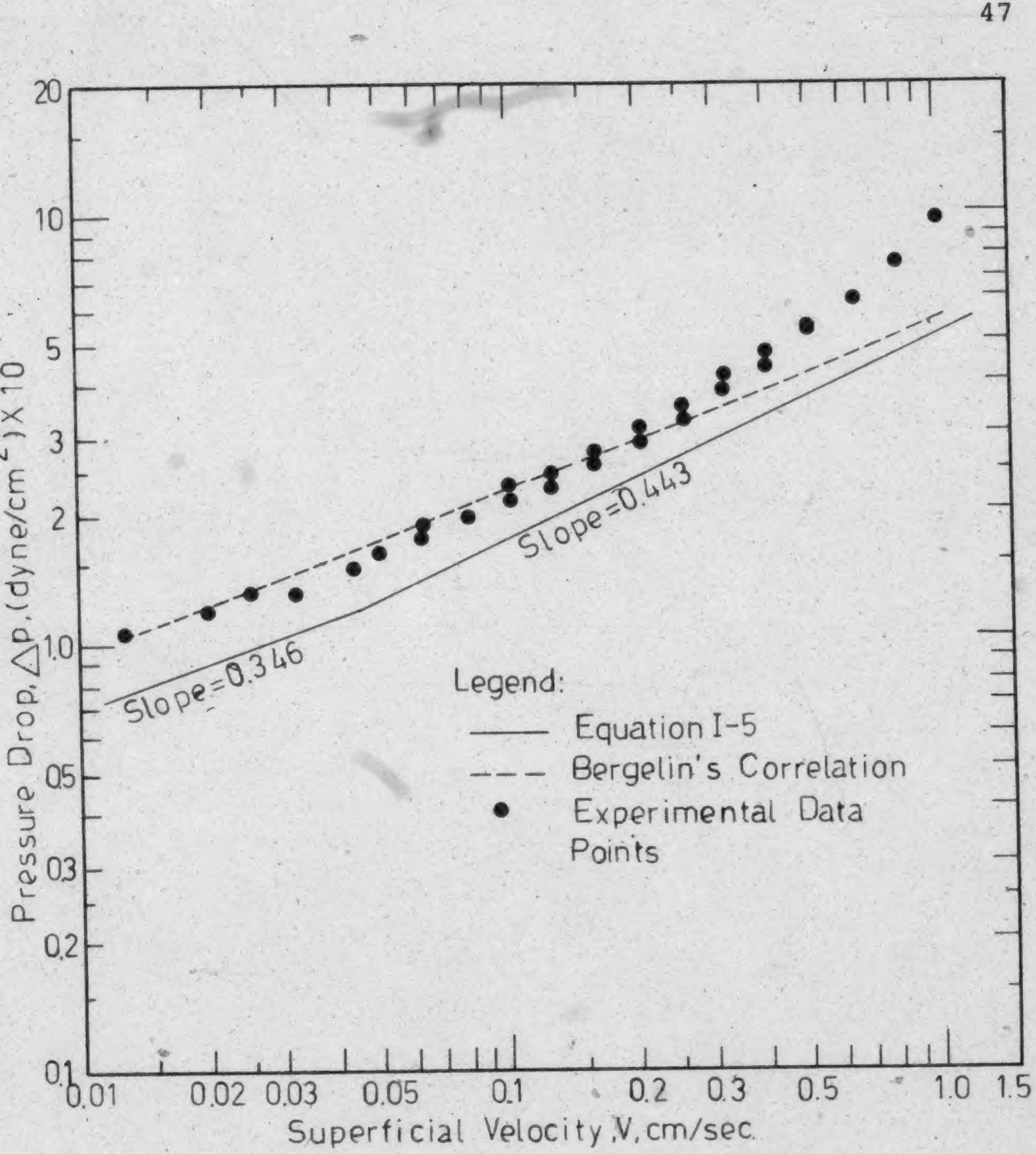

FIGURE IV-2 PRESSURE DROP V.S. FLOW RATE SEPARAN

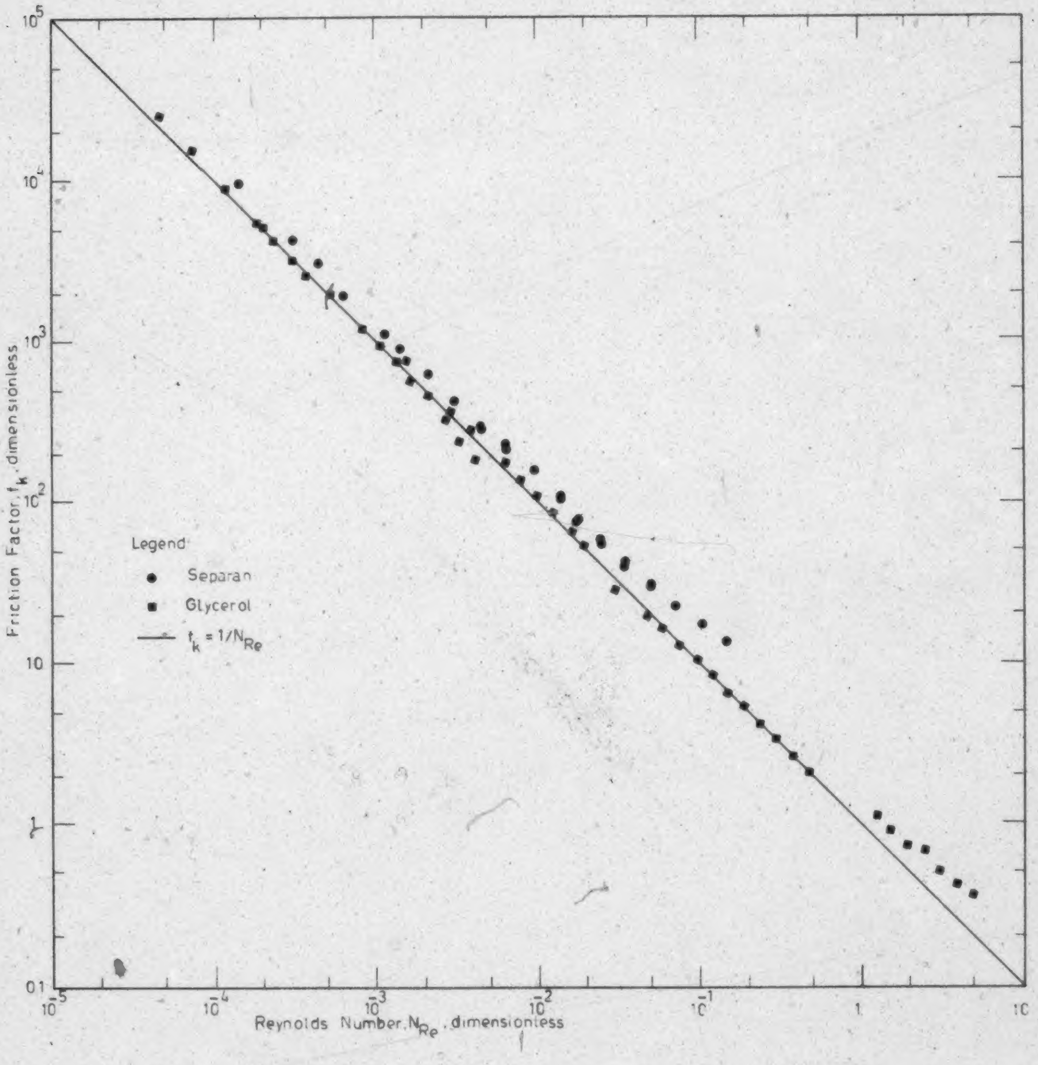

FIGURE IV-3 FRICTION FACTOR V.S. REYNOLDS NUMBER

Figure (IV-3) shows the behavior of friction factor v.s. Reynolds number for Glycerol and polymer solutions. The correlations used in this plot are Equations (II-38, 40, 41). The Separan data points of this plot and also those from Figure (IV-2) are recorded in Table (B-2). The Glycerol data points of Figure (IV-3) are presented in Table (B-1).

IV. 2 Streamlines

Photograph No. 1 in Figure (IV-4) presents the shape of the streamlines of 0.2% polymer solution across a single submerged cylinder. The diameter of the cylinder was 3mm and the exposed length, 5.2 cm. The photograph has been taken in a plane perpendicular to the cylinder at its mid-point. The approach or free stream velocity was 0.437 cm/sec. Photographs No. 2, 3, and 4 in Figure (IV-5), taken from position No. 25, present typical streamlines of pure Glycerol through the bank of glass rods. The flow rates were 0.685, 1.717, and 3.42 cc/sec respectively. Photographs No. 5, 6, and 7 in Figure (IV-6) have been taken from the same position and the same flow rates as Glycerol but with the 0.2% polymer solution.

IV. 3 Local Velocity Profiles

Local velocity profiles have been studied for three rows, namely row numbers 20, 21 and 22, and were established for total flow rates of 0.685, 1.717, 3.42 and 6.84 cc/sec. It was noticed that the percentage of the total flow rate

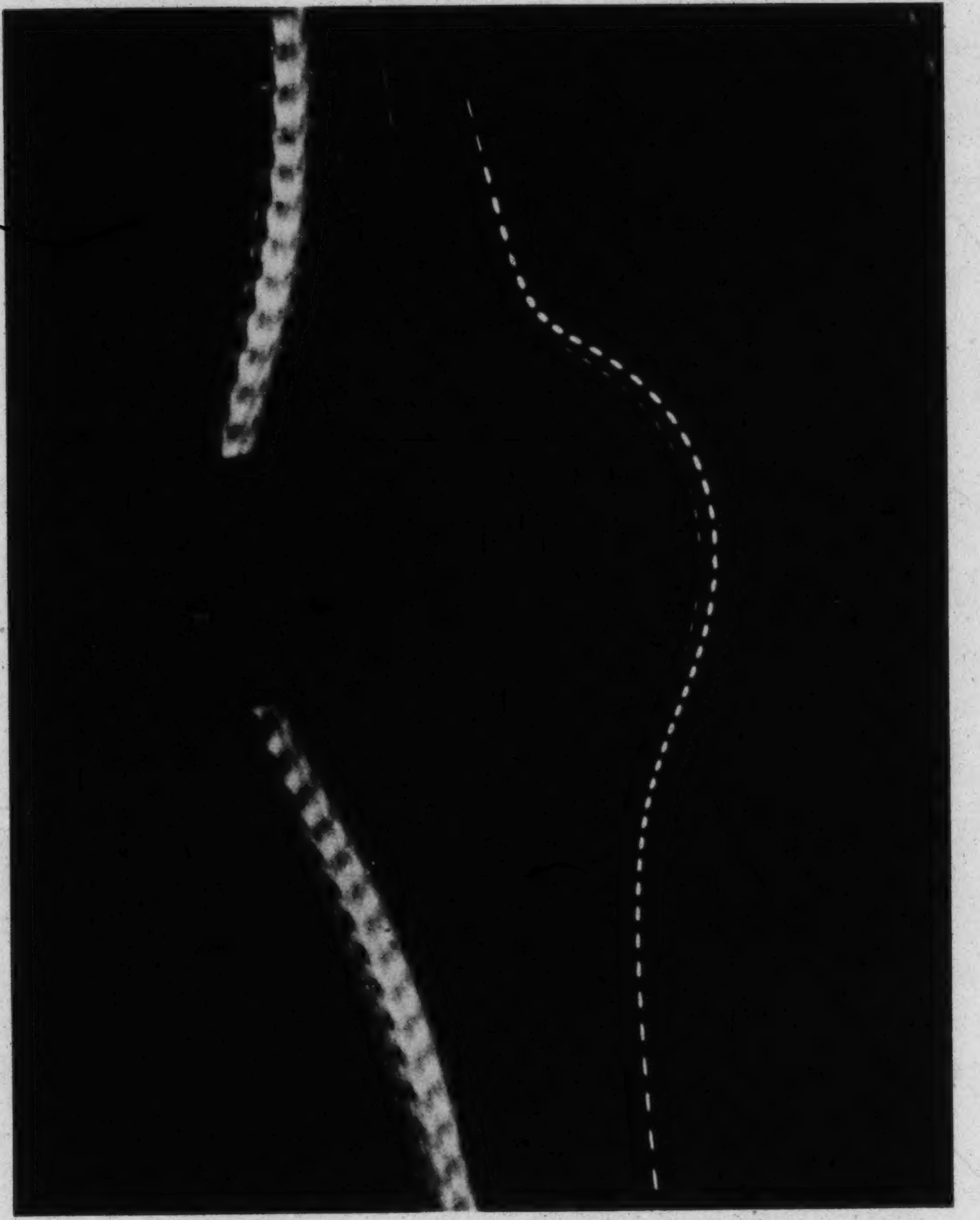

Photograph No. 1
U=0.437cm/sec.

Flow Direction

FIGURE IV-4 VISCOELASTIC FLOW PAST SINGLE CYLINDER

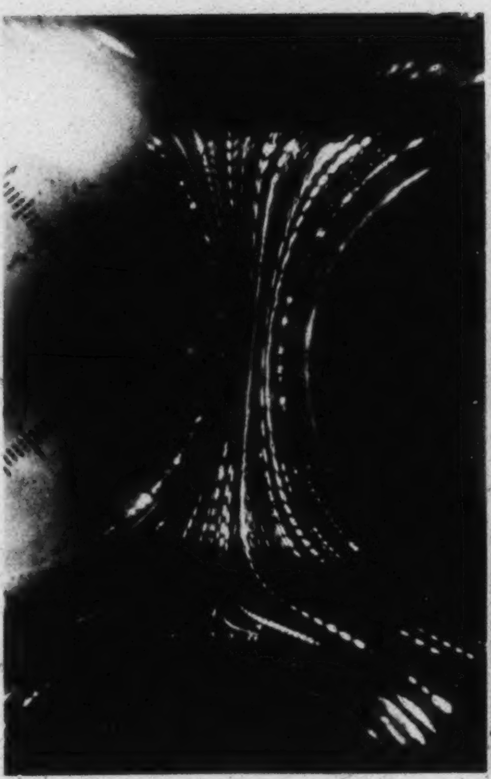

Photograph No.2
q = 0.685 cc/sec

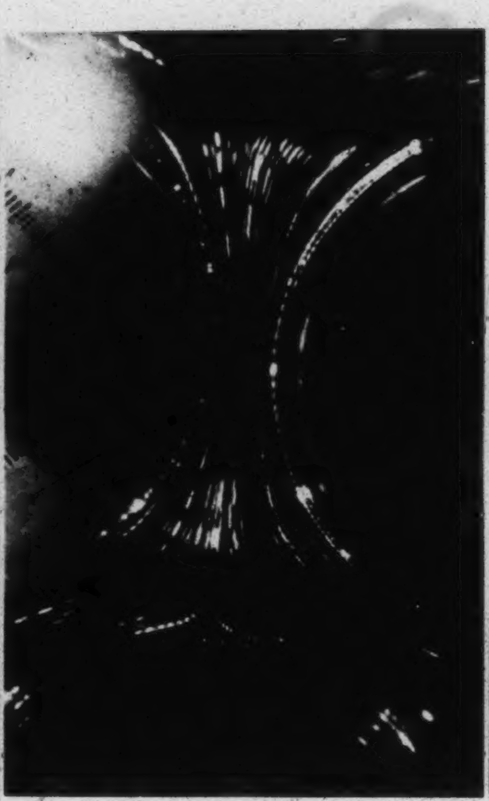

Photograph No.3
q = 1.717 cc/sec

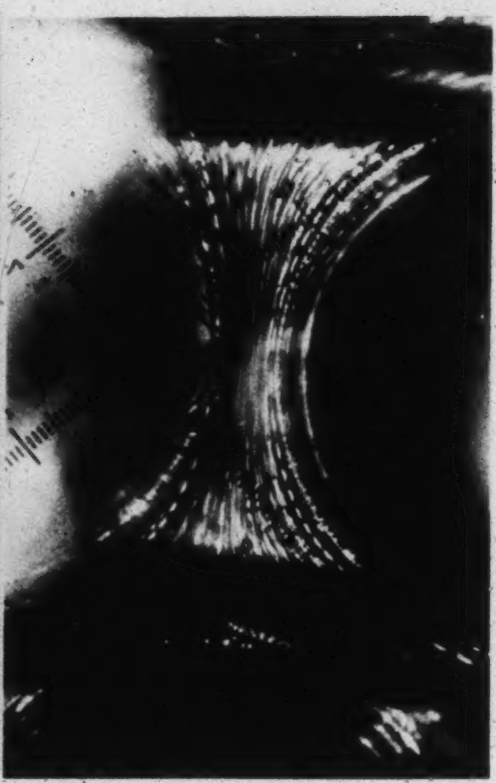

Photograph No.4
q = 3.42 cc/sec

↑ Flow Direction

↑ Flow Direction

FIGURE IV-5 NEWTONIAN FLOW PAST MULTI CYLINDERS — ~~POSITION~~ NO 2

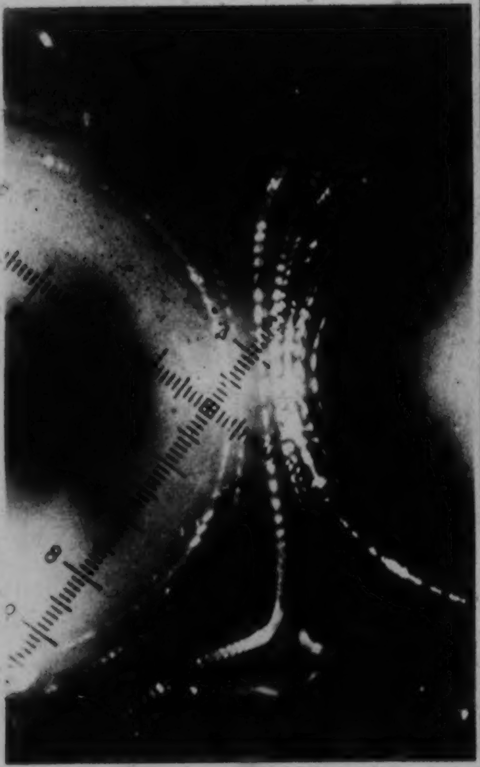

Photograph No.5
q=0.685cc/sec

Flow Direction

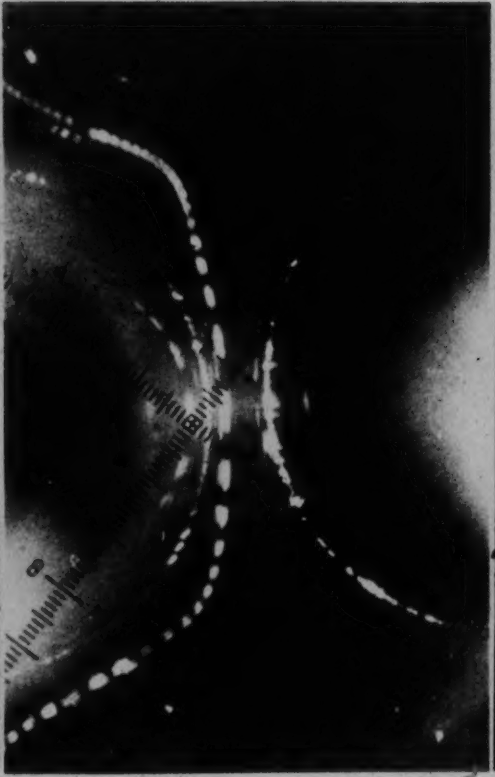

Photograph No.6
q=1.717cc/sec

Flow Direction

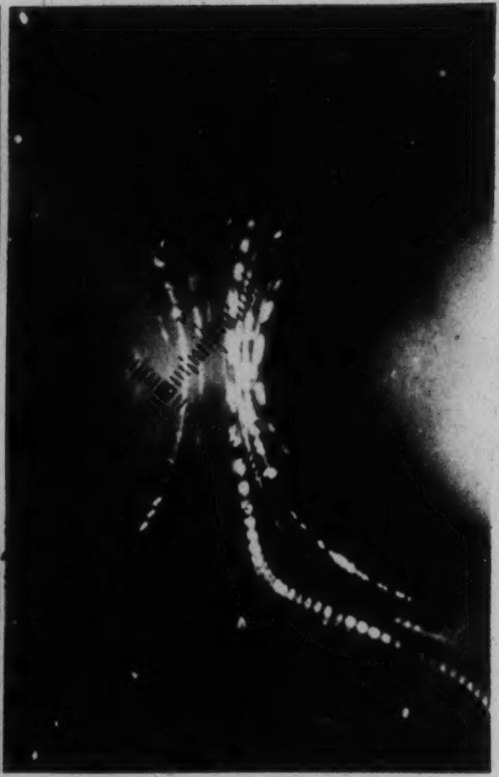

Photograph No.7
q=3.42cc/sec.

FIGURE IV-6 VISCOELASTIC FLOW PAST MULTI CYLINDERS – POSITION NO.25

passing through each opening was independent of the total flow rate through the bed. In other words, flow distribution remained the same for all sets of data. This suggests that by choosing a proper factor, the four sets of local velocity profiles could be superimposed. The data points of different flow rates are shown in the same plot in the Figures (IV-7) to (IV-12) by different symbols. For the sake of brevity, this has been performed only for one position of each row, namely positions No. 2, 17, and 27, and the velocity profiles of the other positions are not presented here.* In these plots projected streak length as measured directly from graph paper at the total magnification of 100 are plotted v.s. the position between two cylinders. However, the scale given in the plots has been chosen so that the profiles present the dimensionless interstitial velocity, i.e. u/V, v.s. position. The procedure to obtain the scale factor is discussed in Appendix C.

The total data points obtained in the present study was over 5000, but the complete set of data points are presented only for row No. 21 and minimum flow rate, i.e. q = 0.685 cc/sec and for one position of each row, namely positions 2, 17, and 27. Again, for the sake of brevity, only some of the data points are presented for the other positions and flow rates. These data points are recorded

---

*The complete set of plotted local velocity profiles is available from the Chemical Engineering Department, University of Alberta, Edmonton 7, Alberta, Canada.

Legend For Figures IV-7 To IV-12

△	q = 0.685 cc/sec.
□	q = 1.717 cc/sec.
○	q = 3.42 cc/sec.
▼	q = 6.82 cc/sec.
-----------	Eye-Fit Curve

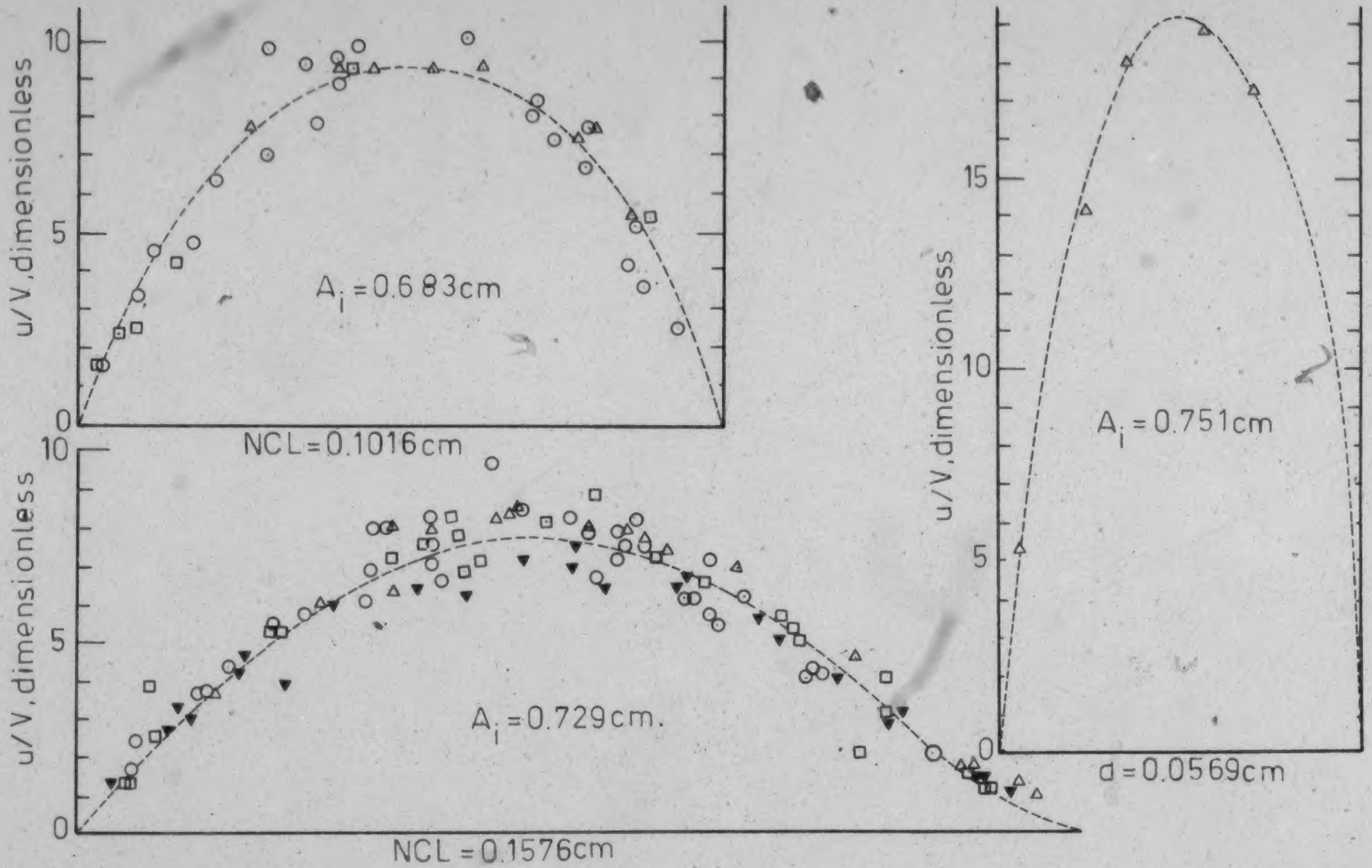

FIGURE IV-7 LOCAL VELOCITY PROFILES OF POSITION NO.2 — GLYCEROL

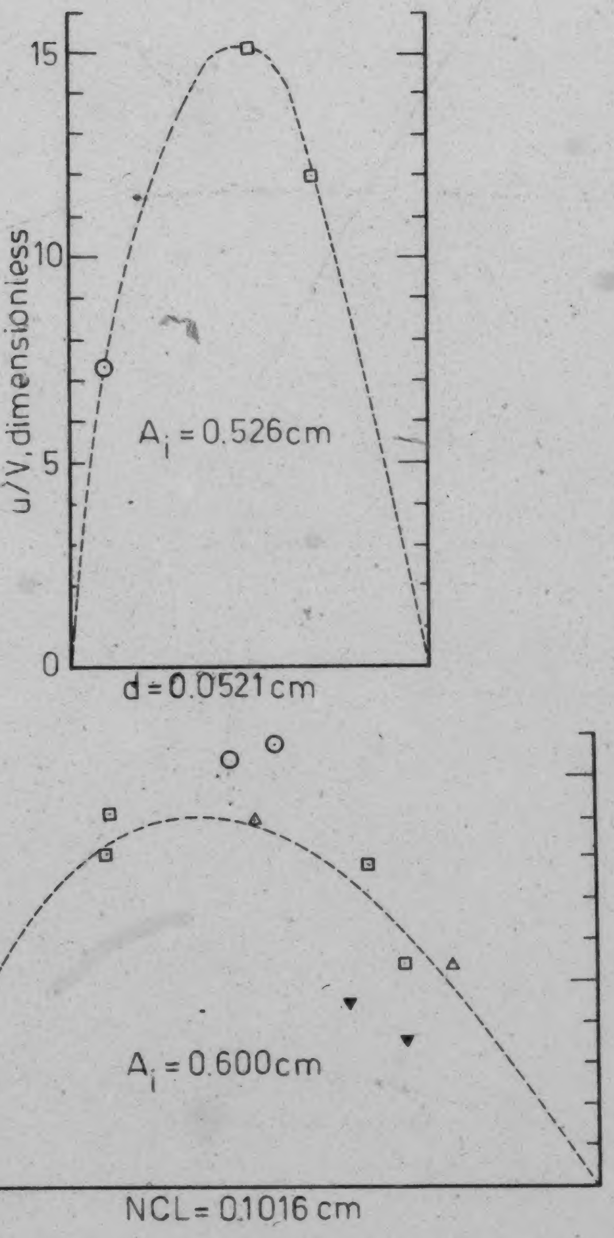

FIGURE IV-8 LOCAL VELOCITY PROFILES OF POSITION NO. 2 — SEPARAN

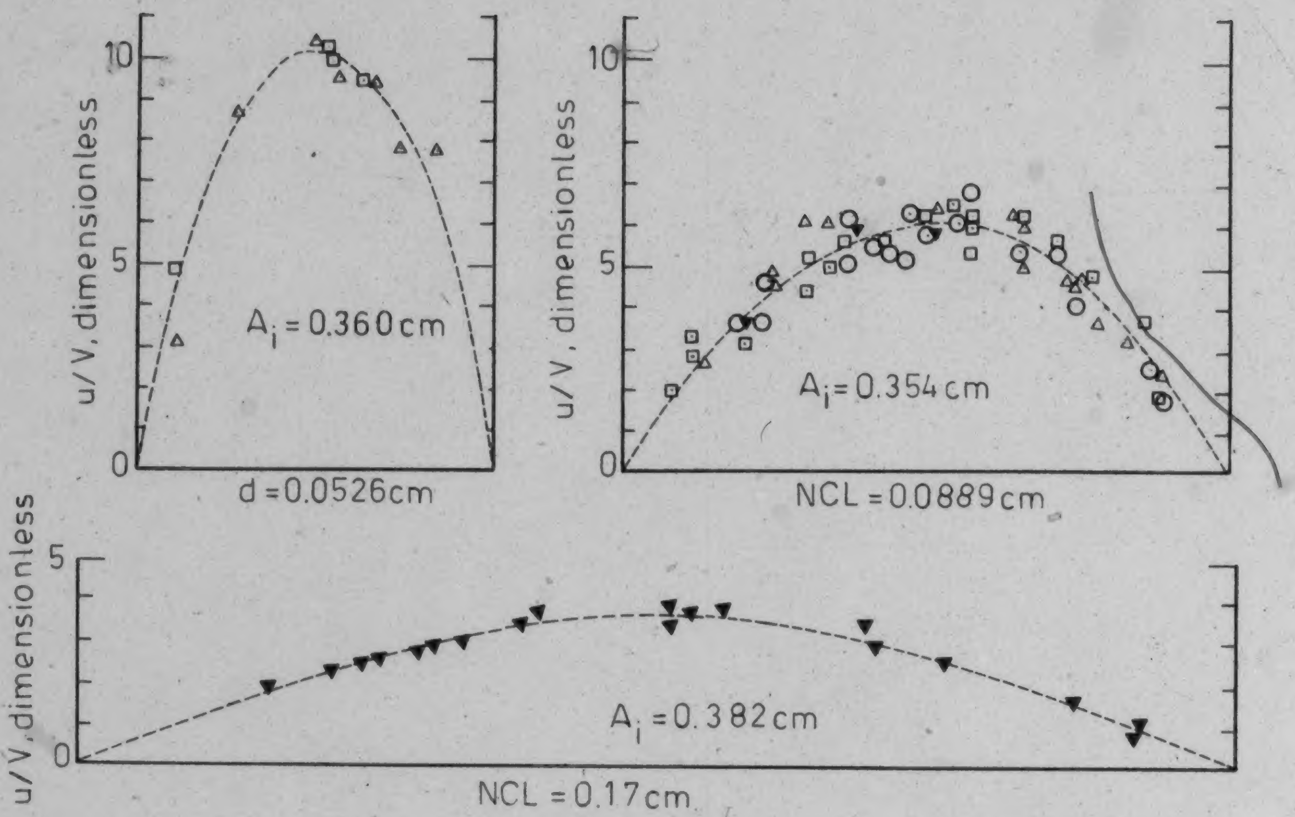

FIGURE IV-9 LOCAL VELOCITY PROFILES OF POSITION NO. 17 — GLYCEROL

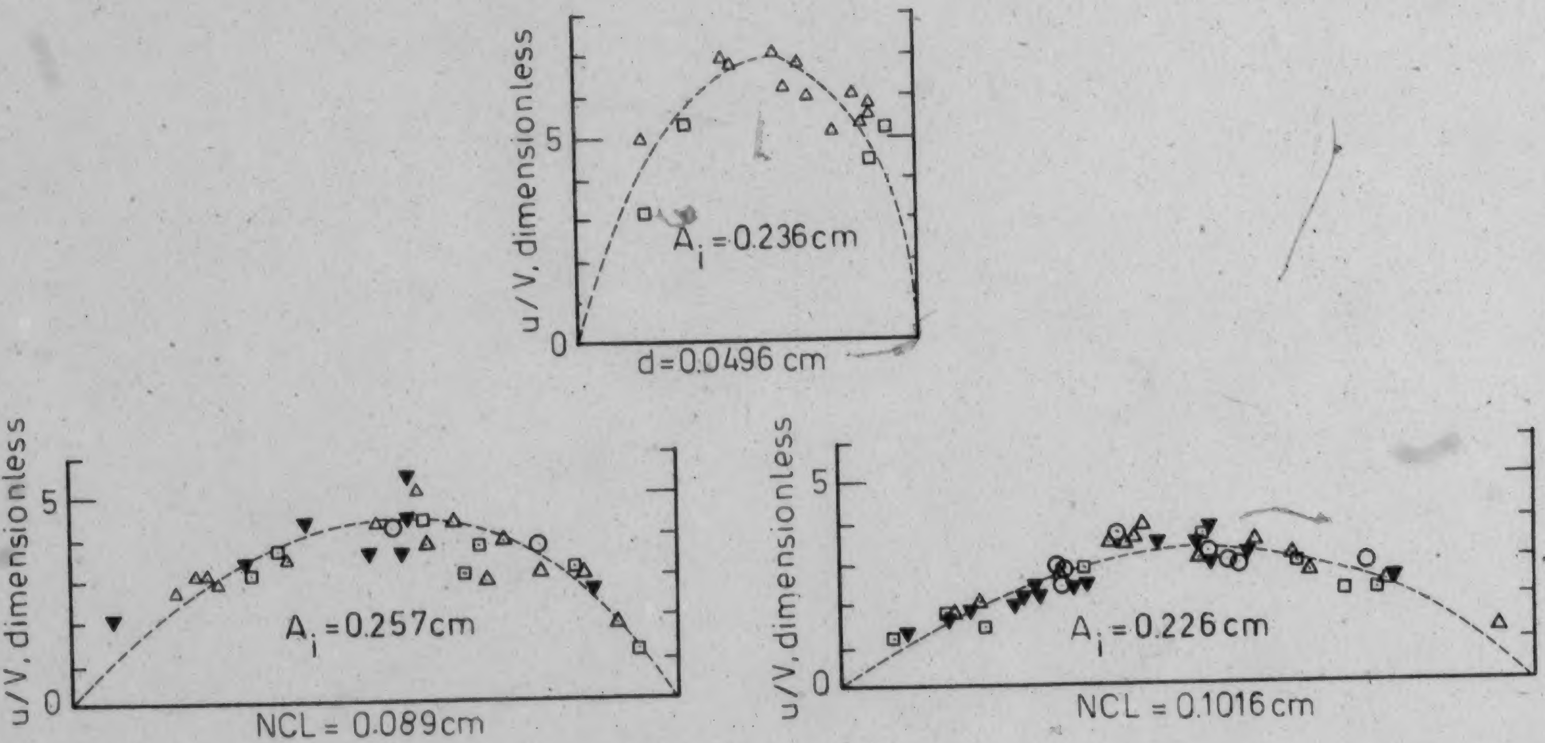

FIGURE IV-10 LOCAL VELOCITY PROFILES OF POSITION NO.17 — SEPARAN

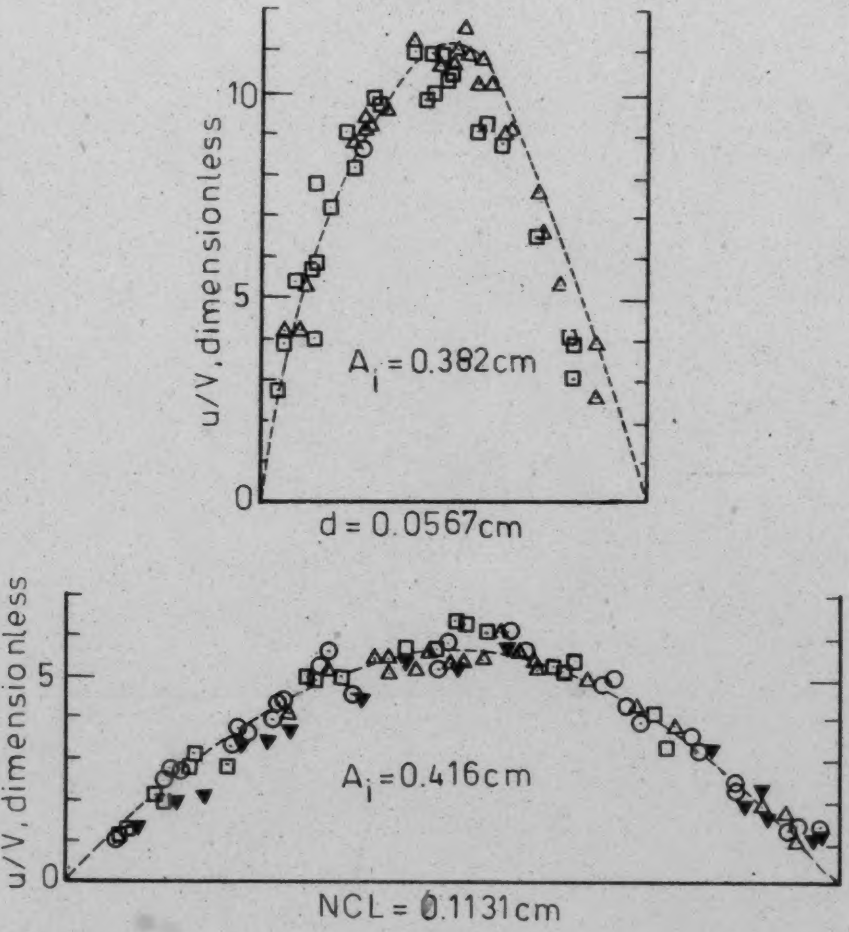

FIGURE IV-11 LOCAL VELOCITY PROFILES OF POSITION NO. 27 — GLYCEROL

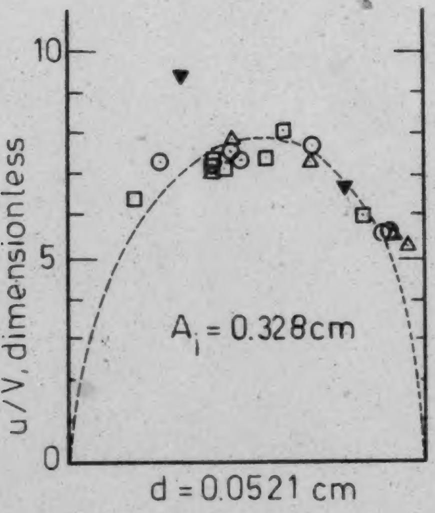

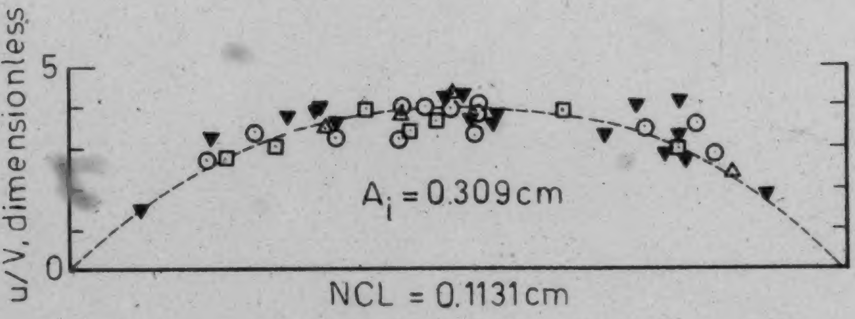

FIGURE IV-12 LOCAL VELOCITY PROFILES OF POSITION NO. 27 — SEPARAN

in Tables (E-1, 2).

The area under the local velocity profiles as well as the d's (i.e. center line openings) are given in Table (C-1). It is evident that the area under the velocity profile--in appropriate units--multiplied by the length of the cylinder gives the portion of the flow passing through that specific opening, no matter whether the velocity profile is chosen at d or NCL. This flow rate will be designated by q_i.

It should be noted from Table (C-1) that some of the values of d's of Glycerol solution runs are different from those of the polymer solution runs, although they were from the same positions. The reason is that, after the runs with polymer solution were completed, the system was taken apart and washed. Therefore, those glass rods which were not perfectly tight in their positions did not return to the same place as before. Also, as was mentioned in Section (III-1), the glass rods were not perfectly uniform; therefore, their relative positions could cause an increase or decrease in d. This, of course, occurred only for a few positions.

The maximum interstitial velocity occurs at the mid-point of d--assuming symmetry in local velocity profile which is not exactly so. Non-symmetry in experimental velocity profiles, which is evident from Figures (IV-7) to (IV-12), is due to nonhomogeneity of the bed. For the positions that the center line local velocity profile could not be obtained, the maximum velocities were calculated by

Equations (D-15,17). The calculated and also experimental values are presented in Table (V-3).

In Figure (IV-13) theoretical parabolic velocity profiles for the flow of Newtonian fluids through parallel plates are compared with experimental data points for three positions. To compare with experimental data points of polymer solution, the velocity profiles predicted from flow of a power-law fluid through parallel plates are also presented in Figure (IV-13). The Equations of these profiles are derived in Appendix D.

Legend:

○ Position No.13

▽ Position No.15

□ Position No.16

━━ Equation D-14

── Equation D-16

FIGURE IV-13 CENTERLINE VELOCITY PROFILE

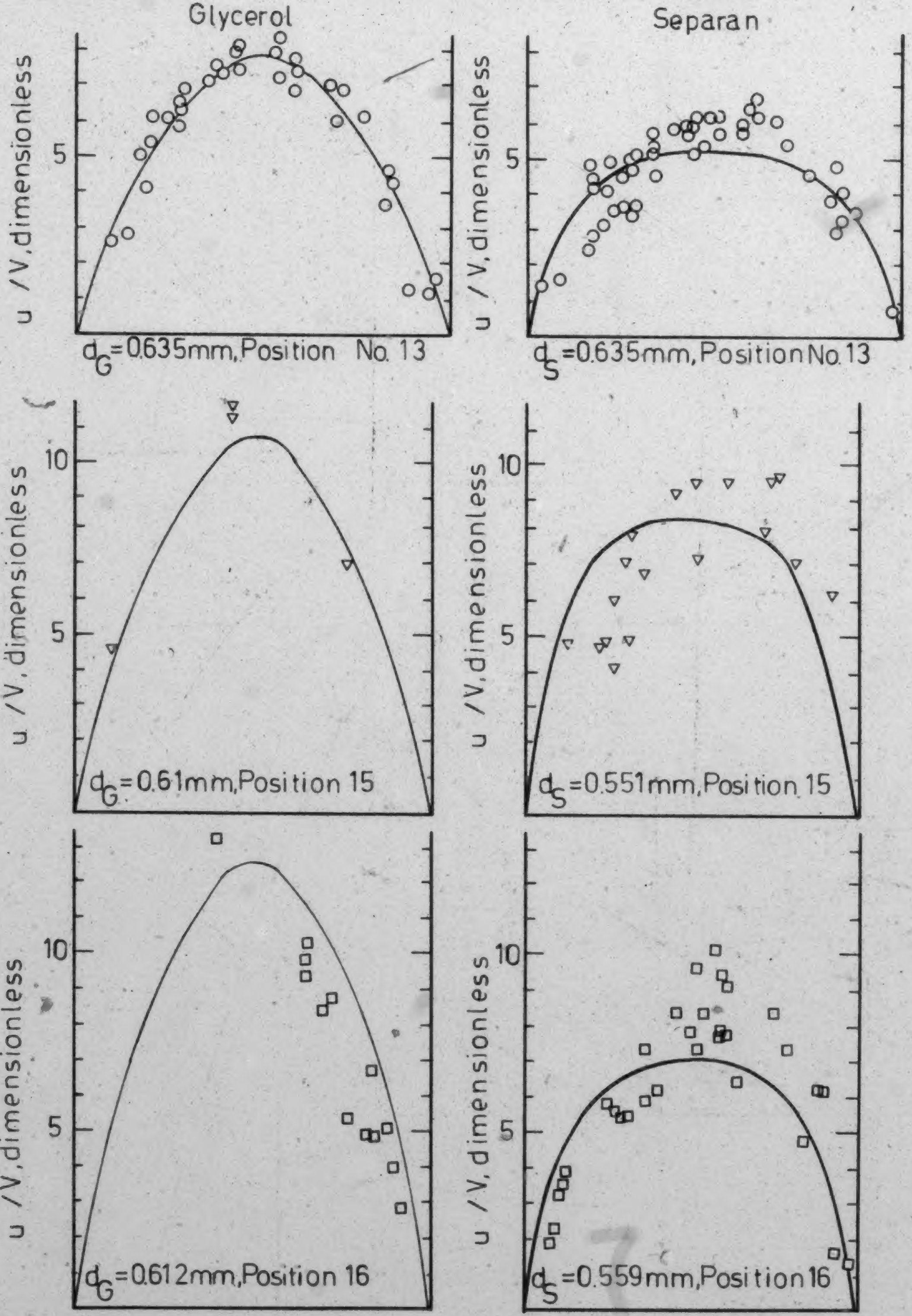

CHAPTER V

DISCUSSION OF THE RESULTS

V. 1 Pressure Drop

The linearity of the pressure drop with superficial velocity is evident from Figure (IV-1) which suggests the applicability of Darcy's law, i.e. Equation (I-4). Except for the water data the empirical correlation of Bergelin, et al. (58) to predict the pressure drop across an ideal bank of tubes is in excellent agreement with the data. The calculations and use of this equation are given in detail in Appendix B. The water data are significantly higher than the predicted line. Since this is simply a Newtonian fluid it is expected inertial effects cause the discrepancy. Although the value of Reynolds number at which inertial effects become important cannot be uniquely defined for different porous media (14b), the particular value for a given media can be determined by experiments over a sufficiently large range of flow rates. Thus the Newtonian data as plotted on Figure IV-3 show that inertial effects become significant at a Reynolds number (defined by Equation II-41) of order unity.

Assuming the flow of the polymer solution is pure viscous, Equation (I-5) which is equivalent to (II-36) can be applied. That is the slope of ΔP v.s. V on log-log coordinates is equal to the power-law parameter, n. The pressure drop measurement v.s. flow rate for the polymer solution in Figure IV-2 indicates the pseudoplastic nature of the polymer solution. However, the slope varied from approximately 0.35 to 0.92 over the range of flow rates while the slope of the viscometric data ranges from 0.35 to 0.44 in Figure A-3. Note in Figure A-3 the best fit lines have been taken over two portions of the curve to define power-law parameters used in the calculations. This is of little consequence in that calculated parameters, such as Reynolds number are not very sensitive to the exact value of the slope. The large slope at high flow rates and the fact that the Reynolds number is significantly below that at which inertial effects are expected suggest elasticity effects are occurring. Thus predictions for the pressure drop of the polymer solution need to be limited to the lower flow rates.

Different approaches were tried to predict the pressure drop of polymer solution in the bed. First the modified capillary model discussed in Chapter II, then, the empirical correlation of Bergelin, et al. (58) with apparent viscosity was applied. For estimation of apparent viscosity Equation (B-38) was assumed to define the shear rate--refer to Appendix B. To predict P from Equation (I-5), one needs to estimate the viscosity level parameter, H. H for the present model is given by Equation (II-37) in which C_4 and K must be determined, experimentally, by a Newtonian fluid. In Section (IV-1) K was reported to be equal to 1.3×10^{-4} cm^2

and surface porosity for the present model is calculated from (II-21) to be,

$$\varepsilon_s = 0.134. \qquad \text{(V-1)}$$

This value is the arithmetic average of two consecutive rows, one without by-pass channel and the other with two by-pass channels near the walls. The values of K and ε_s were used in Equation (II-30) to calculate C_4.

$$C_4 = 0.682, \qquad \text{(V-2)}$$

The calculated pressure drop together with H are recorded in Table (B-2) and the complete predicted curve of ΔP v.s. V is shown in Figure (IV-2).

In this approach the openings of parallel plates are taken equal to the minimum center line openings, d. This gives the highest possible value for a characteristic shear rate, therefore, smallest value for viscosity. In view of Equation (I-5), which is equivalent to (II-36), this gives the lowest possible value for ΔP. In fact, in the bed, there is a range of values of viscosity which occur and, therefore, the bed would have a somewhat higher value of average viscosity, and consequently ΔP, than the minimum which comes from the analysis. This problem does not occur for Newtonian; because, μ is constant. In terms of $f_K - N_{Re}$, the low value of viscosity causes higher N_{Re} which makes the data points of Separan systematically shift to the right of Newtonian in Figure (IV-3).

To further show the possibility of elasticity effect, Deborah number was calculated. Deborah number was defined in Section (I-3) and is rewritten in the following form,

$$N_{Deb} = 2\Theta_f \frac{\partial u_z}{\partial z} . \qquad \text{(V-3)}$$

Referring to the geometry of the bed $\partial u_z/\partial z$ can be estimated via maximum velocity at center line openings. According to Figure (V-1),

$$\frac{\partial u_z}{\partial z} = \frac{\bar{u}_{max} - 0}{\Delta z} = \frac{\bar{u}_{max}}{\Delta z} . \qquad \text{(V-4)}$$

Δz is approximately 0.33 cm for the present model and $\bar{u}_{max}$ is the average value of the maximum velocities at center line openings for two consecutive rows. To be on the conservative side, the shear dependent relaxation time was used for Θ_f which was read from Figure (A-4). This required shear rate to estimate Θ_f. The value of shear rate occurring at the minimum opening is of the order of,

$$\sigma = \frac{u_m}{d/2} = \frac{2u_m}{d} , \qquad \text{(V-5)}$$

and,

$$u_m = \frac{q_i}{d\ell} . \qquad \text{(V-6)}$$

Therefore,

$$\sigma = \frac{2q_i}{\ell d^2} . \qquad \text{(V-7)}$$

Recorded values of σ in Table (V-1) are the arithmatic average value of two consecutive rows. That is q_i/d^2 at a given flow in the bed has been averaged for opening in

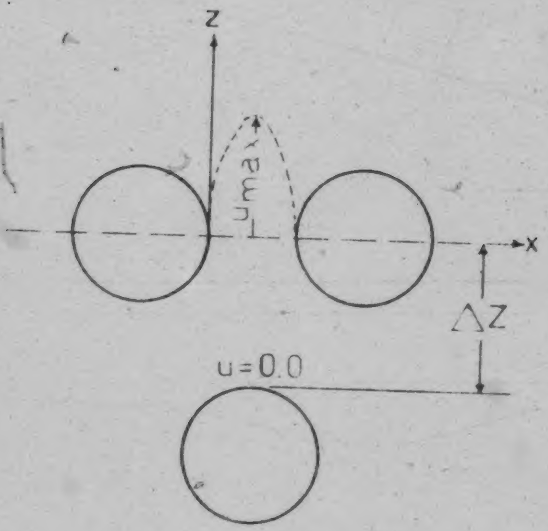
z
umax
x
ΔZ
u=0.0

FIGURE V-1 ESTIMATION OF ELONGATIONAL RATE

TABLE (V-1)

FLOW PARAMETERS OF 0.2% SEPARAN SOLUTION

RUN NO.	q cc/sec	σ sec^{-1}	Θ sec.	$\bar{u}_{max}$ cm/sec	$\partial u_z/\partial z$ sec^{-1}	N_{Deb} Dimensionless	$f_K x N_{Re}$ Dimensionless
1	0.431	3.09	0.68	0.113	0.337	0.458	1.33
2	0.685	4.91	0.47	0.18	0.537	0.505	1.31
3	0.835	6	0.4	0.219	0.654	0.523	1.31
4	1.07	7.68	0.33	0.281	0.839	0.554	1.16
5	1.49	10.7	0.25	0.392	1.17	0.585	1.228
6	1.717	12.3	0.24	0.451	1.343	0.645	1.262
7	2.13	15.28	0.19	0.56	1.67	0.634	1.278
8	2.17	15.58	0.18	0.57	1.7	0.612	1.317
9	2.725	19.55	0.15	0.716	2.137	0.64	1.29
10	3.39	24.3	0.13	0.899	2.68	0.697	1.3
11	3.42	24.55	0.13	0.899	2.68	0.697	1.31
12	4.27	30.6	0.11	1.122	3.35	0.737	1.41
13	4.28	30.6	0.11	1.122	3.35	0.737	1.336
14	5.38	38.55	0.089	1.422	4.24	0.755	1.388

TABLE (V-1) (continued)

RUN NO.	q cc/sec	σ sec^{-1}	Θ sec.	$\bar{u}_{max}$ cm/sec	$\partial u_z/\partial z$ sec^{-1}	N_{Deb} Dimensionless	$f_K \times N_{Re}$ Dimensionless
15	5.41	38.8	0.089	1.422	4.24	0.755	1.388
16	5.76	48.4	0.073	1.8	5.37	0.785	1.418
17	6.84	49.1	0.073	1.8	5.37	0.785	1.51
18	8.53	61.1	0.061	2.255	6.72	0.82	1.267
19	8.58	61.6	0.061	2.255	6.72	0.82	1.35
20	10.76	77.1	0.051	2.85	8.5	0.867	1.31
21	10.84	77.7	0.051	2.85	8.5	0.867	1.41
22	13.6	97.7	0.042	3.58	10.69	0.897	1.34
23	13.62	97.7	0.042	3.58	10.69	0.897	1.445
24	17.06	122.2	0.035	4.51	13.43	0.94	1.476
25	17.19	123	0.035	4.51	13.43	0.94	1.517
26	21.52	154	0.029	5.65	16.85	0.976	1.586
27	27.25	195.8	0.024	7.16	21.37	1.023	1.76
28	34.35	246	0.02	9.02	26.9	1.076	1.968

the two rows.

Calculated Deborah numbers are presented in Table (V-1). According to Marshall and Metzner (45), the magnitude of Deborah number is high enough to expect significant elasticity effect. As mentioned in Section (I-3), Marshall and Metzner revealed that appreciable influences of the fluid elasticity were observed when Deborah number, defined by Equation (I-13), reached 0.05-0.06 or, defined by Equation (V-3), reached 0.2-0.24. It is noted that Deborah number defined by Equation (V-3) is four times as large as that of Equation (I-13).

In Figure (V-2), $f_K N_{Re}$ was plotted v.s. Deborah number for polymer solution. The upward deviation of the data points at high flow rates, is similar to that observed by Marshall and Metzner (45), although the analysis is not sufficient to indicate when this might occur in the figure.

V. 2 Streamlines

The elasticity effect predicted by Ultman, et al. (42) in the flow past a submerged cylinder is obviously present in photograph No. 1 in Figure (IV-4). The early bulge of the upstream streamlines, the earlier return to undisturbed flow downstream of the rod and the non-symmetry of the flow are characteristic behavior of viscoelastic fluid flow past a submerged cylinder. The approach velocity which was calculated from the length of streaks was U=0.437 cm/sec.

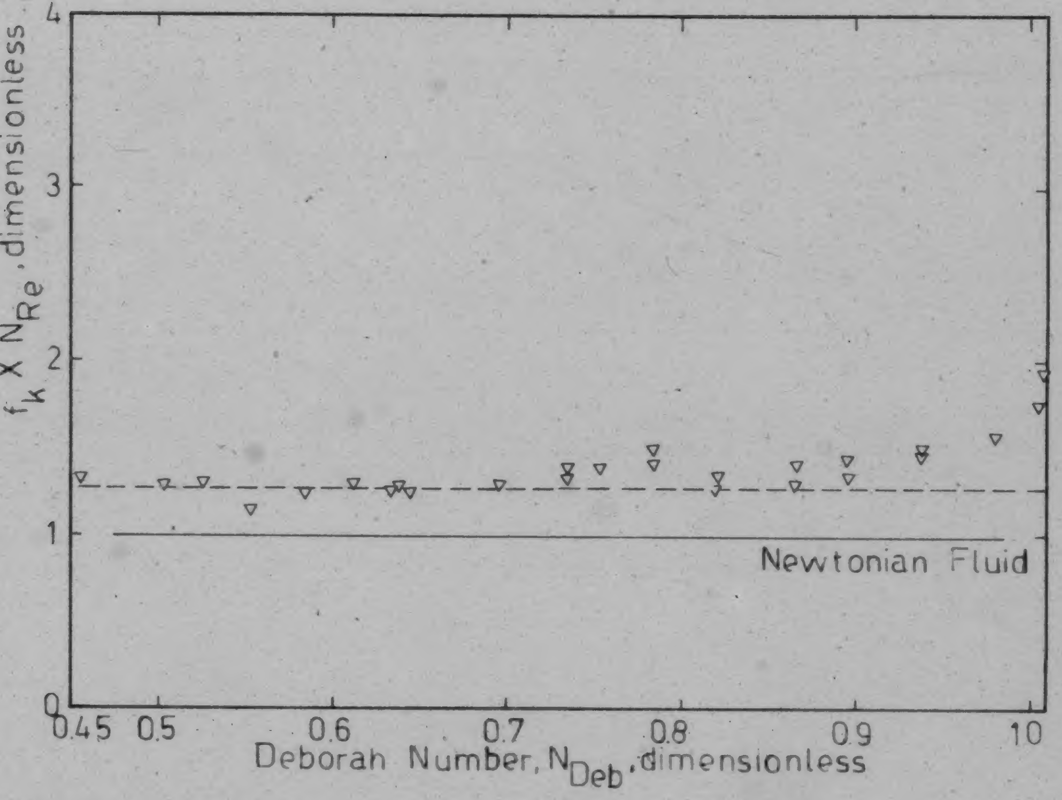

FIGURE V-2 DEPENDENCE OF ELASTICITY EFFECT UPON THE DEBORAH NUMBER OF THE FLOW PROCESS

Reynolds number is defined as,

$$Re_c = \frac{\rho UD}{\mu_o} , \tag{V-9}$$

where density, $\rho = 1$, diameter of the rod, $D = 0.326$ cm, and $\mu_o = 42$ poise is the limit of viscosity at low shear rate. Therefore,

$$Re_c = 0.00339. \tag{V-10}$$

also, Weissenberg number is calculated by Equation (I-11) in which to be consistent with Ultman, et al. (42), $\Theta_o = 3.126$ sec was estimated from Bueche's theory, i.e. Equation (A-6). Therefore,

$$N_{we} = 4.19. \tag{V-11}$$

To compare the situation prevailing in the submerged bank of rods with that of single submerged rod, the following justification is made. The average velocity at the center line opening is taken as the approach velocity,

$$U \equiv u_m = \frac{q}{A\varepsilon_s} . \tag{V-12}$$

The flow rates studied varied from 0.685 to 6.85 cc/sec, therefore, approach velocities varied from $U = 0.151$ cm/sec to 1.51 cm/sec. The other parameters remained the same. Therefore,

$$Re_c = 0.00216 \text{ to } 0.0216, \tag{V-13}$$

$$N_{we} = 0.787 \text{ to } 7.87. \tag{V-14}$$

By comparing the Reynolds and Weissenberg numbers of bank of glass rods with those of single rod, it was felt that the range of flow rates studied was broad enough to cover any elasticity effects observable in the shape of the streamlines.

The initial goal of photographic study was to seek if the bulge effect for the polymer solution would be intensified by the presence of the other rods. The behavior could be, hopefully, related to the increased microscopic sweep efficiency in polymer flooding. However, on observation of streamlines in the bed it was apparent that simple determination of the streamlines would not clearly show the major differences in flow field of the two fluids. Therefore, the direction of study was changed and focused on local velocity profiles and flow distribution.

V. 3 Visual Observations

Visual observations were limited to the positions along rows 19 to 23 for Glycerol and Separan. The flow rates studied were q = 0.685, 1.717, 3.42 and 6.85 cc/sec. The observations at points where the flow was anomalous revealed some significant differences between Newtonian and polymer solution. The positions where anomalous behavior occurred with the description of the peculiarity are given in Figures (V-3, 4). These positions are where no flow exists, i.e. dead zones, flow is slow compared to the normal neighborhood openings, or the flow is in the opposite direction of the normal flow direction. It is noticed from Figures (V-3, 4) that the number of anomalous points for Newtonian fluid are 15 while those from polymer solution are only 5. The observed difference, especially the number of dead zones or nearly dead zones, might be a good qualitative explanation of the increased microscopic sweep efficiency in polymer flooding. These points were usually near the walls where by-pass flow existed, however, this situation is not unexpectable in the oil reservoir fields.

The above observed distinguished difference imply that the streamlines are not the same for Glycerol and Separan solutions. This is also revealed in section (V. 4) by observing the difference in flow distribution.

V. 4 Local Velocity Profiles and Flow Distribution

It is clearly observed from Figures (IV-7) to (IV-12) that the local velocity profiles were not the same in the different openings. That is the small

DESCRIPTION OF ANOMALOUS BEHAVIOR

1. Very small flow in the opposite direction of the normal flow direction at q=0.685, 1.717, 3.42, and 6.85 cc/sec.

2 Very small flow at q=0.685 cc/sec.

3. Same as (1).

4. Same as (1)

5. Same as (1).

6. Almost no flow at q=0.685, 1.717 cc/sec. and same as (1) at q=3.42, 6.34 cc/sec.

7. Almost no flow at all four flow rates.

8. Same as (7).

9. Same as (1).

10. Very small flow at all four flow rates.

11. Same as (10).

12. Same as (2).

13. Same as (1).

14. Same as (10).

15. Same as (10).

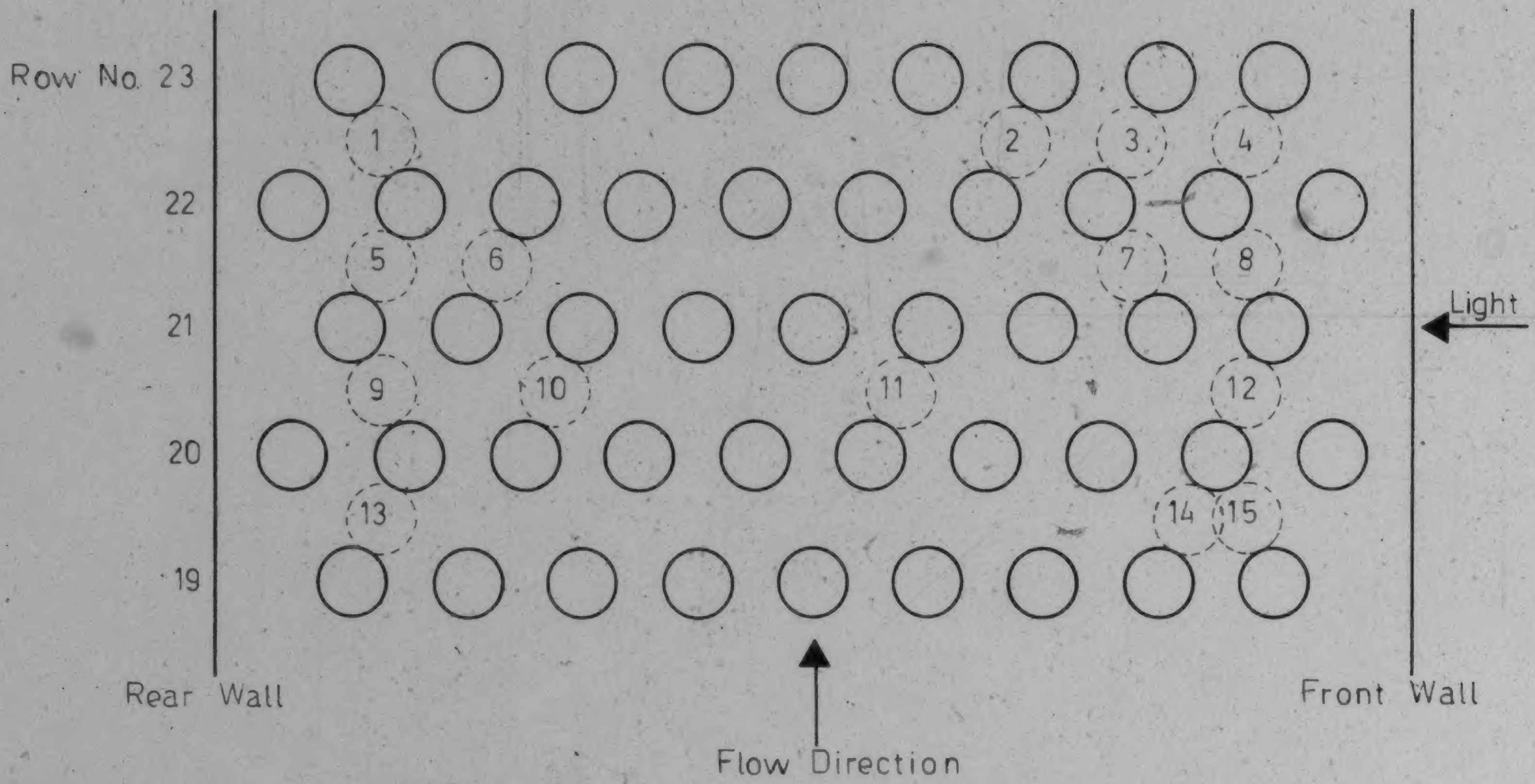
Row No. 23
22
21
20
19
1
2
3
4
5
6
7
8
9
10
11
12
13
14
15
Light
Rear Wall
Front Wall
Flow Direction

FIGURE V-3 VISUAL OBSERVATION - GLYCEROL

DESCRIPTION OF ANOMALOUS BEHAVIOR

1. Almost no flow at q=0.685 cc/sec. and very small flow at q=1.717, 3.42, and 6.85 cc/sec.
2. Very small flow in the opposite direction of the normal flow direction at q=0.685, 1.717, 3.42 and 6.85 cc/sec.
3. Almost no flow at q=0.685, 1.717 cc/sec. and very small flow at q=3.42, 6.85 cc/sec.
4. Very small flow at q=0.685, 1.717, 3.42, and 6.85 cc/sec.
5. Almost no flow at q=0.685, 1.717, and 3.42 cc/sec. and very small flow at q=6.85 cc/sec.

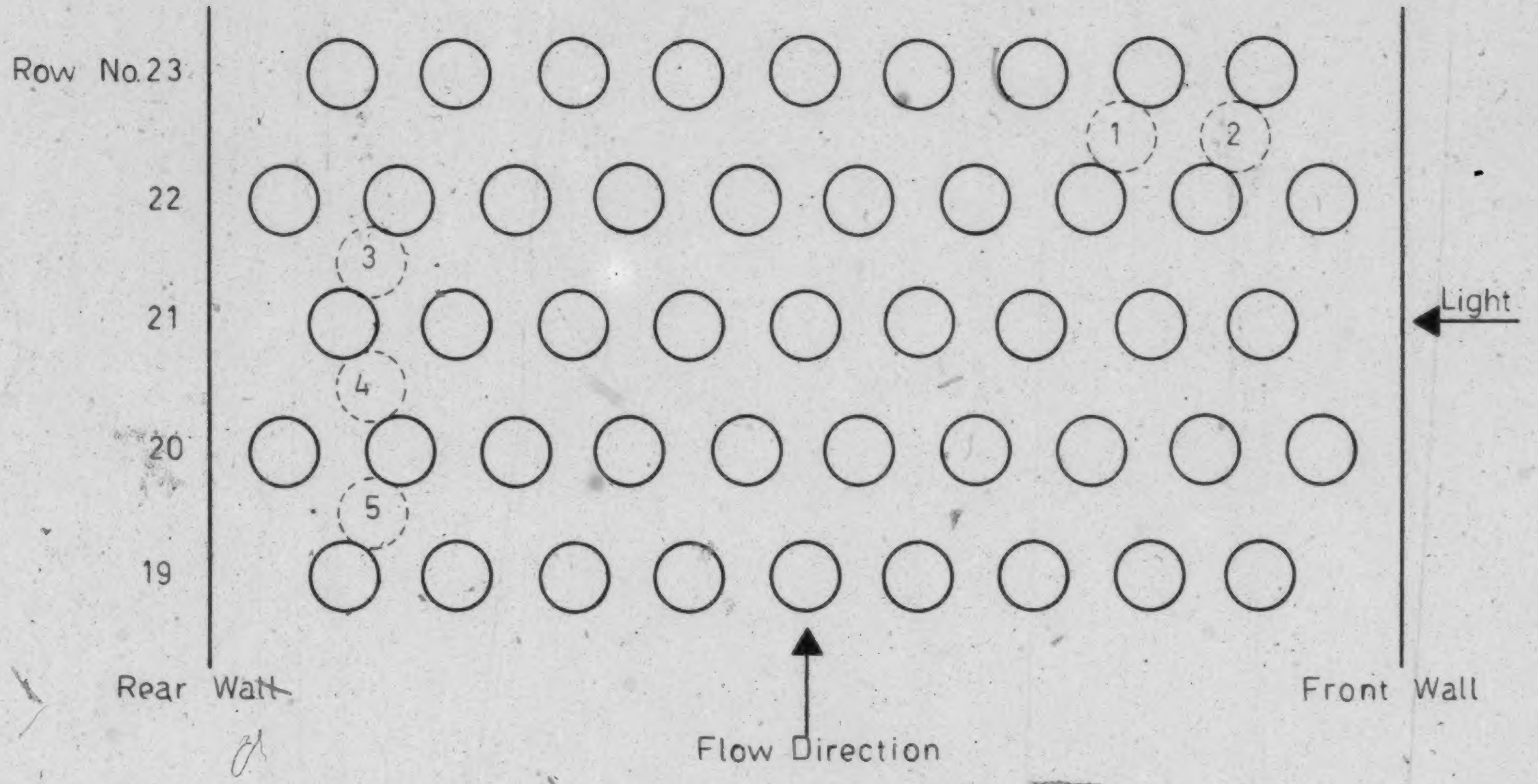
Row No.23
22
21
20
19
1
2
3
4
5
Light
Rear Wall
Front Wall
Flow Direction

FIGURE V-4 VISUAL OBSERVATION - SEPARAN

inhomogeneity of the bed caused significant differences in velocity profiles. Also, the local velocity profiles of glycerol show larger differences between positions than those of Separan. This shows that the nonhomogeneity has less effect on polymer solution than Newtonian. To emphasize the differences in flow distribution, the maximum velocities at the center line openings of rows 20, 21 and 22 are plotted against position for Glycerol and Separan solutions in Figures (V-5) to (V-7). The maximum velocities of the positions which could not be determined directly--due to the difficulty involved in photography at the center line positions--were calculated by Equations (D-15, 17). The justification for this can be found in Table (V-2) where the predicted and experimental maximum velocities are compared. In all cases, except one or two, quantitative agreement was obtained. No usable pictures could be taken from position No. 3 of polymer solution runs--neither at center line nor at NCL. The flow rate through this position was calculated by subtracting the sum of the flow rates passing the other openings of row No. 20 from the total flow rate.

From Figures (V-5) to (V-7) it is clear that there is a greater variation in velocity at the center of the openings with glycerol than with Separan. It should be noticed that the value of u_{max}/V for position No. 3 in Figure (V-5) as

TABLE V-2

MAXIMUM VELOCITIES AT CENTER LINE OPENINGS

u_{max}/V, DIMENSIONLESS

Position No.	Glycerol Calc.	Exp.	Separan Calc.	Exp.
1	23.5	?	31.1	?
2	18.65	18.5	14.2	14.66
3	14.16	?	5.42	?
4	12.7	?	10.76	?
5	11.4	?	8.64	?
6	14.8	?	8.3	9.16
7	10.56	10.28	8.14	8.63
8	12.1	12.32	7.27	8.05
9	16.9	17.1	9.82	10.28
10	13.4	13.14	12.9	?
11	16.93	?	10.7	?
12	6.92	6.57	7.9	8.64
13	7.62	7.6	5.06	6.16
14	10.56	?	7.52	?
15	10.28	11.1	8.35	9.25
16	12.1	12.33	6.57	8.22
17	10.02	9.86	6.29	6.57
18	15.53	14.8	8.06	9.45
19	7.56	?	6.82	7.97
20	6.9	?	6.82	7.4

TABLE V-2 (continued)

Position No.	Glycerol Calc.	Exp.	Separan Calc.	Exp.
21	4.89	4.11	3.8	3.9
22	24.5	?	34.6	?
23	21	?	25	?
24	10	10	6.95	8.85
25	16.55	16.24	8.85	9.87
26	11.36	10.78	6.42	7.82
27	10.4	10.7	7.53	7.82
28	10.7	10.28	6.79	8.1
29	16.03	?	8.24	9.17
30	15.06	?	8.64	10.17
31	13.54	13.6	12.7	?
32	17.5	?	17.4	?

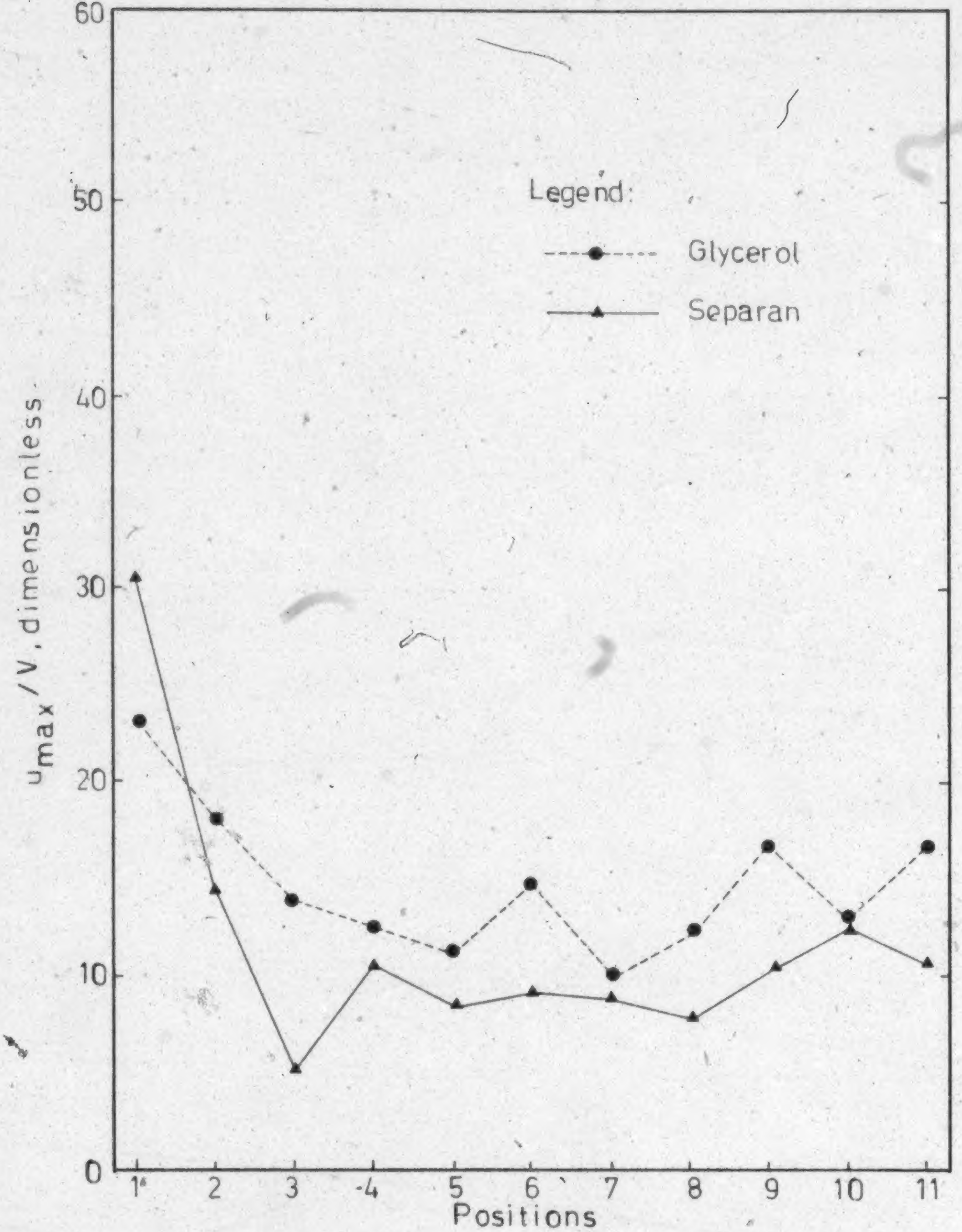

FIGURE V-5 MAXIMUM CENTER LINE VELOCITIES
ROW NO.20

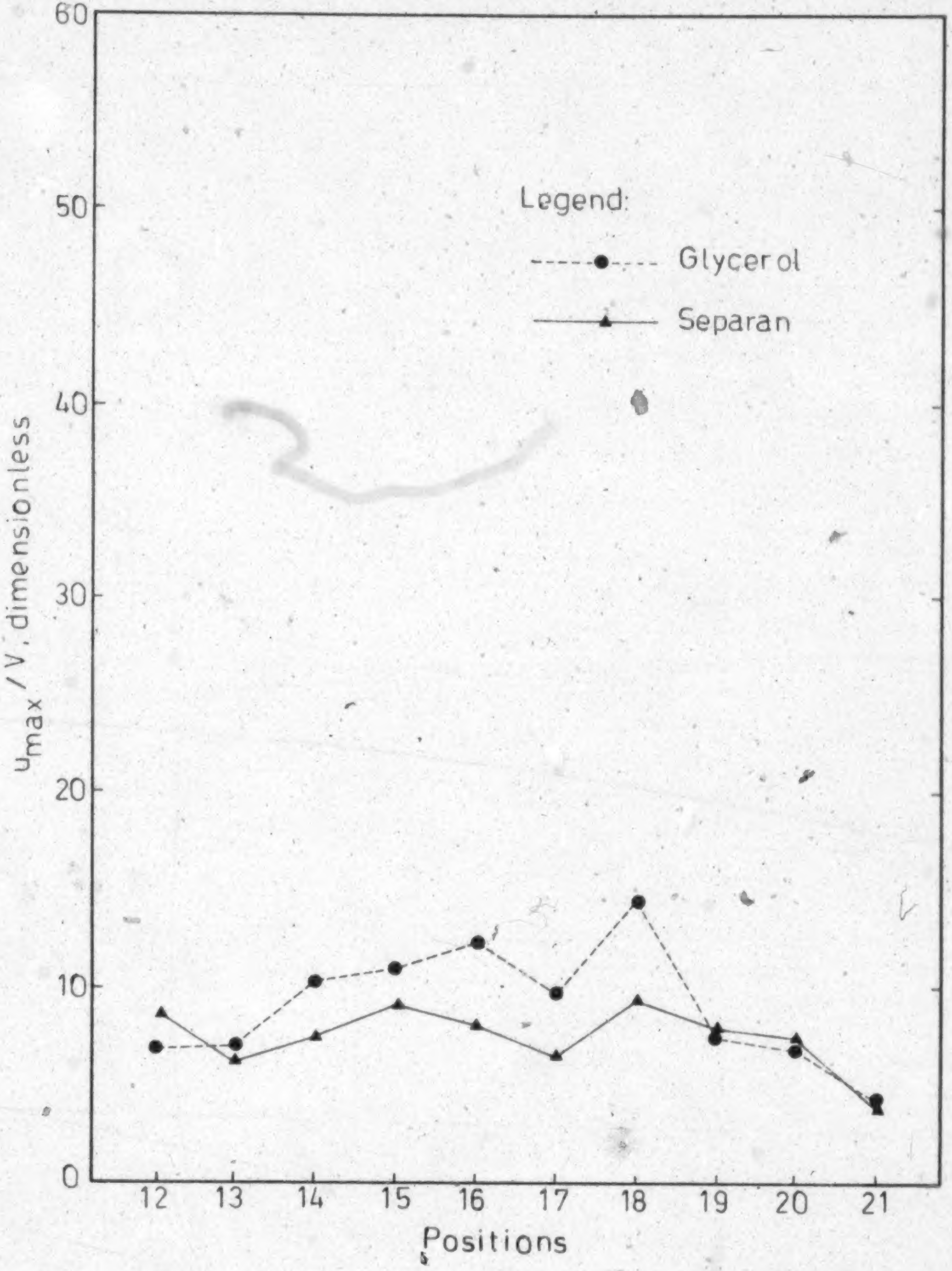

FIGURE V-6 MAXIMUM CENTER LINE VELOCITIES
ROW NO.21

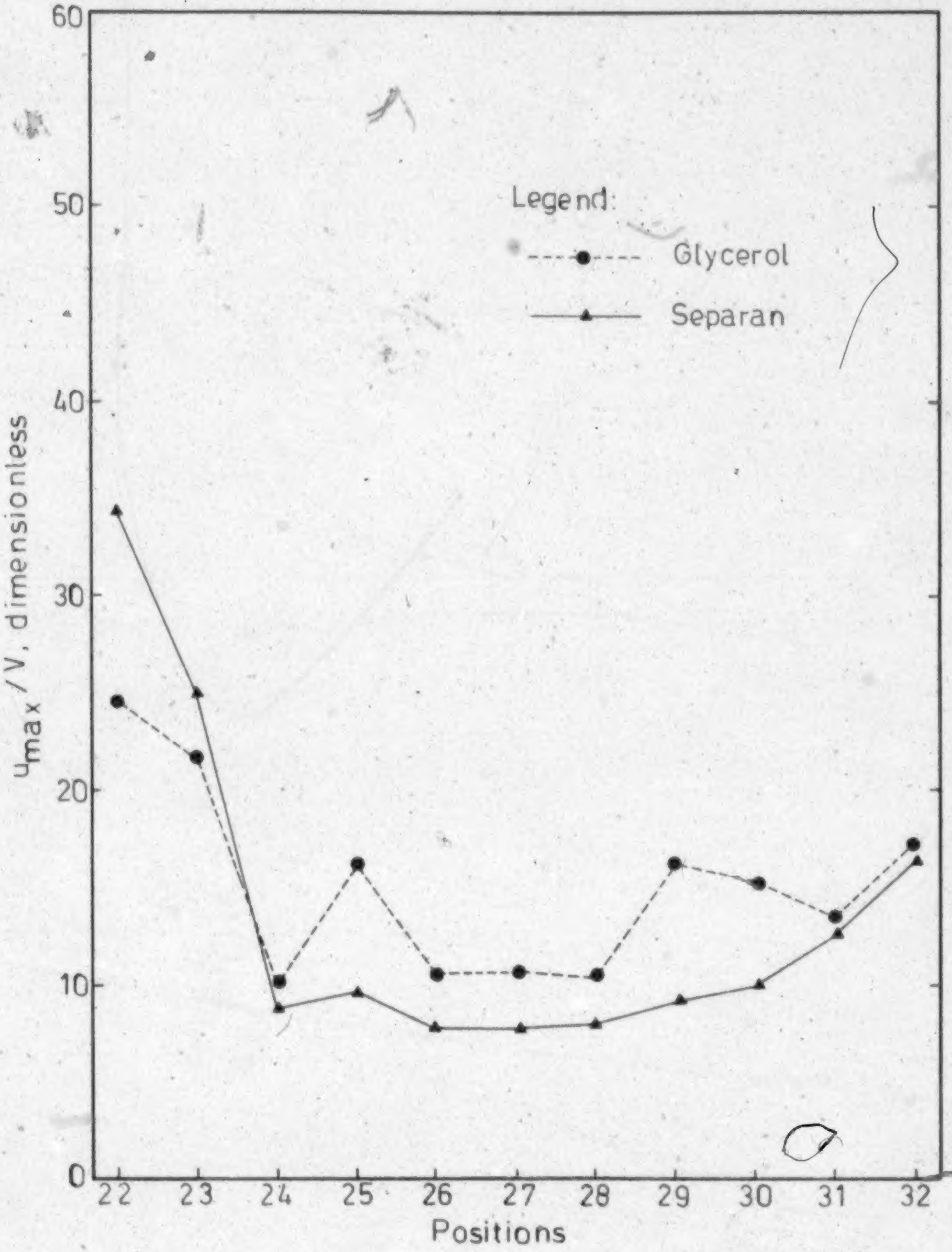

FIGURE V-7 MAXIMUM CENTER LINE VELOCITIES ROW NO. 22

mentioned before is uncertain. Also, as was mentioned before, the openings of some positions have changed from Glycerol runs to Separan which makes a detailed position by position comparison without accounting for the openings invalid.

The three curves of maximum velocities were added together to find the final resultant. They are presented in Figures (V-8, 9). Again, same kind of behavior observed for the single row in Figures (V-5, 6, 7) is noticed. The resultant curve for Separan in Figure (V-9) is much smoother than that for Glycerol in Figure (V-8). To clarify the qualitative conclusion derivable from Figures (V-8, 9), let us assume a straight undisturbed line of fluid particles before row No. 20. The shape of this line of fluid particles after passing through rows No. 20, 21 and 22 would be, roughly, the resultant curve--assuming that the major disturbances were at the minimum center line openings.

It is also shown from Figures (V-5, 6, 7) that the flow rate passing through positions 1, 12 and 22, which are next to the wall, are significantly larger for the case of Separan than those of Glycerol. The increase in by-pass flow should not only be attributed to the wall effect, but the relative magnitude of the openings next

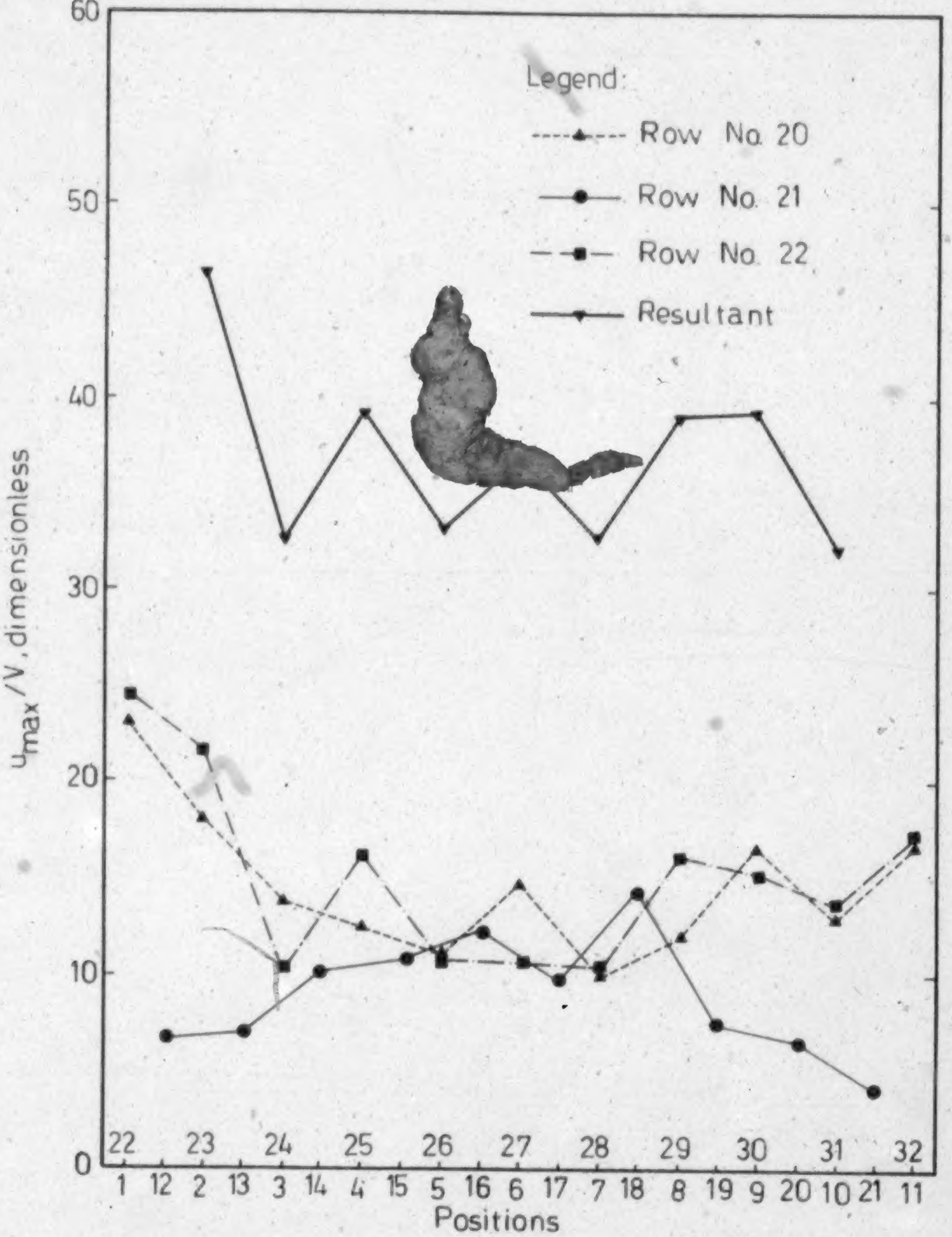

FIGURE V-8 RESULTANT OF MAXIMUM CENTER LINE VELOCITIES OF THREE ROWS - GLYCEROL

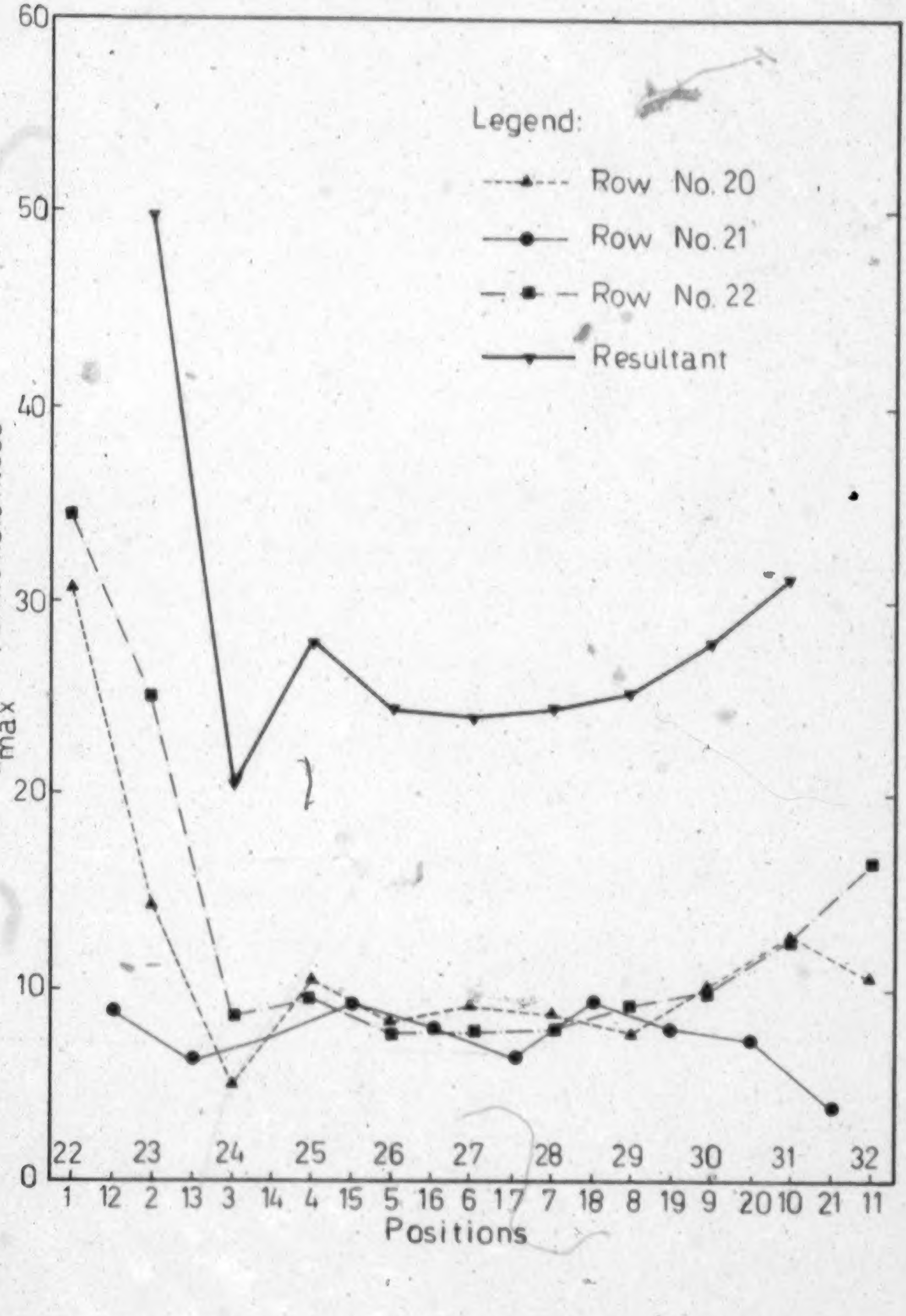

FIGURE V-9 RESULTANT OF MAXIMUM CENTER LINE VELOCITIES OF THREE ROWS - SEPARAN

to the walls and also the effect of the other neighborhood openings.

To eliminate the effect of by-pass flow, the following procedure was undertaken. Positions 1, 2, 10, 11, 12, 13, 21, 22, 23, 31 and 32 which were near the walls were ignored. The flow rates of the remaining openings of each row were added together. Then the percentage of this total flow rate passing through each opening of a row was calculated. These values will be referred to as "corrected fractional flow rates", f. This procedure makes it also possible to compare, quantitatively, the flow rates of the individual openings in different rows. Since every alternate row has two by-pass openings and more flow rate will pass from these openings, therefore, less flow would be available for the openings far from the walls comparing with the openings of those rows without by-pass channel. However, by applying the above procedure, all the remaining openings of the three rows are scaled up on the same basis. Corrected fractional flow rates are recorded in Table (V-3), but fractional flow rates without applying by-pass correction are presented in Table (C-1).

An attempt was made to find the behavior of flow

TABLE (V-3)

CORRECTED FRACTIONAL FLOW RATES

Position No.	d_G/d_{min} Dimensionless	d_S/d_{min} Dimensionless	f_G Dimensionless	f_S Dimensionless
3	1.54	1.54	12.7	?
4	1.74	1.38	12.8	15.14
5	1.71	1.48	11.32	12.9
6	2.03	2.03	17.5	17.1
7	1.66	1.66	10.2	13.65
8	1.73	1.73	12.1	12.77
9	2.38	2.01	23.4	20
14	2	2	15.5	17.1
15	1.84	1.67	12.9	15.9
16	1.85	1.69	15.27	12.6
17	1.59	1.5	10.83	10.73
18	2.04	2.04	21.6	18.7
19	1.575	1.575	12.2	12.2

TABLE (V-3) (continued)

Position No.	d_G/d_{min} Dimensionless	d_S/d_{min} Dimensionless	f_G Dimensionless	f_S Dimensionless
20	1.645	1.645	11.6	12.77
24	1.69	1.69	10.5	12.6
25	2.03	2.03	20.8	19.3
26	1.64	1.54	11.57	10.57
27	1.71	1.58	11.07	12.78
28	1.54	1.54	10.23	11.3
29	2.04	2.04	20.36	18.1
30	1.65	1.65	15.44	15.3

distribution with respect to pore openings. Equation (D-8) predicts that the flow rate varies with opening to the power $(1 + 2n)/n$. Since $n < 1$, it is expected that the effect of openings is aggravated for pseudoplastic fluid compared to Newtonian in which $n = 1$. In Figures (V-10) and (V-11) corrected fractional flow rates for Glycerol and Separan, respectively, are plotted v.s. dimensionless openings, i.e. d/d_{min}, where $d_{min} = 0.33$mm is the minimum d from Table (C-1). The line with slope 3 is the theoretical equation for a Newtonian fluid through parallel plates, i.e. Equation (D-11), and the line with slope 4.5 in Figure (V-11) is presenting Equation (D-8) with $n = 0.4$. It is evident from Figures (V-10,11) that the effect of openings on polymer fractional flow rates is somewhat less than expected theoretically. Furthermore a line with slope even less than 3, probably, will fit the experimental data points of Separan.

Since the openings are coupled, i.e. the effect of the neighborhood openings can not be eliminated; therefore, the data points of Figures (V-10, 11) are expected to be scattered. However, f_G is a measure of local permeability and portrays the combined effect of the neighborhood openings. Since the fractional flow rates of Glycerol and Separan are directly proportional to local permeability, therefore, it is felt that a plot of f_G and f_s v.s. $f_G\, d_G/d_{min}$ and $f_G\, d_s/d_{min}$, respectively, will be less scattered. These are presented in Figures (V-12, 13). The eye-fit line passing through the points of Figure (V-13) has less slope

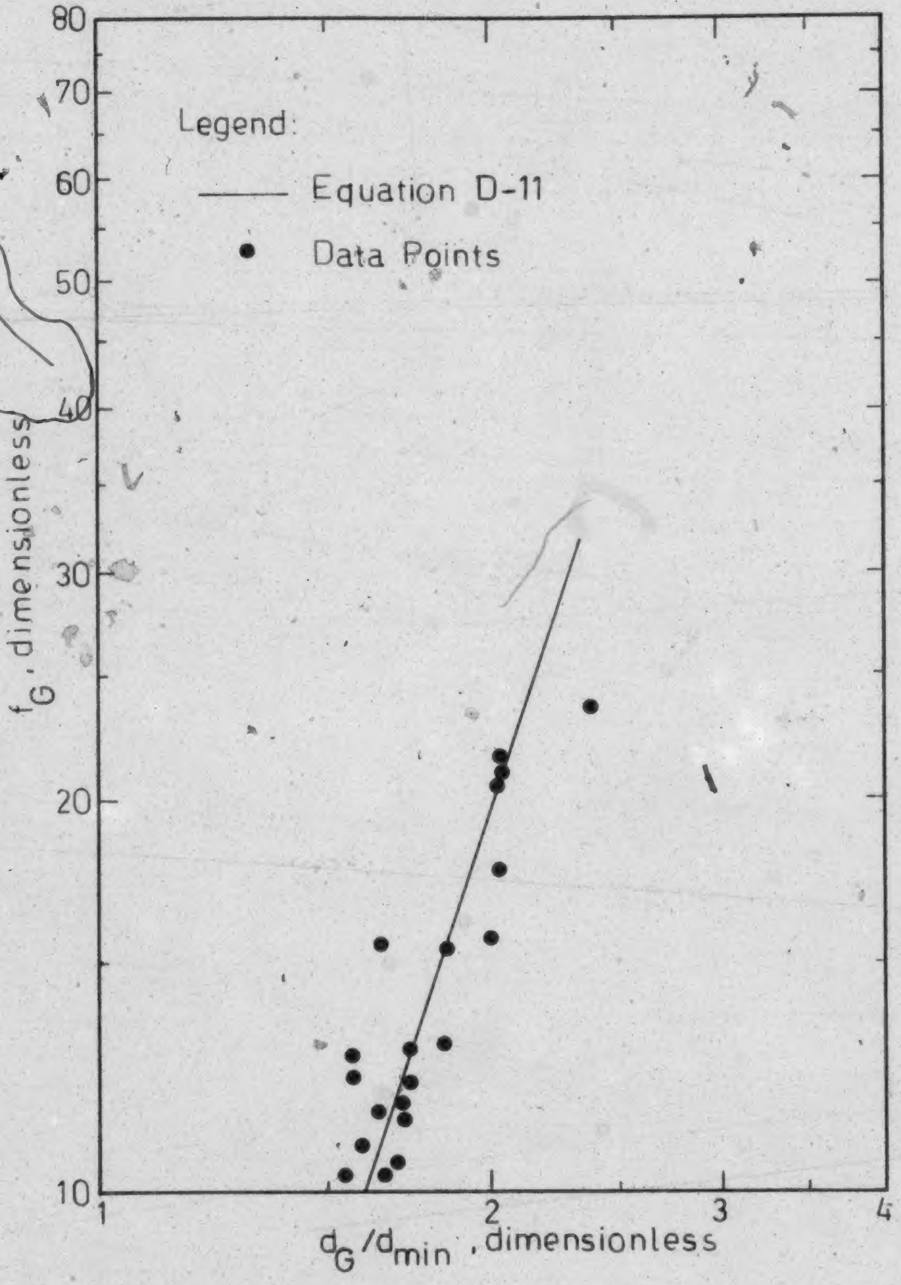

FIGURE V-10 FLOW DISTRIBUTION WITH OPENING, GLYCEROL

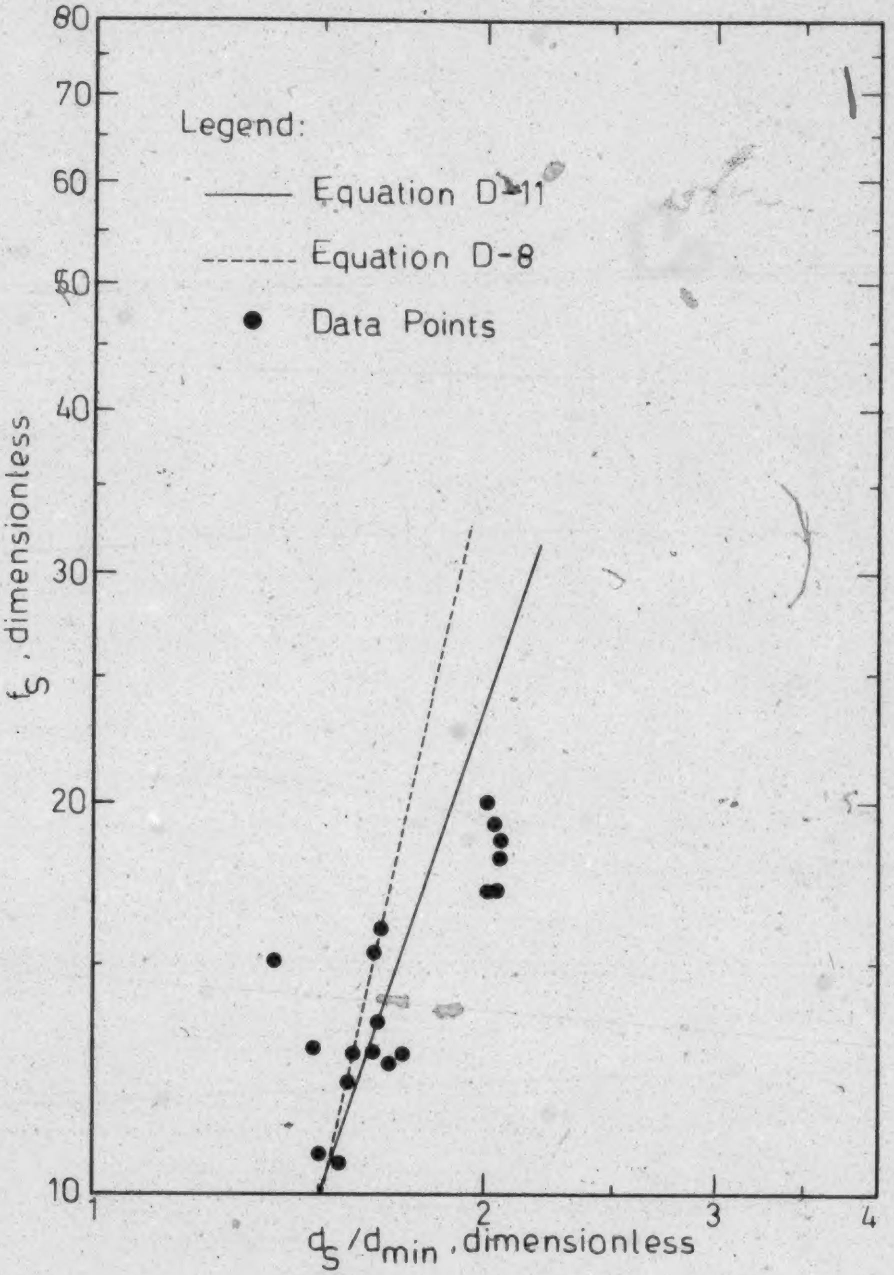

FIGURE V-11 FLOW DISTRIBUTION WITH OPENING, SEPARAN

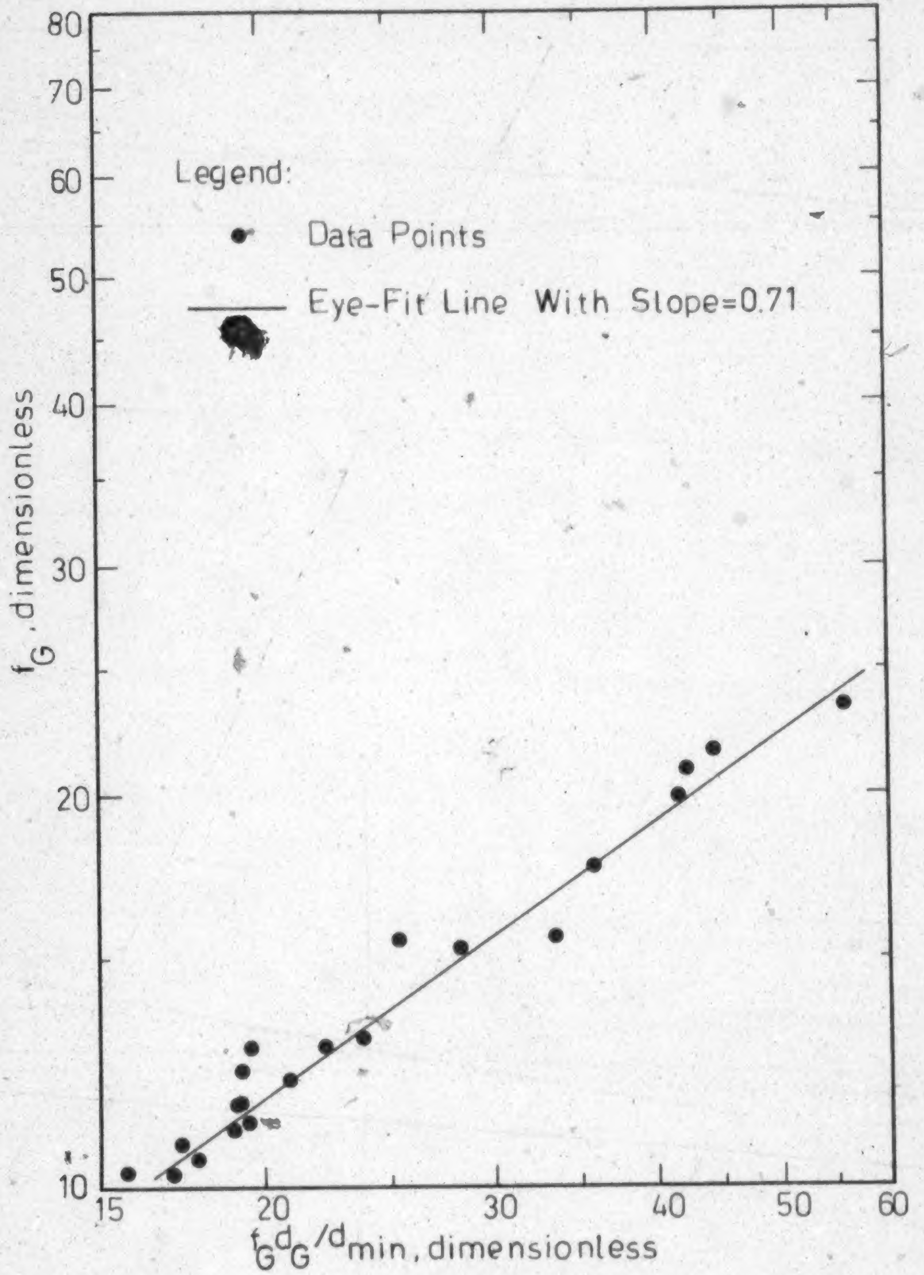

FIGURE V-12 FLOW DISTRIBUTION WITH OPENING, GLYCEROL

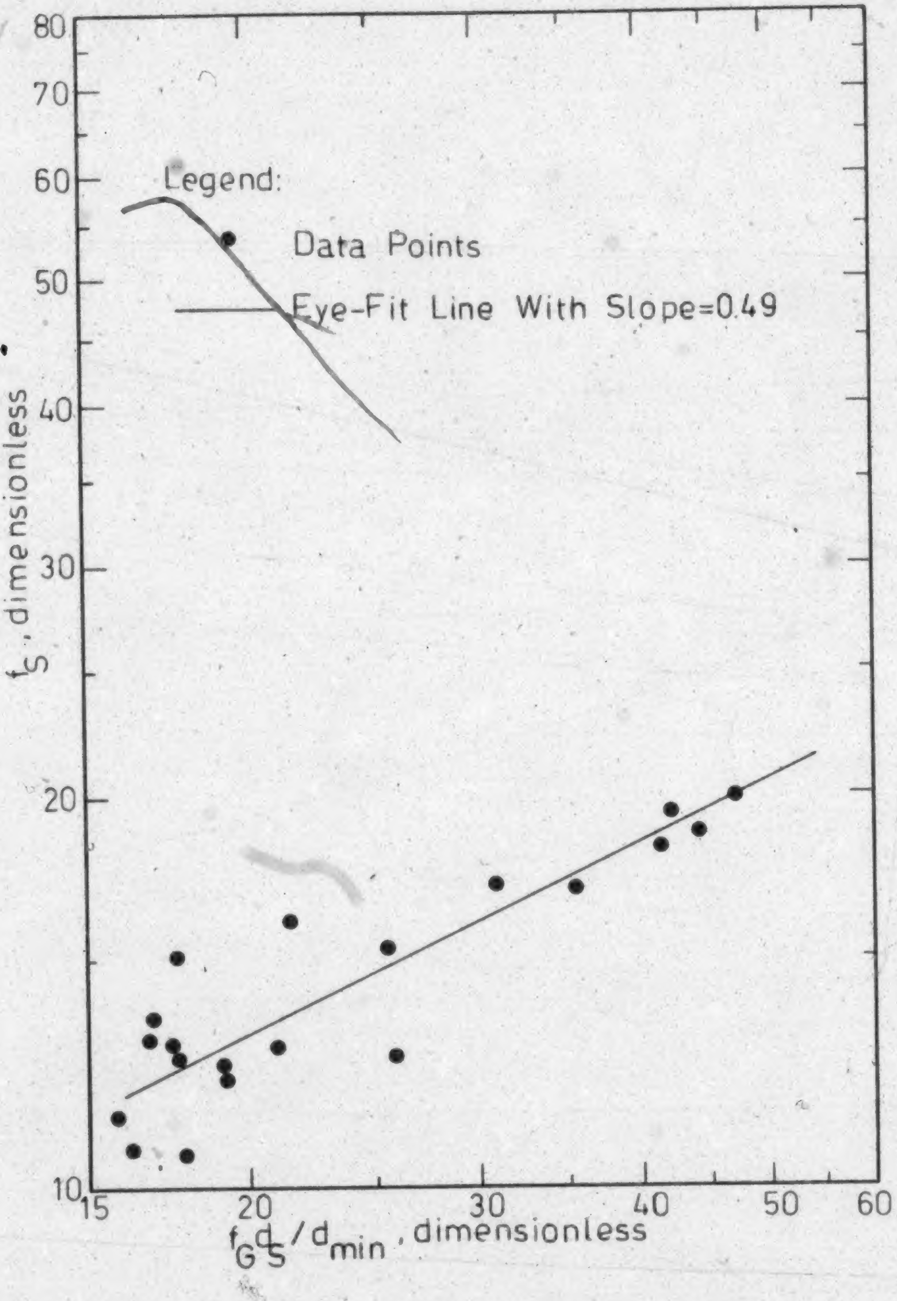

FIGURE V-13 FLOW DISTRIBUTION WITH OPENING, SEPARAN

than that of Figure (V-12) which confirms the former discussion. From Figure (V-12) one can conclude,

$$f_G \sim (f_G\ d_G)^{0.71} \qquad \text{(V-15)}$$

or, approximately,

$$f_G \sim d^3 \qquad \text{(V-16)}$$

And from Figure (V-13),

$$f_S \sim (f_G\ d_S)^{0.5} \qquad \text{(V-17)}$$

or, substituting for f_G from (V-16),

$$f_S \sim d^2 \qquad \text{(V-18)}$$

That is the fractional flow rates of the Glycerol solution is proportional with the openings to the power three, while those of Separan solution is proportional with the openings to the power two.

The fact that the effect of openings is suppressed due to the use of polymer solution may have major effects on the stability of a displacement front: one via conventional dispersion and the other via dispersion coefficient. According to Scheidegger (14c), the most conservative dependency of dispersion coefficient on interstitial velocity is,

$$C_D = b_1\ u \qquad \text{(V-19)}$$

where C_D is dispersion coefficient, b_1, a constant, and u, interstitial velocity. This implies that by adding some little amount of polymer to the water not only the nonuniform interstitial velocities will tend to be more uniform, but the effect of non-homogeneity of the bed on dispersion coefficient would, also, be damped out.

The above experimental observation reveals that the flow distribution of polymer solution in the bed can not be predicted simply by power-law model and some other effects such as elasticity have a significant influence. The failure of the power-law model in prediction of the flow behavior of polymer solution is also shown by direct comparison of the experimental data with predicted velocity profiles. The experimental data and predicted velocity profiles by power-law were given for positions No. 13, 15 and 16 in Figure (IV-13). As it is noticed from the Figure (IV-13), the experimental data of Glycerol solution is fairly close to the parabola obtained from flow of Newtonian fluid through parallel plates. In contrast, although not shown vividly by the particular profiles plotted, predicted power-law profiles are significantly flatter than the polymer solution data. This feature is best shown by Table (V-2) where the calculated values of u_{max}/V, which are based on power-law fluid flow through parallel plates, are, without exception, less than the experimental values.

CHAPTER VI

CONCLUSIONS AND RECOMMENDATIONS

VI. 1 Conclusions

The following are the main conclusions of this study.

1. Nonhomogeneity of the bed affected the flow distribution significantly. The effect of polymer solution was to suppress variations in velocity with pore opening to levels even below those for Newtonian fluids.

2. The experimental velocity profiles for Glycerol solution were consistent with prediction for Newtonian fluid flow through parallel plates. On the other hand those of the polymer solution were much more rounded than the predicted velocity profiles for a power-law fluid.

3. Consistent with earlier studies, increased pressure drop because of elasticity were observed. However, these occurred at flow rates in excess of those at which velocity measurements were made. Therefore, the elasticity of the fluid affects the flow distribution before it affects the pressure drop.

4. Qualitative visual observations revealed that the number of the dead zones or nearly dead zones and recirculation regions for polymer solution were reduced relative to

the Newtonian case. This implies the possibility of enhanced displacement efficiency in a microscopic sense.

VI. 2 Recommendations

1. Two-phase flow, i.e. displacing oil with Newtonian and also polymer solution in the present bed, could be useful in visualizing fingering which, hopefully, could be related to the present single phase behavior. It is recommended that the by-pass channels be eliminated in the future model design.

2. A study of local velocity profiles and flow distribution should be undertaken using the same kind of model with more diversified pore size distributions.

BIBLIOGRAPHY

1. Sandiford, B. B. "Laboratory and Field Studies of Water Floods Using Polymer Solutions to Increase Oil Recoveries." J. Pet. Tech., (August, 1964), p. 917.

2. "History of Petroleum Engineering." A Publication of the American Petroleum Inst., (1961), p. 850.

3. Muskat, M. "Physical Principles of Oil Production." McGraw-Hill Book Co. Inc., (1949), p. 648.

4. Aronofsky, J. S. "Mobility Ratio-Its Influence on Flood Patterns During Water Encroachment." Trans. AIME, 195 (1952), p. 15.

5. Aronofsky, J. S., and Ramey, H. J., Jr. "Mobility Ratio--Its Influence on Injection or production Histories in Five-Spot Water Flood." Trans., AIME, 207 (1956), p. 205.

6. Hurst, W. "Determination of Performance Curve in Five-Spot Water Flood." Petroleum Engineer, 25, P.B.-40 (April 1953).

7. Craig, F. F., Jr., Geffen, T. M., and Morse, K. A. "Oil Recovery Performance of Pattern Gas or Water Injection Operations from Model Tests." Trans., AIME, 204, (1955), p. 7.

8. Dyes, A. B., Candle, B. H., and Erickson, R. A. "Oil Production After Breakthrough as Influenced by Mobility Ratio." Trans. AIME, 201, (1954), p. 81.

9. Mahaffey, J. L., Rutherford, W. M., and Mathews, C. S. "Sweep Efficiency of Miscible Displacement in a Five-Spot." Soc. Pet. Eng. J., 6 (March 1966), p. 73.

10. Slobod, R. L., and Candle, B. H. "X-Ray Shadowgraph Studies of Areal Sweepout Efficiencies." Trans. AIME, 195 (1952), p. 265.

11. Slobod, R. L., and Thomas, R. A. "Effect of Transverse Diffusion on Fingering in Miscible-Phase Displacement." Soc. Pet. Eng. J. (March 1963), p. 9.

12. Caudle, B. H., and White, M. S. "Production Potential Changes During Sweep-Out in a Five-Spot System." Trans., AIME, 216 (1959), p. 446.

13. Collins, R. E. "Flow of Fluids Through Porous Materials." Reinhold Publishing Corporation, New York: (1961), p. 174.

14. Scheidegger, A. E. "The Physics of Flow Through Porous Media." University of Toronto Press, (a) p. 69, (b) p. 160, (c) p. 259 (1963).

15. Christopher, R. H., and Middleman, S. "Power-Law Flow Through a Packed Tube." I & EC Fundamentals, 4, No. 4 (November 1965), p. 422.

16. Pirson, S. J. "Oil Reservoir Engineering." McGraw-Hill Book Co. Inc., (a) p. 558, (b) p. 560, (1958).

17. Welge, H. J. "A Simplified Method for Computing Oil Recovery by Gas or Water Drive." Trans., AIME, 195, (1952), p. 91.

18. Jones, M. A. "Waterflood Mobility Control: A Case History." J. Pet. Tech. 18 (September 1966), p. 1151.

19. Mungan, N. "Improved Waterflooding Through Mobility Control." Paper prepared for the 19th Canadian Chemical Engineering Conference and 3rd Symposium on Catalysis, Edmonton, Alberta (October 1969).

20. Mungan, N., Smith, F. W., and Thompson, J. L. "Some Aspects of Polymer Floods." J. Pet. Tech., 18 (September 1966), p. 1143.

21. Stiles, W. E. "Use of Permeability Distribution in Water-Flood Calculations." Trans., AIME, 186 (1949), p. 9.

22. Dykstra, H., and Parsons, R. L. "The Prediction of Oil Recovery by Water Flood." Secondary Recovery of Oil in the United States, API, New York: (1950), p. 160.

23. Pye, D. J. "Improved Secondary Recovery by Control of Water Mobility." J. Pet. Tech. (August 1964), p. 911.

24. Gogarty, W. B. "Mobility Control with Polymer Solutions." Soc. Pet. Eng. J., 7 (June 1967), p. 161.

25. Dauben, D. L., Menzie, D. E. "Flow of Polymer Solutions Through Porous Media." J. Pet. Tech. (August 1967), p. 1065.

26. Slater, G. E., and Farough Ali, S. M. "Prediction of Sweep Efficiency in Polymer Flooding." Prod. Monthly, 32, No. 10 (October 1968), p. 22.

27. Lee, K. S., and Claridge, E. L. "Areal Sweep Efficiency of Pseudoplastic Fluids in a Five-Spot Hele-Shaw Model." Soc. Pet. Eng. J. (March 1968), p. 52.

28. Smith, F. W. "The Behavior of Partially Hydrolyzed Polyacrylamide Solutions in Porous Media." J. Pet. Tech. (February 19), p. 148.

29. McCartney, J. A., and Sloat, B. "Polymer Reduce Risk in Waterflooding." Pet. Eng., (December 1970), p. 74.

30. Lozanski, W. R., and Martin, I. "Taber South-Canada's First Polymer Flood." Paper prepared for the 21st Annual Technical Meeting of the Petroleum Society of CIM in Calgary, Alberta (May 1970).

31. White, J. L., Goddard, J. E., and Phillips, H. M. "Use of Polymers to Control Water Production in Oil Wells." J. Pet. Tech. (February 1973), p. 143.

32. Jewett, R. L., and Schurz, G. F. "Polymer Flooding --A Current Appraisal." Paper prepared for the 44th Annual Fall Meeting of the Society of Petroleum Engineers of AIME, Denver, Colorado: September 28-October 1, 1969.

33. Ustick, R. E., and Hillhouse, J. D. "Comparison of Polymer Flooding and Water-Flooding at Huntington Beach, California." J. Pet. Tech., 19 (September 1967), p. 1103.

34. Jennings, R. R., Rogers, J. H., and West, T. J. "Factors Influencing Mobility Control by Polymer Solutions." J. Pet. Tech. (March 1971), p. 391.

35. Burcik, E. J. "A Note on the Flow Behavior of Polyacrylamide Solutions in Porous Media." Prod. Monthly, 29 No. 6, (June 1965), p. 14.

36. ________. "Pseudo Dilatant Flow of Polyacrylamide Solutions in Porous Media." Prod. Monthly, 31, No. 3 (March 1967), p. 27.

37. Burcik, E. J., and Ferrer, J. "The Mechanism of Pseudo Dilatant Flow." Prod. Monthly, 32, No. 3 (March 1968), p. 7.

38. Burcik, E. J. "What, Why and How of Polymers for Waterflooding." Pet. Eng. (August 1968), p. 60.

39. ________, and Walrond, K. W. "Microgel in Polyacrylamide Solutions and Its Role in Mobility Control." Prod. Monthly, 32, No. 9, (September 1968), p. 12.

40. Lynch, E. J., and MacWilliams, D. C. "Mobility Control with Partially Hydrolyzed Polyacrylamide--A Reply to Emil Burcik." J. Pet. Tech., 21 (October 1969), p. 1247.

41. Patton, J. T., Coats, K. H., and Colegrave, G. T. "Prediction of Polymer Flood Performance." Soc. Pet. Eng. J., (March 1971), p. 72.

42. Ultman, J. S. "Viscoelastic Uniform Streaming Flow Past Submerged Obstacles." Ph.D. dissertation, University of Delaware, Newark: (1970).

43. Harvey, A. H. "An Investigation of the Flow of Polymer Solutions Through Porous Media." Ph.D. dissertation, University of Oklahoma, Norman (1967).

44. Sadowski, T. J., and Bird, R. B. "Non-Newtonian Flow Through Porous Media." Trans. Soc. Rheol., 9 (2), (1965), p. 243.

45. Marshall, R. J., and Metzner, A. B. "Flow of Viscoelastic Fluids Through Porous Media." SPE paper 1687, prepared for the Society of Petroleum Engineers Symposium on Mechanics of Rheologically Complex Fluids, Houston, Texas: December 15-16, 1966.

47. Astarita, G. "Two Dimensionless Groups Relevant in the Analysis of Steady Flows of Viscoelastic Materials." I & EC Fundamentals, 6, No. 2 (May 1967), p. 257.

48. Gaitonde, N. Y., and Middleman, S. "Flow of Viscoelastic Fluids Through Porous Media." SPE Paper 1685, prepared for the Society of Petroleum Engineers Symposium on Mechanics of Rheologically Complex Fluids, Houston, Texas: December 15-16, 1966.

49. Harrington, R. E., and Zimm, B. H. "Anomalous Plugging of Sintered Glass Filters by High Molecular Weight Polymers." J. Polymer Science, Part A-2, 6 (1968), p. 294.

50. Jones, W. M., and Maddock, J. L. "Flow of Viscoelastic Liquids: Comparison of Departures from Laminar Flow in Porous Beds and in Tubes." SPE Paper 1686, (cont.)

prepared for the Society of Petroleum Engineers symposium on Mechanics of Rheologically Complex Fluids, Houston, Texas: December 15-16, 1966.

51. Savins, J. G. "Non-Newtonian Flow Through Porous Media." I & EC, 16, No. 10 (October 1969), p. 18.

52. Bird, R. B., Stewart, W. E., and Lightfoot, E. N. "Transport Phenomena." John Wiley & Sons, Inc. (a) p. 62, (b) p. 79, (c) p. 197 (1966).

53. McKelvey, J. M. "Polymer Processing." John Wiley & Sons, Inc. (1962), p. 100.

54. Ergun, S. "Fluid Flow Through Packed Columns."Chem. Eng. Prog., 48, No. 2 (1952), p. 89.

55. Kyle, C. R., and Perrine, R. L. "An Experimental Model for Visual Studies of Turbulent Flow in Porous Materials." C. J. Ch. E., 49 (February 1971), p. 19.

56. Rollin, A. L. "Similarity Laws and Turbulence Structure of Drag Reducing Fluids." Ph.D. dissertation, University of Alberta, Edmonton (1971).

57. Catania, P. Ph.D. dissertation, under print, University of Alberta, Edmonton (1973).

58. Bergelin, O. P., Bell, K. J., and Leighton, M. D. "Heat Transfer and Fluid Friction During Flow Across Banks of Tubes." VII "By-passing Between Tube Bundle and Shell." Chem. Eng. Prog. Symposium Series, 55, No. 29 (1959), p. 45.

59. Ishihara, K. "Incompressible Viscous Flow Across Banks of Tubes at Low Reynolds Numbers." Ph.D. dissertation, Oklahoma State University (1971).

60. Boger, D. V., and Rama Murthy, A. V. "Normal Stress Measurement and Evaporation Effects on the Weissenberg Rheogoniometer." Trans. Soc. Rheol., 13 (1969), p. 405.

61. The Weissenberg Rheogoniometer, Instruction Mannual, Model R. 18, Sagamo Controls limited, Section D, Theory.

62. Seyer, F. A., and Metzner, A. B. "Turbulence Phenomena in Drag Reducing Systems." AICHE J., 15, No. 3 (May 1969), p. 426.

63. Middleman, S. "The Flow of High Polymers." Interscience Publishers (1968), p. 148.

APPENDIX A

RHEOLOGICAL PROPERTIES OF THE SOLUTIONS

A WEISSENBERG Rheogoniometer was used to measure viscosity of the Glycerol and polymer solutions. It was calibrated with a standard oil. Also, normal forces were measured for polymer solution to estimate relaxation time of the solutions. To eliminate the surface evaporation of the solution at the edge of the platen a thin film of a light nonvolatile oil was used as recommended in reference (60). However, inconsistency in the different sets of the measurements for the same fluid forced us to change the procedure and diameter-correction method, which will be discussed later, was performed to correct for evaporation.

Plots of shear stress and viscosity v.s. shear rate are given in Figure (A-2) and (A-3). Figure (A-2) includes standard oil, pure Glycerol and 96% Glycerol, while the viscometric behavior of polymer solution is presented in Figure (A-3). The straight lines of shear stress v.s. shear rate with slope unity obtained for standard oil and Glycerol solution indicate the Newtonian behavior of these fluids. It is also checked by constant viscosity horizontal lines obtained for these fluids. The curve of 0.2% (by weight) polymer solution indicated pseudoplastic behavior in the range of shear rates studied. The flow behavior index varied from 0.8 to 0.346 for low shear rate region and from 0.346 to 0.443 for high shear rate region. The apparent viscosity varied from 0.2 to 42 poise at the lowest shear rate. Table (A-2) represents the viscometric data and the results obtained from the Rheogoniometer for all the fluids used in the present study.

I. Rheogoniometer Parameters

From (61), the shear stress is given by,

$$\tau = \frac{3T_r}{2\pi\ R_{Pl}^3} = \frac{3.82T_r}{d_{Pl}^3} \qquad \text{(A-1)}$$

where,

τ = shear stress, dynes/cm^2

T_r = torque = $S_1 \Delta t\ K_t$

S_1 = torque transducer sensitivity, micron/volt

Δt = movement of torsion head transducer, volts

K_t = torsion bar constant in dyne cm per micron movement of the transducer,

R_{Pl} = radius of the platen, cm.

d_{Pl} = diameter of the platen cm.

The shear rate is given by,

$$\sigma = \frac{360}{\alpha t}, \qquad \text{(A-2)}$$

where,

σ = shear rate, sec^{-1}

α = angle of cone, degrees

$t = 2\pi/\beta$, second/revolution

β = angular rotation of the platen, rad./sec.

The normal force is calculated by,

$$P_{11}-P_{22} = \frac{4F}{\pi\, d_{P1}{}^2}\ , \qquad \text{(A-3)}$$

where,

$P_{11} - P_{22}$ = primary normal stress difference, dyne/cm^2

$F = S_2\, g v_t$, normal force, dyne,

S_2 = sensitivity of the normal force transducer, gr/volt

g = acceleration of gravity, cm/sec^2

v_t = output of transducer, volt.

The normal force transducer was calibrated by placing analytic weights on the plate while rotating and the sensitivity was found to be $S_2 = 0.2$ gr/volt. The calibration curve is presented in Figure (A-1) and the data in Table (A-1).

Apparent viscosity was calculated by,

$$\mu = \frac{\tau}{\sigma}\ , \qquad \text{(A-4)}$$

and relaxation time (62) by,

$$\Theta = \frac{P_{11} - P_{22}}{2\,\tau\,\sigma}\ . \qquad \text{(A-5)}$$

The plot of relaxation time v.s. shear rate is given in Figure (A-4). The maximum relaxation time was estimated by Bueche's theory (63),

$$\Theta_o = \frac{12(\mu_o - \mu_s)\, M}{\pi^2\, C\, R_g\, T}\ , \qquad \text{(A-6)}$$

where,

μ_s = viscosity of the solvent, poise,

M = solute molecular weight, g-mole

C = solute concentration, gr/cm^3

R_g = gas constant, gr cm^2/sec^2 g-mole ok

T = absolute temperature, ok

The above parameters for 0.2% (by weight) Separan AP-273 solution are,

μ_o = 42 poise

μ_s = 0.013 poise

$M \simeq 3 \times 10^6$ g-mole

$C = 0.2/100 = 0.002$ gr/cm^3

$R_g = 8.3 \times 10^7$ gr cm^2/sec^2 g-mole ok

T = 292 ok

Therefore,

$$\Theta_o = 3.126 \text{ sec.} \tag{A-7}$$

For the entire set of runs two different platens but only one torsion bar was used.

Runs with small platen,

d_{P1} = 5 cm

α = 2° - o' - 53"

K_t = 106.6 dynes cm/micron.

S_1 = 1.008 micron/volt.

S_2 = 0.2 gr/volt.

Therefore, Equations (A-1, 2, 3) becomes,

$$\tau = 3.285\,\Delta t, \tag{A-8}$$

$$\sigma = \frac{180}{t}\,, \tag{A-9}$$

$$P_{11} - P_{22} = 10\ v_t. \qquad \text{(A-10)}$$

Runs with Large Platen,

$d = 7.5$ cm

$\alpha = 55', 10''$

$K_t = 106.6$ dyne cm/micron,

$S_1 = 1.008$ micron/volt.

Therefore, Equations (A-1, 2, 3) become,

$$\tau = 0.974\ \Delta t, \qquad \text{(A-11)}$$

$$\sigma = \frac{392}{t}, \qquad \text{(A-12)}$$

$$P_{11} - P_{22} = 4.443\ v_t. \qquad \text{(A-13)}$$

II. Evaporation Correction

Care should be taken that the fluid covers the whole area of the platens. However, due to the evaporation at the edges of the platens, the area covered by the liquid would always be less than the platen's area. Therefore, the platen's diameter in former calculation should be replaced by the exact diameter of the portion of the platen which is covered with liquid.

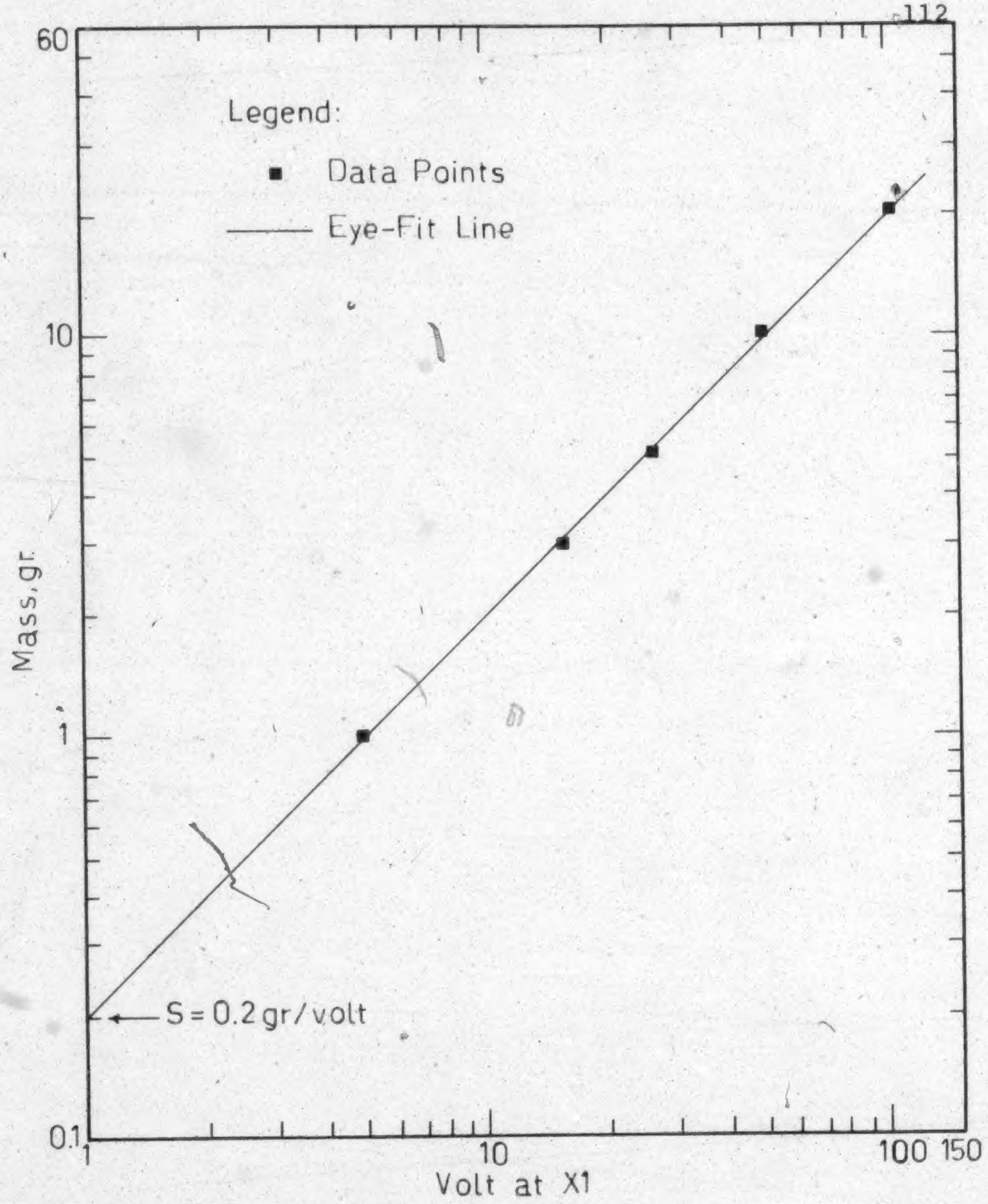

FIGURE A-1 NORMAL FORCE TRANSDUCER CALIBRATION

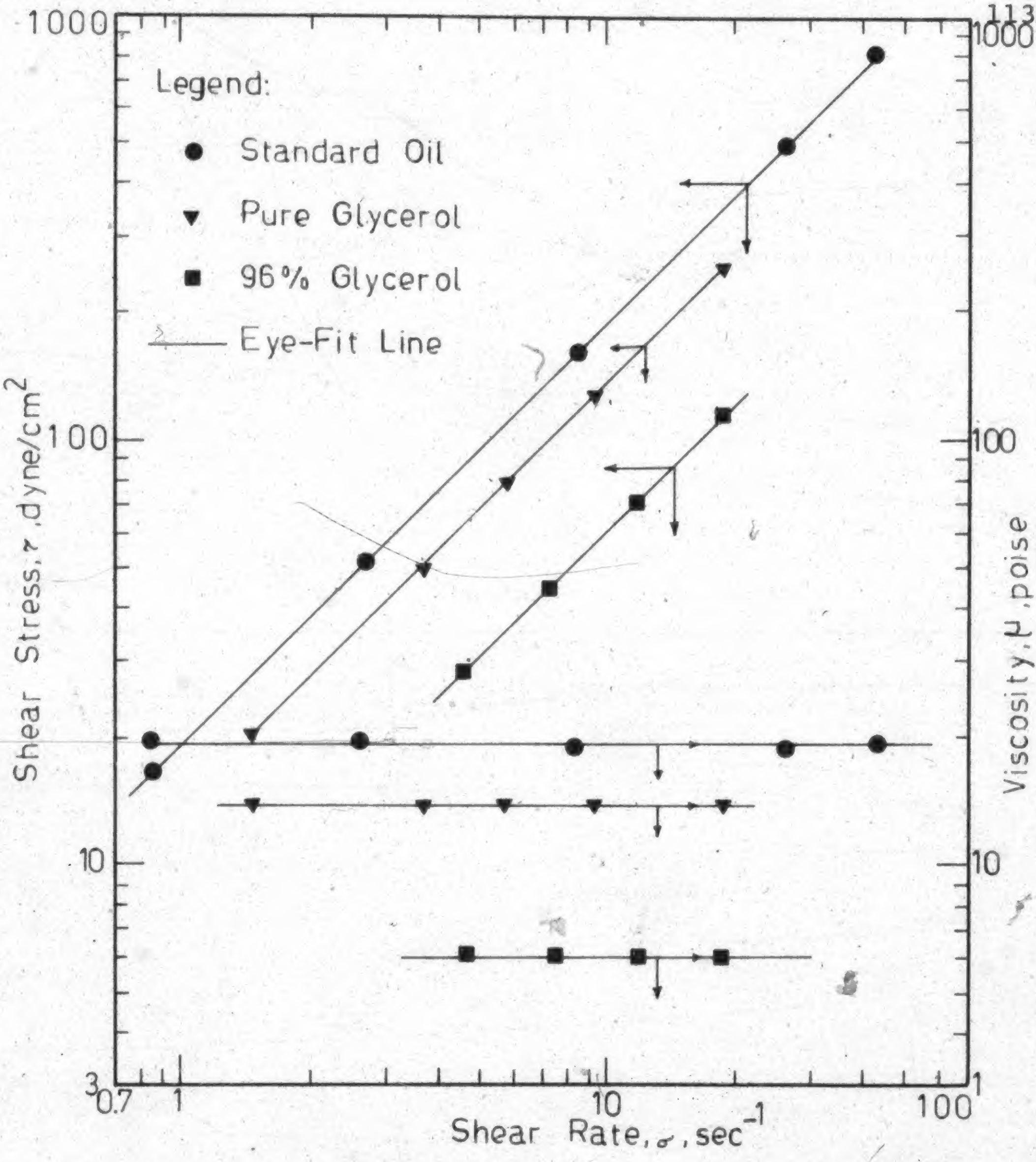

FIGURE A-2 VISCOMETRIC BEHAVIOR OF NEWTONIAN FLUIDS

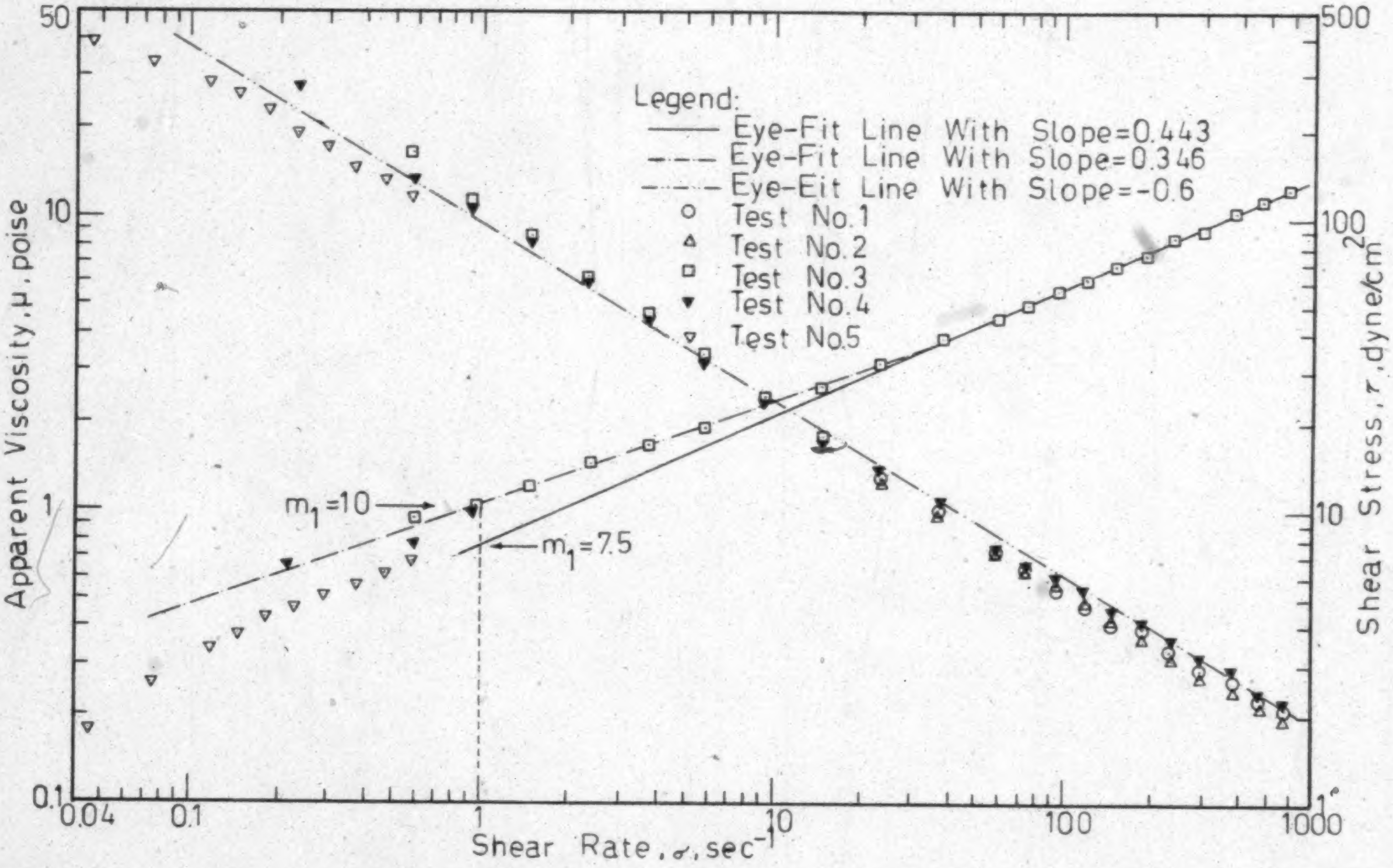

FIGURE A-3 VISCOMETRIC BEHAVIOR OF SEPARAN AP-273, 0.2% (by weight)

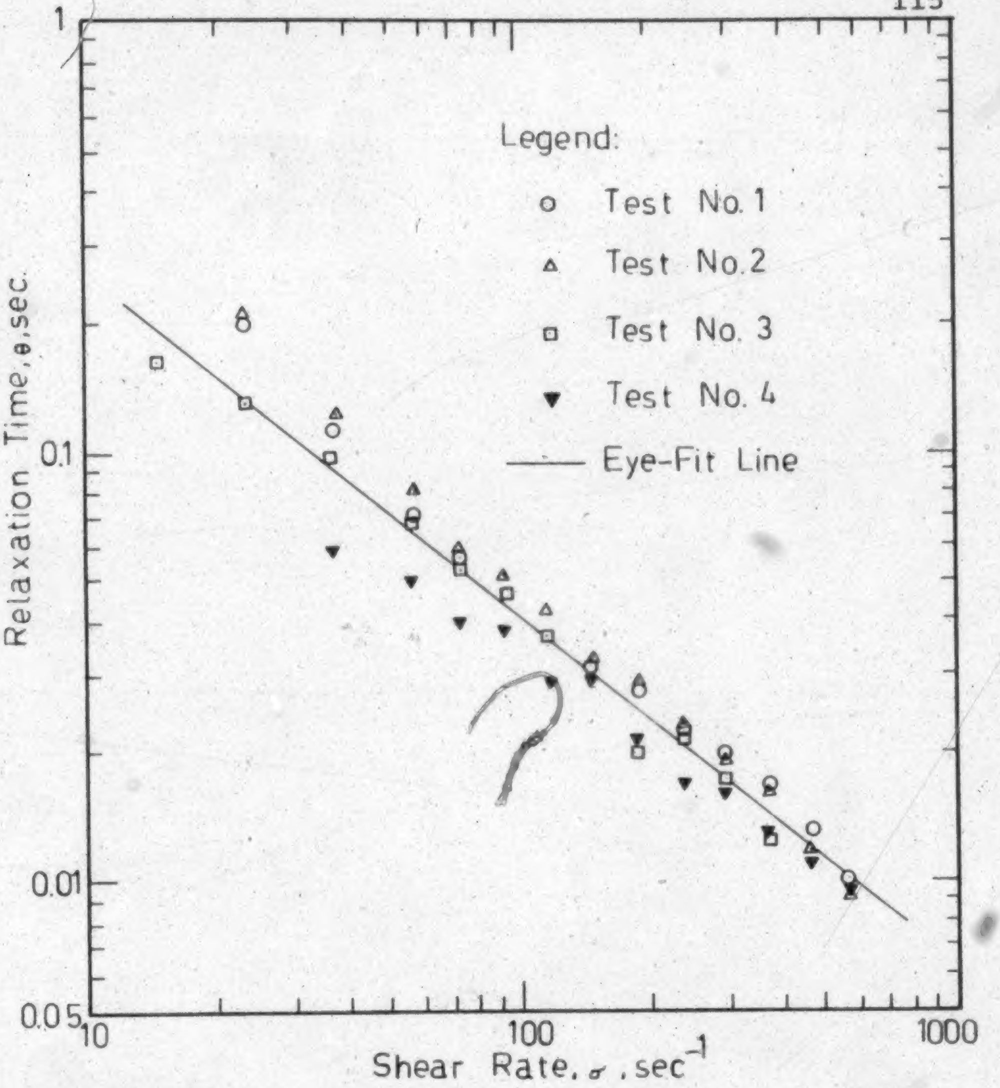

FIGURE A-4 RELAXATION TIME OF SEPARAN AP-273, 0.2%(by weight)

TABLE A-1

CALIBRATION OF NORMAL FORCE TRANSDUCER

Run No.	Mass (gr.)	Volt (at XI)
1	1	4.9
2	3	15.4
3	5	26
4	10	49.4
5	20	101.5
6	30	150
7	50	247

TABLE A-2

VISCOMETRIC MEASUREMENTS FOR STANDARD OIL, GLYCEROL, AND POLYMER SOLUTION

1. Standard Oil

VISC. No. S-600-68-1h was used as standard oil, which had viscosity of 1974 C.P. at 20°C. and 1294 C.P. at 25°C. The temperature of this experiment was 21°C.

Run No.	σ sec^{-1}	Δt Volt	τ $dyne/cm^2$	μ C.P.
1	26.5	150	493	1861
2	42.6	248	815	1915
3	84.8	490	1610	1900
4	8.48	48	157.7	1860

TABLE A-2 (continued)

Run No.	σ sec^{-1}	Δt Volt	τ dyne/cm^2	μ C.P.
5	2.65	15.5	50.9	1922
6	0.848	5	16.42	1934
7	0.265	1.6	5.26	1982
8	0.0848	0.55	1.808	2130

2. Pure Glycerol, T = 21°C

1	9.23	130	126.7	1373
2	18.4	260	253.5	1377
3	5.75	80	78	1356
4	1.464	20.8	20.25	1382
5	3.68	51	49.7	1350
6	9.23	128	124.8	1350

NOTE: Run No.'s 1-3 are for the pure Glycerol before being used, while runs 4-6 are for the same solution after being used in the system.

3. 96% Glycerol, T = 21°C

1	18.4	115	112	609
2	4.62	29	28.25	611
3	7.35	45	43.8	596
4	11.6	72.5	70.6	608

4. 81% Glycerol, T = 20°C

1	35.5	65	26.65	75
2	22.4	42	172	76.8

TABLE A-2 (continued)

Run No.	σ sec^{-1}	Δt Volt	τ dyne/cm^2	μ C.P.
3	14.13	27	11.08	78.3
4	55.5	105	43.1	77.5
5	89	165	67.5	75.8
6	141.3	260	106.6	75.3
5. 58% Glycerol, T = 20°C				
1	44.6	10.5	4.31	9.66
2	71	17	6.98	9.83
3	112	26	10.67	9.6
4	177.5	41	16.8	9.47
6. Domestic Tap Water				
1	71	1.8	0.739	1.04
2	112	2.8	1.148	1.025
3	177.5	4.5	1.844	1.039
4	112	2.8	1.148	1.025
5	224	5.75	2.36	1.053
6	355	9.2	3.77	1.061

7. 0.2% Separan AP-273 Solution, Test No. 1, T = 20°C

Run No.	σ sec^{-1}	Δt Volt	τ dyne/cm^2	μ C.P.	v_t Volt	$P_{11}-P_{22}$ dyne/cm^2	Θ sec.
1	23.24	26	28.55	122.6	57.5	277	0.209
2	36.8	31.2	34.25	93.1	61.5	296.5	0.1177

Run No.	σ sec^{-1}	Δt Volt	τ dyne/cm^2	μ C.P.	v_t Volt	$P_{11}-P_{22}$ dyne/cm^2	θ sec.
3	57.5	36.5	40.1	69.6	86	414	0.0897
4	73.5	40.5	44.4	60.4	80	385.5	0.059
5	92.3	44.5	48.8	52.9	91	439	0.0486
6	116	49	53.8	46.3	110	531	0.0426
7	146.4	54.5	59.8	40.8	120	579	0.033
8	184	59.5	65.3	35.5	144	694	0.0289
9	232.4	65	71.4	30.7	160	771	0.0232
10	292.5	72.5	79.6	27.2	188	906	0.0194
11	368	80	87.8	23.9	220	1061	0.01645
12	462	89	97.7	21.1	240	1158	0.0128
13	575	100	109.8	19.1	240	1158	0.00916

NOTE: The sample was taken from a freshly prepared solution before being used for the experiment and the period between the time of solution preparation and the time of performing viscometric measurements was 15 days.

Test No. 2, T = 19.5°C

1	23.24	27.2	29.85	128.3	64.5	311	0.224
2	36.8	32.6	35.8	97.3	65	313.5	0.1189
3	57.5	39	42.8	74.4	73.5	354.5	0.072
4	73.5	42	46.1	62.7	88	424	0.0625
5	92.3	46.5	51	55.3	95	458	0.0486
6	116	50.5	55.4	47.8	100	482	0.03745
7	146.4	55.5	60.9	41.6	118	569	0.0319
8	184	61	66.9	36.4	146	704	0.0286

Run No.	σ sec^{-1}	Δt Volt	τ $dyne/cm^2$	μ C.P.	v_t Volt	$P_{11}-P_{22}$ $dyne/cm^2$	θ sec.
9	232.4	68.5	75.2	32.4	169	815	0.0233
10	292.5	75	82.4	28.2	204	984	0.0203
11	368	84.5	96.6	26.2	240	1188	0.0167
12	462	94	107.5	23.2	262	1298	0.01306
13	575	105	120	20.9	282	1395	0.0101

NOTE: The sample was taken from the same solution as Test No. 1 but after experimental runs and viscometric measurements were performed same day as Test No. 1.

Test No. 3, T = 19.5°C

1	0.575	8	9.16	1159	-	-	-
2	0.923	9	10.3	1117	-	-	-
3	1.464	10.5	12.02	821	-	-	-
4	2.324	12.5	14.3	615	-	-	-
5	3.68	14.5	16.6	451	-	-	-
6	5.75	16.5	18.9	328.5	-	-	-
7	9.23	19.5	22.3	241.5	-	-	-
8	14.64	23	26.35	180	22.6	111.9	0.1455
9	23.24	27	30.9	133	37.2	184.2	0.1282
10	36.8	32	38.25	104	53.5	273	0.097
11	57.5	37.5	44.8	77.8	70	357	0.0693
12	73.5	41.5	49.6	67.4	75	382.5	0.0525
13	92.3	45	56.1	60.8	94	494	0.0477
14	116	49	61.1	52.4	100	525	0.037
15	146.4	54	67.4	46.1	120	630	0.0319

Run No.	σ sec^{-1}	Δt Volt	τ dyne/cm^2	μ C.P.	v_t Volt	$P_{11}-P_{22}$ dyne/cm^2	θ sec.
16	184	59	73.6	40	100	525	0.01938
17	232.4	67	83.6	36	153	803	0.0206
18	292.5	72.5	90.5	30.95	170	893	0.01686
19	368	82	102.3	27.8	180	945	0.01252
20	462	90	112.3	24.3	220	1156	0.01113
21	575	100	124.8	21.7	262	1375	0.0958
Test No. 4, T = 19.5°C							
1	0.232	6	6.23	2730	-	-	-
2	0.575	6.8	7.47	1300	-	-	-
3	0.923	8.9	9.77	1060	-	-	-
4	1.464	10.9	11.98	817	-	-	-
5	2.324	12.2	13.4	576	-	-	-
6	3.68	14.8	16.25	442	-	-	-
7	5.75	16.8	18.44	321	-	-	-
8	9.23	19.0	20.85	226	-	-	-
9	14.64	22.4	24.6	168	-	-	-
10	23.24	27.6	31.6	136	-	-	-
11	36.8	32.5	38.83	105.5	34	173.4	0.0607
12	57.5	37	44.2	76.9	50	255	0.0501
13	73.5	40	47.8	65	55	280.5	0.0399
14	92.3	45	53.8	58.3	75	382.5	0.0385
15	116	50	59.8	51.6	80	408	0.0294
16	146.4	54	67.4	46.1	90	472	0.02395
17	184	60	74.8	40.7	111	583	0.0212

Run No.	σ sec^{-1}	Δt Volt	τ $dyne/cm^2$	μ C.P.	v_t Volt	$P_{11}-P_{22}$ $dyne/cm^2$	Θ sec.
18	232.4	68	84.8	36.5	125	656	0.01664
19	292.5	72	89.8	30.7	158	830	0.0158
20	368	82	102.2	27.8	184	966	0.01283
21	462	90	112.2	24.3	213	1118	0.01082
22	575	101	126	21.9	260	1365	0.00942

Test No. 5, T = 20°C

Run No.	σ sec^{-1}	Δt Volt	τ $dyne/c^2$	μ C.P.
1	0.02925	0.9	1.228	4200
2	0.0462	1.3	1.774	3840
3	0.0735	1.8	2.46	3345
4	0.116	2.4	3.275	2820
5	0.1464	3.0	3.74	2555
6	0.184	3.4	4.24	2310
7	0.2324	3.6	4.49	1930
8	0.2925	4	4.99	1706
9	0.368	4.5	5.38	1462
10	0.462	5.5	6.04	1308
11	0.575	6	6.59	1146

NOTE: Tests No. 3, 4, and 5 were performed on the samples of the same solution which was different from that of tests No. 1 and 2. However, the sample of test No. 3 was one day old and was taken from the freshly prepared solution, while the samples of tests No. 4 and 5 were 10 and 17 days old, respectively, and were taken after the experimental runs. The results of the different tests indicate the lack of major degradation of the samples.

APPENDIX B

PRESSURE DROP AND RELATED CORRELATIONS

Bergelin, et al. (58) suggested the following empirical correlation to predict pressure drop of the flow across an ideal bank of tubes,

$$\Delta P_B = \frac{4K_1 \ \mu \ W_B \ N}{2 \ \rho \ S_B \ D} \left(\frac{\mu}{\mu_w}\right)^m . \qquad \text{(B-1)}$$

For isothermal flow the viscosity correction need not be considered; therefore,

$$\Delta P_B = \frac{4K_1 \ \mu \ W_B \ N}{2 \ \rho \ S_B \ D} , \qquad \text{(B-2)}$$

where,

$W_B = \rho\, q$ = mass flow rate, gr/sec.

$S_B = d x \ell x N_m$ = minimum free flow area, cm^2

N_m = number of the minimum openings in one row,

N = number of major restriction encountered in flow through the bank,

B = indicates an ideal bundle of tubes, i.e. without by-pass flow.

K_1 = dimensionless constant which is determined by the following procedure,

$$f_B = \frac{K_1}{Re_t} , \qquad \text{(B-3)}$$

where f_B is friction factor and Re_t is tube bank Reynolds number, defined as,

$$Re_t = \frac{D\ W_B}{\mu\ S_B} \quad . \qquad \text{(B-4)}$$

In general, for tube banks (59),

$$f_B = \frac{6}{Re_t}\ \frac{P_t - 1}{P_t^{\ 3}}\ F\ (P_t) \qquad \text{(B-5)}$$

This is obtained (59) by integrating the Hagen-Poiseuille equation for a creeping flow between two tubes and using the tube bank friction factor defined as,

$$f_B = \frac{2\ \Delta P\ \rho\ S_B^{\ 2}}{4\ W_B^{\ 2}\ N_t} \quad . \qquad \text{(B-6)}$$

In Equation (B-5), $F(P_t)$ is equal to,

$$F(P_t) = \int_0^1 \frac{dx}{[P_t - \sqrt{2x - x^2}]^3} \quad . \qquad \text{(B-7)}$$

P_t is pitch ratio and is defined as,

$$P_t = \frac{S_T}{D} \quad , \qquad \text{(B-8)}$$

where S_T is transverse pitch as shown in Figure (III-1). It is worthwhile to mention that in staggered configuration the smaller pitch (i.e. S_L or S_T whichever is smaller) should be taken to calculate pitch ratio. For the present model,

$$S_T = 0.65 \text{ cm} \ . \qquad \text{(B-9)}$$

Therefore,

$$P_t = 1.08. \qquad \text{(B-10)}$$

By graphical integration, $F(P_t)$ from Equation (B-7) was determined to be,

$$F(P_t) = F(1.08) = 462.8. \qquad \text{(B-11)}$$

Hence, by substituting into Equation (B-5),

$$f_B = \frac{176}{Re_t} . \qquad \text{(B-12)}$$

comparing (B-12) with (B-3),

$$K_1 = 176. \qquad \text{(B-13)}$$

As mentioned before, the Equation (B-1) was for an ideal bundle of tubes, i.e. without by-pass flow. To apply this equation to the present model, the by-pass flow should be eliminated. That is according to Figure (III-3), only the flow passing through the positions 13 to 20 should be considered. Hence, an imaginary wall is assumed to pass through the centers of the outermost cylinders which was shown by dashed-line in Figure (III-3). Therefore, ideal bundle volumetric flow rate, q_B, is,

$$q_B = \frac{\sum_{i=13}^{20} A_i}{\sum_{i=12}^{21} A_i} \; q . \qquad \text{(B-14)}$$

From Table (C-1), q_B for Glycerol is,

$$q_B = \frac{3.405}{6.128} q = 0.556 \; q . \qquad \text{(B-15)}$$

That is approximately 50% of the flow passes between the cylinders in row No. 21. For Separan,

$$q_B = \frac{2.465}{5.654} q = 0.436 \; q . \qquad \text{(B-16)}$$

In the above calculations, the flow rate passing through the imaginary wall and the outermost cylinders of row No. 21 was neglected. A further assumption made is that the flow distribution would remain the same for the whole range of flow rates studied in pressure drop measurement.

Considering the above assumptions, the Equation (B-2) can be used for the present model with the following known parameters,

$K_1 = 176$

$W_B = 0.556\ \rho q$

$N = 35$ (i.e. the number of rows between the two pressure taps)

$S_B = d \times \ell \times N_m = (0.05)(5.2)(9) = 2.34\ \text{cm}^2$

$D = 0.6$ cm

$\mu = 13.6$ poise (pure Glycerol solution)

$\mu = 6.06$ poise (96% Glycerol solution)

$\mu = 0.765$ poise (81% Glycerol solution)

$\mu = 0.0964$ poise (58% Glycerol solution)

$\mu = 0.0104$ poise (Domestic Tap Water)

Substituting into Equation (B-2) and performing the necessary algebraic operations,

$$\Delta P_B = 6.63 \times 10^4\ q \quad \text{dyne/cm}^2 \ \text{(pure Glycerol)} \tag{B-17}$$

$$\Delta P_B = 2.96 \times 10^4\ q \quad \text{dyne/cm}^2 \ \text{(96\% Glycerol)} \tag{B-18}$$

$$\Delta P_B = 3.75 \times 10^3\ q \quad \text{dyne/cm}^2 \ \text{(81\% Glycerol)} \tag{B-19}$$

$$\Delta P_B = 4.7 \times 10^2\ q \quad \text{dyne/cm}^2 \ \text{(58\% Glycerol)} \tag{B-20}$$

$$\Delta P_B = 50.6\ q \quad \text{dyne/cm}^2 \ \text{(Dom. Tap W.)} \tag{B-21}$$

In terms of superficial velocity, one can write,

$$V = \frac{q}{A}\ , \tag{B-22}$$

where $A = 33.8\ cm^2$ is the cross sectional area of the box, therefore,

$$\Delta P_B = 2.24 \times 10^6\ V\ \text{dyne/cm}^2 \text{ (pure Glycerol)} \quad (B-23)$$

$$\Delta P_B = 1.0 \times 10^6\ V\ \text{dyne/cm}^2 \text{ (91\% Glycerol)} \quad (B-24)$$

$$\Delta P_B = 1.27 \times 10^5\ V\ \text{dyne/cm}^2 \text{ (81\% Glycerol)} \quad (B-25)$$

$$\Delta P_B = 1.59 \times 10^4\ V\ \text{dyne/cm}^2 \text{ (58\% Glycerol)} \quad (B-26)$$

$$\Delta P_B = 1.71 \times 10^3\ V\ \text{dyne/cm}^2 \text{ (Dom. Tap W.)} \quad (B-27)$$

Equations (B-23) to (B-27) together with the experimental data points were presented in Figure (IV-1).

To apply Bergelin's correlation, i.e. Equation (B-2), to the polymer solution, an apparent viscosity must be defined for each flow rate, which the flow behavior indices, i.e. m_1 and n, can be considered constant. As a first approximation, these parameters are estimated directly from the experimental curve of pressure drop v.s. superficial velocity in Figure (IV-2). According to the figure (IV-2), the whole region of flow rates studied can be divided into four parts,

Region of flow rate cc/sec.	n	m_1
0.431 - 1.717	0.346	10
2.13 - 6.84	0.443	7.5
8.53 -21.52	0.632	2.93
27.25 -34.35	0.917	0.778

n is the slope of the eye-fit line through the data points in Figure (IV-2). These lines have not been shown. m_1 was calculated by assuming power-law

$$m_1 = \mu \, \sigma^{1-n}. \tag{B-28}$$

To estimate the apparent viscosity, the following procedure was undertaken.

The wall shear rate for flow through parallel plates is given by,

$$\sigma_w = \frac{2n+1}{n} \, \frac{\bar{V}}{d/2}, \tag{B-29}$$

where σ_w is wall shear rate, $\bar{V}$, average velocity and d is shown in Figure (II-2). Equation (B-29) can be easily derived from equation of motion for power-law fluid flow through parallel plates (53). To modify Equation (B-29) for the present model, $\bar{V}$ should be replaced by average interstitial velocity, i.e.

$$\bar{V} \equiv \frac{V}{\varepsilon}, \tag{B-30}$$

and d/2 should be replaced by volumetric hydraulic radius of the bed. Therefore,

$$\sigma_w = \frac{2n+1}{n} \, \frac{V}{\varepsilon R_H} \tag{B-31}$$

on the other hand, R_H can be calculated as follows (52c),

$$R_H = \frac{\text{volume of voids}}{\text{wetted surface}}$$

$$= \frac{\dfrac{\text{volume of voids}}{\text{volume of bed}}}{\dfrac{\text{wetted surface}}{\text{volume of bed}}} = \frac{\varepsilon}{s_v}, \tag{B-32}$$

where s_v represents the wetted surface per volume of bed. Specific surface, s_s, is defined as,

$$s_s = \frac{\text{wetted surface}}{\text{solid volume}}. \tag{B-33}$$

For the present bed,

$$S_s = \frac{(\pi D \ell)\ N_T}{(\pi D^2 \ell/4)\ N_T} = \frac{4}{D} \qquad \text{(B-34)}$$

In calculation of s_s, the area of the surrounding walls has been neglected. One can also write,

$$S_V = S_s\ (1-\varepsilon). \qquad \text{(B-35)}$$

From Equations (B-32, 34, 35),

$$R_H = \frac{\varepsilon D}{4(1-\varepsilon)}\ . \qquad \text{(B-36)}$$

Substituting (B-22, 36) into (B-31),

$$\sigma_w = \frac{4(1-\varepsilon)}{A\varepsilon^2 D}\ \frac{2n+1}{n}\ q. \qquad \text{(B-37)}$$

Knowing the following parameters,

$A = 33.8\ \text{cm}^2$

$\varepsilon = 0.357$

$D = 0.6\ \text{cm}.$

Equation (B-37) becomes,

$$\sigma_w = 0.995\ \frac{2n+1}{n}\ q. \qquad \text{(B-38)}$$

The estimated σ_w from Equation (B-38) laid in the region of 2.1 to 100.5 sec^{-1}. Over this range of shear rates Figure A-4 shows n to be approximately .346 to .443. After the initial estimate of shear rate using (B-38) by n estimated from the pressure drop measurements, these new values of flow behavior indices were used in apparent viscosity calculation. Therefore, the calculated apparent viscosity, consequently, the predicted pressure drops were based on the viscometric measurement of the fluid.

The calculated values of wall shear rate, apparent viscosity, and pressure drop are recorded in Table (B-3) and the predicted curve of pressure drop v.s. superficial velocity by Equation (B-2) is presented in Figure (IV-2).

TABLE B-1

FLOW BEHAVIOR PARAMETERS OF 96% GLYCEROL SOLUTION

Run No.	q cc/sec.	V cm/sec.	$\Delta P \times 10^{-4}$ dyne/cm^2	$K \times 10^4$ cm^2	$f_K \times 10^{-2}$ Dimensionless	$N_{Re} \times 10^4$ Dimensionless	$f_K \times N_{Re}$
1	0.835	0.0248	2.785	1.198	48.9	2.057	1.005
2	1.49	0.443	4.36	1.369	25.3	3.65	0.924
3	2.13	0.0633	6.75	1.261	19.2	5.23	1.004
4	3.39	0.1007	10.36	1.308	11.62	8.32	0.967
5	3.39	0.1007	10.5	1.291	11.8	8.32	0.982
6	4.28	0.127	13.04	1.31	9.21	10.5	0.966
7	5.38	0.1598	16.19	1.328	7.23	13.2	0.955
8	6.76	0.201	19.68	1.372	5.54	16.64	0.921
9	8.53	0.2535	25.4	1.342	4.51	20.95	0.944
10	8.53	0.2535	21.8	1.564	3.87	20.95	0.81
11	10.76	0.3195	29.05	1.481	3.24	27	0.875
12	13.6	0.404	32.5	1.672	2.27	33.4	0.757
13	17.06	0.507	40.2	1.698	1.79	41.9	0.75
				PURE GLYCEROL			
14	0.431	0.0128	3.6	1.07	251	0.471	1.18
15	0.685	0.02037	5.27	1.165	145	0.748	1.085
16	1.07	0.0318	7.69	1.25	86.6	1.17	1.01
17	1.717	0.0511	11.78	1.311	51.6	1.88	0.97

TABLE B-1 (continued)

Run No.	q cc/sec.	V cm/sec.	$\Delta P x10^{-4}$ dyne/cm^2	$Kxk0^4$ cm^2	$f_K x10^{-2}$ Dimensionless	$N_{Re} x10^4$ Dimensionless	$f_K x N_{Re}$
18	2.17	0.0645	14.63	1.332	40.2	2.37	0.954
19	2.725	0.081	18	1.37	31.35	2.98	0.934
20	3.42	0.1017	22.3	1.379	24.55	3.75	0.92
PURE GLYCEROL							
1	0.431	0.0128	3.6	1.07	251	0.471	1.18
2	0.685	0.02037	5.27	1.165	145	0.748	1.085
3	1.07	0.0318	7.69	1.25	86.6	1.17	1.01
4	1.717	0.0511	11.78	1.311	51.6	1.88	0.97
5	2.17	0.0645	14.63	1.332	40.2	2.37	0.954
6	2.725	0.081	18	1.37	31.35	2.98	0.934
7	3.42	0.1017	22.3	1.379	24.55	3.75	0.92
96% GLYCEROL SOLUTION							
8	0.835	0.0248	2.785	1.198	48.9	2.057	1.005
9	1.49	0.0443	4.36	1.369	25.3	3.65	0.924
10	2.13	0.0633	6.75	1.261	19.2	5.23	1.004
11	3.39	0.1007	10.36	1.308	11.62	8.32	0.967
12	3.39	0.1007	10.5	1.291	11.8	8.32	0.982
13	4.28	0.127	13.04	1.31	9.21	10.5	0.966

TABLE B-1 (continued)

Run No.	q cc/sec.	V cm/sec.	$\Delta P \times 10^{-4}$ dyne/cm^2	$K \times 10^4$ cm^2	$f_K \times 10^{-2}$ Dimensionless	$N_{Re} \times 10^4$ Dimensionless	$f_K \times N_{Re}$
14	5.38	0.1598	16.19	1.328	7.23	13.2	0.955
15	6.76	0.201	19.68	1.372	5.54	16.64	0.921
16	8.53	0.2535	25.4	1.342	4.51	20.95	0.944
17	8.53	0.2535	21.8	1.564	3.87	20.95	0.81
18	10.76	0.3195	29.05	1.481	3.24	27	0.875
19	13.6	0.404	32.5	1.672	2.27	33.4	0.757
20	17.06	0.507	40.2	1.698	1.79	41.9	0.75
			81% GLYCEROL SOLUTION				
21	0.835	0.0248	0.392	1.075	7.51	15.72	1.18
22	1.49	0.0443	0.597	1.258	3.59	28.1	1.008
23	2.13	0.0633	0.938	1.146	2.76	40.1	1.107
24	3.39	0.1007	1.484	1.15	1.72	63.9	1.1
25	4.28	0.127	1.86	1.16	1.358	80.5	1.093
26	5.38	0.1598	2.34	1.16	1.08	101.2	1.092
27	6.76	0.201	2.88	1.184	0.84	127.5	1.071
28	8.53	0.2535	3.58	1.2	0.656	160.7	1.054
29	10.76	0.3195	4.43	1.222	0.511	202.5	1.034
			58% GLYCEROL SOLUTION				
30	2.13	0.063	0.0882	1.53	0.275	302	0.83

TABLE B-1 (continued)

Run No.	q cc/sec.	V cm/sec.	$\Delta P\times10^{-4}$ dyne/cm^2	$K\times10^4$ cm^2	$f_K\times10^{-2}$ Dimensionless	$N_{Re}\times10^4$ Dimensionless	$f_K\times N_{Re}$
31	3.39	0.1007	0.1588	1.356	0.1935	483	0.934
32	4.28	0.1262	0.206	1.31	0.16	605	0.968
33	5.38	0.16	0.253	1.35	0.1222	766	0.936
34	6.76	0.2	0.3235	1.325	0.1	959	0.959
35	8.53	0.254	0.418	1.3	0.08	1218	0.974
36	10.76	0.321	0.524	1.31	1.0629	1538	0.966
37	13.6	0.403	0.676	1.275	0.0515	1930	0.994
38	17.06	0.505	0.864	1.25	0.419	2420	1.015
39	21.52	0.636	1.088	1.25	0.0333	3045	1.014
40	27.25	0.806	1.372	1.256	0.02615	3860	1.01
41	34.35	1.015	1.723	1.26	0.0207	4860	1.006
				TAP WATER			
42	10.76	0.321	0.0809	0.916	0.01118	12380	1.384
43	13.6	0.403	0.1029	0.905	0.00902	15530	1.4
44	17.06	0.505	0.1322	0.882	0.00738	19460	1.434
45	21.52	0.636	0.1983	0.74	0.00698	24500	1.71
46	27.25	0.806	0.228	0.816	0.005	31000	1.55
47	34.35	1.015	0.3015	0.779	0.00416	39100	1.625
48	42.8	1.262	0.404	0.722	0.00361	48700	1.758

TABLE B-2

FLOW BEHAVIOR PARAMETERS OF 0.2% SEPARAN

Run No.	q cc/sec.	V cm/sec.	$\Delta P \times 10^{-4}$ dyne/cm^2	H grcm^{-n}sec.$^{n-2}$	$f_K \times 10^{-2}$ Dimensionless	$N_{Re} \times 10^3$ Dimensionless
1	0.431	0.01272	1.049	0.202	92.6	0.1436
2	0.685	0.02025	1.186	0.202	41.3	0.318
3	0.835	0.0247	1.28	0.202	29.9	0.438
4	1.07	0.0316	1.3	0.202	18.58	0.624
5	1.49	0.0441	1.47	0.202	10.81	1.134
6	1.717	0.0508	1.586	0.202	8.8	1.436
7	2.13	0.063	1.739	0.202	6.19	2.065
8	2.17	0.0642	1.835	0.202	6.27	2.1
9	2.725	0.0805	1.911	0.202	4.21	3.06
10	3.39	0.103	2.1	0.202	2.82	4.6
11	3.42	0.1011	2.31	0.202	2.93	4.47
12	4.27	0.1262	2.43	0.202	2.18	6.45
13	4.28	0.1262	2.31	0.202	2.07	6.45
14	5.38	0.16	2.6	0.202	1.45	9.57
15	5.41	0.1602	2.7	0.202	1.45	9.57
16	6.76	0.2	2.87	0.202	1.02	13.9
17	6.84	0.202	3.12	0.202	1.07	14.1

TABLE B-2 (continued)

Run No.	q cc/sec.	V cm/sec.	$\Delta P \times 10^{-4}$ dyne/cm^2	H grcm^{-n}sec.$^{n-2}$	$f_K \times 10^{-2}$ Dimensionless	$N'_{Re} \times 10^3$ Dimensionless
18	8.53	0.254	3.265	0.276	0.72	17.58
19	8.58	0.254	3.46	0.276	0.77	17.58
20	10.76	0.321	3.82	0.276	0.53	24.8
21	10.84	0.321	4.11	8.276	0.57	24.8
22	13.6	0.403	4.37	0.276	0.38	35.3
23	13.62	0.403	4.66	0.276	0.409	35.3
24	17.06	0.505	5.28	0.276	0.295	50.1
25	17.19	0.507	5.4	0.276	0.3	50.6
26	21.52	0.636	6.28	0.276	0.221	71.8
27	27.25	0.806	7.7	0.276	0.1693	104
28	34.35	1.015	9.56	0.267	0.132	149

TABLE B-3

PREDICTED PRESSURE DROPS BY BERGELIN'S CORRELATION--0.2% SEPARAN

Run No.	q cc/sec.	n Dimensionless	m_1 $\mathrm{grcm}^{-1}\mathrm{sec}^{n-2}$	σ_w sec^{-1}	μ Poise	ΔP_B $\mathrm{dyne/cm}^2$
1	0.431	0.346	10	2.1	6.2	1.02
2	0.685	0.346	10	3.34	4.8	1.258
3	0.835	0.346	10	4.07	4	1.277
4	1.07	0.346	10	5.21	3.5	1.432
5	1.49	0.346	10	7.26	2.6	1.482
6	1.717	0.346	10	8.36	2.5	1.64
7	2.13	0.346	10	10.4	2.2	1.79
8	2.17	0.346	10	10.5	2.2	1.82
9	2.725	0.346	10	13.3	1.9	1.976
10	3.39	0.346	10	16.5	1.6	2.07
11	3.42	0.346	10	16.9	1.6	2.09
12	4.27	0.346	10	20.8	1.4	2.28
13	4.28	0.346	10	20.8	1.4	2.29
14	5.38	0.346	10	26.2	1.2	2.46
15	5.41	0.346	10	26.3	1.2	2.48
16	6.76	0.346	10	33	1.05	2.71
17	6.84	0.346	10	33.3	1.05	2.71

TABLE B-3 (continued)

Run No.	q cc/sec.	n Dimensionless	m_1 $grcm^{-1}sec^{n-2}$	σ_w sec^{-1}	μ Poise	ΔP_B $dyne/cm^2$
18	8.53	0.443	7.5	36.2	1	3.26
19	8.58	0.443	7.5	36.4	1	3.28
20	10.76	0.443	7.5	45.7	0.86	3.53
21	10.84	0.443	7.5	46	0.86	3.56
22	13.6	0.443	7.5	57.7	0.74	3.85
23	13.62	0.443	7.5	57.9	0.74	3.86
24	17.06	0.443	7.5	72.4	0.64	4.17
25	17.19	0.443	7.5	73	0.64	4.2
26	21.52	0.443	7.5	91.2	0.58	4.76
27	27.25	0.443	7.5	115.5	0.5	5.21
28	34.35	0.443	7.5	138.6	0.44	5.77

APPENDIX C

CONSTRUCTION OF VELOCITY PROFILE FROM STREAK LENGTH

As was mentioned in Section III-4-2, the length of the streaks and openings were taken from 0.1-inch division graph paper at total magnification of 100. Data points presented in Appendix E and the local velocity profile plotted in Figure (IV-7 to 12) are based on this magnified scale. However, the scale given in the plots has been chosen so that the profiles present the dimensionless interstitial velocity, i.e. u/V v.s. position. The RPM's reported in Tables (E-1, 2) are based on the chopper disk with one radial slit. That is, if the experimental RPM was 25 revolution per minute with a 4-slit chopper disk, it would be reported 100 RPM. Because the time duration of every period of opening or closing the light would be same for a 4-slit chopper at 25 RPM as for one-slit at 100 RPM. For every rotating disk, one can write,

$$t = \frac{60}{\text{RPM}} \quad \text{sec/rev.} \tag{C-1}$$

where t, is the duration of one revolution. For a one-slit chopper disk,

$$t_P = \frac{60}{\text{RPM}} \times \frac{1}{2} = \frac{30}{\text{RPM}} \quad \text{sec.} \tag{C-2}$$

where t_P is the time of every period of opening or closing the light. Therefore, taking s as the length of streak, the velocity is calculated by,

$$u = \frac{s}{t_p} = \frac{RPM}{30} s. \qquad \text{(C-3)}$$

The flow rate passing through each opening is obtained by,

$$q_i = \ell \int_0^d u dx, \qquad \text{(C-4)}$$

where x-direction is shown in Figure (V-1). Substituting (C-3) into (C-4),

$$q_i = \frac{RPM}{30} \ell \int_0^d s dx. \qquad \text{(C-5)}$$

The area under the velocity profiles, A_V, is obtained by,

$$A_V = \int_0^d u dx = \frac{RPM}{30} \int_0^d s dx. \qquad \text{(C-6)}$$

However, the plots in Figures (IV-7 to 12) are u/V v.s. x. Therefore, the area under the profiles, A_i, which have been presented for three positions in Figures (IV-7 to 12), is given by,

$$A_i = \frac{A_V}{V} = \frac{RPM}{30V} \int_0^d s dx. \qquad \text{(C-7)}$$

A_i's are recorded in Table (C-1). Comparing (C-5) with (C-7), q_i can be obtained in terms of A_i,

$$q_i = A_i \ell V. \qquad \text{(C-8)}$$

It is understood from Tables (E-1, 2) that all the lengths are reported in inches, i.e.

$$d = 2.54 d_M,$$

$$s = 2.54S,$$

$x = 2.54\ X$.

Total volumetric flow rate can be obtained by using sum of the A_i's for each row in place of A_i in Equation (C-8). These values were in a good agreement with the flow rates measured by the formerly calibrated pump. For instance, for the Glycerol solution,

row No. 20 $\rightarrow\rightarrow\rightarrow\rightarrow$ $\Sigma A_i = 6.632$ cm.

row No. 21 $\rightarrow\rightarrow\rightarrow\rightarrow$ $\Sigma A_i = 6.497$ cm.

row No. 22 $\rightarrow\rightarrow\rightarrow\rightarrow$ $\Sigma A_i = 6.567$ cm.

Therefore, the calculated flow rate from Equation (C-8) in the case of minimum flow rate, i.e. $q = 0.685$ cc/sec. or $V = (0.685/33.8)$cm/sec.

row No. 20 $\rightarrow\rightarrow\rightarrow\rightarrow$ $q = 0.698$ cc/sec.

row No. 21 $\rightarrow\rightarrow\rightarrow\rightarrow$ $q = 0.684$ cc/sec.

row No. 22 $\rightarrow\rightarrow\rightarrow\rightarrow$ $q = 0.691$ cc/sec.

and for the Separan solution,

row No. 21 $\rightarrow\rightarrow\rightarrow\rightarrow$ $\Sigma A_i = 5.956$ cm.

row No. 22 $\rightarrow\rightarrow\rightarrow\rightarrow$ $\Sigma A_i = 6.142$ cm.

Therefore, the calculated flow rate,

row No. 21 $\rightarrow\rightarrow\rightarrow\rightarrow$ $q = 0.628$ cc/sec.

row No. 22 $\rightarrow\rightarrow\rightarrow\rightarrow$ $q = 0.648$ cc/sec.

TABLE C-1

OPENINGS, d, AREA UNDER THE DIMENSIONLESS VELOCITY PROFILES, A_i, AND FRACTIONAL FLOW RATES, q%

Position No.	$d \times 10^2$, cm.		$A_i \times 10^3$, cm.		q%	
	Glycerol	Separan	Glycerol	Separan	Glycerol	Separan
ROW NO. 20						
1	7.5	7.5	1193	1891	18.4	31.3
2	5.69	5.21	720	562	11.1	9.29
3	5.08	5.08	488	?	7.51	?
4	5.74	4.57	493	400	7.59	6.61
5	5.64	4.87	437	340	6.73	5.63
6	6.7	6.7	673	451	10.37	7.45
7	5.49	5.49	392	337	6.04	5.57
8	5.71	5.71	467	312	7.18	5.16
9	7.87	6.66	901	528	13.89	8.74
10	4.9	4.9	446	512	6.86	8.46
11	3.68	3.68	422	440	6.5	7.27
ROW NO. 21						
12	40	37.1	1877	2380	28.9	39.25
13	6.35	6.35	326	249	5.03	4.9
14	6.6	6.6	509	402	7.84	6.82
15	6.1	5.51	424	374	6.53	6.17
16	6.12	5.59	502	297	7.72	4.91
17	5.26	4.96	356	252	5.49	4.17
18	6.76	6.76	710	418	10.93	6.19
19	5.21	5.21	401	288	6.17	4.75
20	5.44	5.44	382	286	5.88	4.73
21	32.8	32.8	1010	1010	15.56	16.64
ROW NO. 22						
22	5.94	5.94	986	1660	15.2	27.45

TABLE C-1 (continued)

Position Nol	$dx10^2$, cm. Glycerol	$dx10^2$, cm. Separan	A_ix10^3, cm. Glycerol	A_ix10^3, cm. Separan	q% Glycerol	q% Separan
23	6,99	5.14	991	1038	15.27	17.13
24	5.59	5.59	378	300	5.83	4.96
25	6.7	6.7	790	461	12.16	7.61
26	5.41	5.08	417	301	6.41	4.98
27	5.67	5.21	399	318	6.14	5.26
28	5.11	5.11	369	258	5.69	4.26
29	6.76	6.76	734	451	11.3	7.45
30	5.46	5.46	557	381	8.57	6.29
31	4.96	4.96	509	510	7.84	8.42
32	3.3	3.3	437	464	6.73	7.67

NOTE: q% for Separan are based on average ΣA_i of row No. 21 and 22, while q% for Glycerol are based on the minimum total flow rate, i.e. q = 0.685 which is equivalent to A_i = 6.49 cm.

APPENDIX D

FLOW THROUGH PARALLEL PLATES--POWER LAW MODEL

The equation of motion can be, easily, solved for a power-law fluid flow through two parallel plates to obtain the velocity profile. The direction of the coordinates are given in Figure (II-2)

$$u_z = m_1^{-\frac{1}{n}} \frac{n}{1+n} \left(\frac{\Delta P}{\Delta L}\right)^{\frac{1}{n}} R^{\frac{1+n}{n}} \left[1-\left(\frac{x}{R}\right)^{\frac{1+n}{n}}\right] \qquad \text{(D-1)}$$

where m_1 and n are power-law model parameters and $R = d/2$ shown in Figure (II-2). Also,

$$\frac{q}{\ell} = 2\int_0^R u_z \, dx. \qquad \text{(D-2)}$$

After ingegrating with Equation (D-1)

$$\frac{q}{\ell} = 2m_1^{-\frac{1}{n}} \frac{n}{1+2n} \left(\frac{\Delta P}{\Delta L}\right)^{\frac{1}{n}} R^{\frac{1+2n}{n}} . \qquad \text{(D-3)}$$

Equations (D-1) and (D-3) may approximate the rectilinear flow through the bundle of glass rods, assuming that the minimum center line opening between two contiguous rods of the same row, with length ℓ, is d and the flow rate passing through that opening is q_i. Therefore,

$$u_z = m_1^{-\frac{1}{n}} \frac{n}{1+n} \left(\frac{\Delta P}{\Delta L}\right)^{\frac{1}{n}} \left(\frac{d}{2}\right)^{\frac{1+n}{n}} \left[1-\left(\frac{2x}{d}\right)^{\frac{1+n}{n}}\right], \qquad \text{(D-4)}$$

$$\frac{q_i}{\ell} = 2m_1^{-\frac{1}{n}} \frac{n}{1+n} \left(\frac{\Delta P}{\Delta L}\right)^{\frac{1}{n}} \left(\frac{d}{2}\right)^{\frac{1+n}{n}} . \qquad \text{(D-5)}$$

where $\frac{\Delta P}{\Delta L}$ is unknown, but can be eliminated by dividing Equation (D-4) by (D-5). Hence,

$$u_z = \frac{1+2n}{1+n} \frac{q_i}{\ell d} [1-(\frac{2x}{d})^{\frac{1+n}{n}}] , \quad \text{(D-6)}$$

where q_i is known experimentally. Therefore, the velocity profile can be established for each opening. Also, by setting $x = 0$, the maximum velocity at center line opening can be obtained, i.e.

$$u_{max} = \frac{1+2n}{1+n} \frac{q_i}{\ell d} . \quad \text{(D-7)}$$

From Equation (D-5) one can write,

$$q_i = C_5 d^{(1+2n)/n} \quad \text{(D-8)}$$

where C_5 is a constant. Equation (D-8) is based on the assumption that $\Delta P/\Delta L$ is the same for all the openings.

Equations (D-6, 7, 8) can be applied to a Newtonian fluid by setting $n = 1$, i.e.

$$u_z = \frac{3}{2} \frac{q_i}{\ell d} [1-(\frac{2x}{d})^2], \quad \text{(D-9)}$$

$$u_{max} = \frac{3}{2} \frac{q_i}{\ell d} , \quad \text{(D-10)}$$

$$q_i = C_6 d^3 . \quad \text{(D-11)}$$

Equations (D-6, 7) can, also, be written in terms of the dimensionless velocity,

$$\frac{u_z}{V} = \frac{1+2n}{1+n} \frac{q_i}{\ell d V} [1-(\frac{2x}{d})^{\frac{1+n}{n}}], \quad \text{(D-12)}$$

$$\frac{u_{max}}{V} = \frac{1+2n}{1+n} \frac{q_i}{\ell dV}. \tag{D-13}$$

Using Equation (C-8),

$$\frac{u_z}{V} = \frac{1+2n}{1+n} \frac{A_i}{d} [1-(\frac{2x}{d})^{\frac{1+n}{n}}], \tag{D-14}$$

$$\frac{u_{max}}{V} = \frac{1+2n}{1+n} \frac{A_i}{d}. \tag{D-15}$$

For Newtonian fluids,

$$\frac{u_z}{V} = \frac{3}{2} \frac{A_i}{d} [1-(\frac{2x}{d})^2], \tag{D-16}$$

$$\frac{u_{max}}{V} = \frac{3}{2} \frac{A_i}{d}. \tag{D-17}$$

The calculated values of u_{max}/V by Equations (D-15, 17) are recorded in Table (V-2) and the velocity profiles obtained from Equations (D-14, 16) have been shown in Figure (IV-13) for three positions.

APPENDIX E

EXPERIMENTAL DATA POINTS

The complete data points of row No. 21 for the volumetric flow rate of 0.685 cc/sec, and the complete data points of one arbitrary position in each row will be presented. For the other rows and other flow rates only a few necessary points to show the shape of the profiles will be given. The RPM reported in the following tables are based on the chopper disk with one radial slit--refer to Appendix C for more details. The pictures are labeled by the number of rolls and the number of exposure, E. The reported data in the following tables have already been converted to the same RPM. The necessary correction due to the error of the stroboscope reading mentioned in Section (III-4-1 b) is also included in the reported data.

The length of the streaks, S, position X, and the openings, d_M, were read directly from the 0.1 - inch division graph paper on which the pictures were projected and the total magnification was 100 in all cases. The procedure to analyze the data points was discussed in Appendix C. The position numbers are presented in Figure (III-3) and the direction of X and the origin with respect to the light and flow direction is given in Figure (E-1).

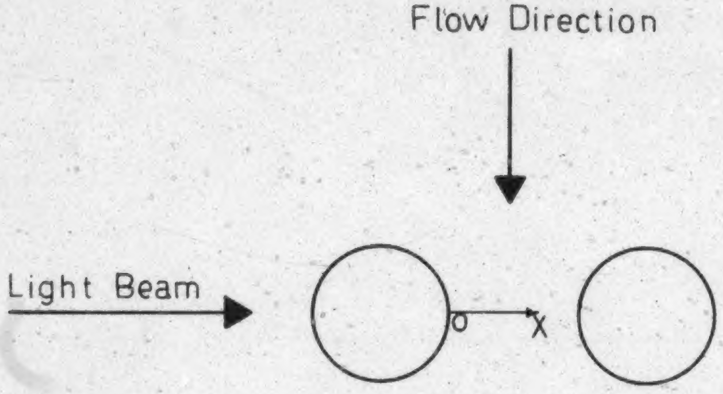
Flow Direction
Light Beam
o
x

FIGURE E-1 DIRECTION OF X AND THE POSITION OF ORIGIN WITH RESPECT TO THE LIGHT AND FLOW DIRECTION

TABLE E-1

STREAK LENGTH DATA OF GLYCEROL

Xx10^3 Inch	Sx10^3 Inch	Xx10^3 Inch	Sx10^3 Inch	Xx10^3 Inch	Sx10^3 Inch	Xx10^3 Inch	Sx10^3 Inch
Position No. 1		55	15.5	E19		NCL=62x10^{-3}in.	
		73	15.1	7.5	42.6	4.8	5.8
Roll No. 238		79	15.1	NCL=40x10^{-3}in.		23	19.5
NCL=91x10^{-3}in.		86	14.6	E17		32	20.7
q=0.685cc/sec.				10.5	18.5	44.6	11.8
RPM=100		q=3.42cc/sec.		22	22.2	48.2	5
E1		RPM=500		31	17.8	E12	
12	6.3	E11		E18		3	3.1
29	11.1	10	6.4	25	22.2	4.5	9
37	12.9	32	12.6	E19		12.5	12.4
42	14.8	37	13.5	16	22.2	19.5	17
47	15.5	47	14.2	E20		23.5	18.2
58	15.9	63	15.4	32	18.5	43.6	13.3
61	15.9	71	15.2	NCL=62x10^{-3}in.		50	7.4
82	14.8	86	15.2	E18		55	3.8
91	14.8			26.7	19.6	E13	
E2		q=6.82cc/sec.		27.1	20	12	12.4
25	11.1	RPM=1000		33.6	18.5	24	16
44	14.8	E16		35	18.1	29	19.2
51	15.5	77	15.6	E19		35.8	17
64	14.8	50	15.6	19.5	14.8	38.7	15.4
74	15.5	E17		21.8	18.5	44.3	12.6
83	15.5	50	15.6	36.5	17.4	E14	
		55	15.6	58.3	2.96	9	10.1
q=1.717cc/sec.		82	15.2			25	16.7
RPM=250		E18		q=1.717cc/sec.		E15	
E6		40	15.2	RPM=250		3.4	3.1
12	6.9	53	15.2	d=20.5x10^{-3}in.		21.5	17.8
34	13.3			E11		50	9.6
44	14.1	Position No. 2		1.1	12.6		
54	15.2			NCL=40x10^{-3}in.		q=3.42cc/sec.	
57	15.5	Roll No. 239		E11		RPM=500	
66	16.1	d=20.5x10^{-3}in.		2.5	5.9	NCL=40x10^{-3}in.	
76	15.5	q=0.685cc/sec.		35.4	13	E6	
79	15.5	RPM=100		E12		7	11.5
91	14	E16		1.6	3.7	37	6.2
E7		5.2	33.3	6	10.1	NCL=62x10^{-3}in.	
22	9.9	15.5	40.7	E15		E6	
35	13.5	E18		3.7	6.2	3.4	3.9
51	15.5	12.4	44.4	17	22.2	7.4	8.5

TABLE E-1 (continued)

$X\times10^3$ Inch	$S\times10^3$ Inch	$X\times10^3$ Inch	$S\times10^3$ Inch	$X\times10^3$ Inch	$S\times10^3$ Inch	$X\times10^3$ Inch	$S\times10^3$ Inch
10.2	10.9	41	12.6			E1	
18	16.2	44.4	10.9	q=6.82cc/sec.		37.5	15.8
22.5	15.5	48	8.6	RPM=1000		57.8	2.4
33.4	18.5	52.2	5.4	NCL=62×10^{-3}in.		E2	
35	17.7	54.2	3.7	E1		9.9	9.9
39.5	12.8	E18		7.6	8.4	15.8	14
45.5	10.1	4.5	5.4	E2		42	13.1
52.8	4.7	15	15.4	6.2	7.7	43.3	11.8
56.4	2.7	18.6	18.7	10.2	10.9	47	9.6
E7		22	17.7	30.7	17.7	E3	
9.2	10.3	27.6	19.8	56	3.3	27.5	16.8
12	12.8	30.5	19.4	E3		51	7.2
14	13.5	39	16.8	37	15.2	E5	
45	9.6	50.5	7.6	55.6	3.5	7	6.9
49	7.2	NCL=40×10^{-3}in.		E4		12.8	9.1
56	2.6	E11		5.4	6.1	43.5	12
E8		14.8	18.8	50	6.7		
3.6	5.7	24	24	E5		Position No. 3	
18.1	18.5	35	8.8	2	3		
32	15.8	E13		6.2	7.8	Roll No. 263	
33.3	16.8	4.6	10.9	49	8.4	NCL=58×10^{-3}in.	
37.5	14.5	16	22.8	54.5	3.8	q=0.685cc/sec.	
39	13.5	E14		E6		RPM=100	
46	9.9	3.8	8.3	40	14.3	E16	
55.8	3	34	10.1	53	5.3	20	11
E9		E15		56.3	3	22	12.4
8	8.5	11.8	16.8	E7		33	13.2
21.8	16.5	28	19.4	4	4.4	35.8	9.9
34.4	19.4	34.4	12.6	E8		41	8
38	14.5	E16		7	8.6	47	6.2
41	14.5	1.6	3.9	30	16.9	50.5	4
E10		8.5	15.2	51	6.7	E17	
5	4.9	17.2	23.6	E9		10.4	5.9
17.8	14.2	31.3	16.1	9	12.2	14.8	9.1
36.5	16.1	E17		21	15	24.2	12.8
52.5	6.2	29.5	17.7	24	14.7	31.8	12.1
Roll No. 262		E18		32.5	15.2	35	12.1
E11		11.8	23.4	34.3	14.7	36.8	12.1
3	5.9	14	22.4	E10		47.4	6.6
19	18.9	28.3	20.2	30.5	16.4		
21.7	19.4	E19		50.7	6.2	q=1.717cc/sec.	
25.5	22.8	31.6	18.5	52.5	5.6	RPM=250	
31.6	18.5	E20		55.5	3.4	E11	
33.8	17.7	16	21.1	Roll No. 239		3.4	2.5

TABLE E-1 (continued)

Xx10^3 Inch	Sx10^3 Inch	Xx10^3 Inch	Sx10^3 Inch	Xx10^3 Inch	Sx10^3 Inch	Xx10^3 Inch	Sx10^3 Inch
8.8	5.1	q=0.685cc/sec.				15	9.9
29.4	13.2	RPM=100		q=3.42cc/sec.		22	14.1
39.4	9.4	NCL=57x10^{-3}in.		RPM=500		38	6.2
44.8	7	E1		E9		E13	
48	5.1	15.2	10.2	30	14.4	7.2	5.9
53	2.2	18.8	11.7	44	8.1	9.8	7.4
E12		24.4	13.2	E10		16	10.4
5	3.7	32.5	13.9	5	4.2	40.5	6.1
7.8	4.7	37.5	12.4	34	11.8		
11	6.6	43.7	8	44.2	7.6	q=3.42cc/sec.	
27	11.7	48	5.5	49.5	4.6	RPM=500	
38	10.7	NCL=37x10^{-3}in.		E11		E6	
47	5.9	10.8	15.4	9	5	17.4	11.8
49.5	4	27.3	15.7	49	6.6	30.4	12.9
55	1.76	30	9.1			E7	
		32	8.8	q=6.82cc/sec.		5	4.2
q=3.42cc/sec		34.3	5.5	RPM=100		26	11.3
RPM=500		E2		E15		31.5	11.8
E1		17.4	18.3	28	13.5	E8	
11.5	6.2	25.8	14.6	32.4	13.7	15	9.9
19.3	10.3	28.3	11			24.6	12.6
35.5	11.3	NCL=57x10^{-3}in.		Position No. 5			
46.8	5.7	25.5	14.3			q=6.82cc/sec.	
E2		38.2	11	Roll No. 265		RPM=1000	
8	4.2	41.5	8.8	q=0.685cc/sec.		E1	
20	12.3	46	5.9	RPM=100		29.4	11.8
48	5.4	49	3.7	NCL=48.2x10^{-3}in.		E3	
51.5	3.3			E16		8.9	5.9
		q=1.717cc/sec.		13.4	10	29	9.7
q=6.82cc/sec.		RPM=250		17	12.2	39	6.7
RPM=1000		E5		24.5	14	E4	
E6		NCL=37x10^{-3}in.		40.5	7.4	22	12.2
7.4	5.4	12	17.9	43	5.5		
E7		NCL=57x10^{-3}in.		E17		Position No. 6	
11	6.2	11	8.8	20.5	13.3		
44	7.2	19	12.5	27	13.3	Roll No. 243	
E8		35.3	12.9	43.5	4.4	q=0.685cc/sec.	
21.2	11.2	45	6.4			RPM=100	
E9		E6		q=1.717cc/sec.		NCL=43x10^{-3}in.	
5	3.5	10.5	7.2	RPM=250		E16	
		13	7.9	E11		6.6	11.3
Position No. 4		24	13.9	23	14.1	11.2	15.7
		31	13.6	42	5.2	18.7	22
Roll No. 264		45	6.6	E12		20	23.8

TABLE E-1 (continued)

Xx10^3 Inch	Sx10^3 Inch	Sx10^3 Inch	Xx10^3 Inch	Sx10^3 Inch	Xx10^3 Inch	Sx10^3 Inch	Xx10^3 Inch
21.5	24.2	E14				5	25.2
28	22.3	32.7	17.5	8	12.6	10.3	31
32	18.3	E15		17	18.3	15.5	26.3
38	11	14	8.1	17.9	18.7		
E17		E16		21.4	16.8	q=1.717cc/sec.	
8.6	12.8	8.8	6.2			RPM=250	
34.8	12.4	48	10.9	q=3.42cc/sec.		E11	
				RPM=500		1	6.8
q=1.717cc/sec.		q=6.82cc/sec.		E11		4.1	19.3
RPM=250		RPM=1000		2.2	3.6	6.1	25.5
E11		E2		5	9.3	12.4	29.1
7	12.3	16	13.1	10.5	11.8	E12	
16.6	21	E3		16.5	15.2	1.2	12.1
23.3	22.7	7	4.6	21.3	15.5	3	17.6
32	16.3	11.8	8.8	E12		5.4	23.8
E12				5	8.5	12.2	28.8
7.3	11.6	Position No. 7		6.3	10.1	14	25.9
16.5	19.5			12.5	16.8	17.7	14.5
26	20.5	Roll No. 244		22.1	12.6		
E13		q=0.685cc/sec.				q=3.42cc/sec.	
10	12	RPM=100		q=6.822cc/sec.		RPM=500	
11	14.6	NCL=32.8x10^{-3}in.		RPM=1000		E6	
20.6	23.4	E1		E16		2.1	13.5
		5.2	9.1	4.8	5.7	3.8	18.5
q=3.42cc/sec.		10	14.3	23	13	4.8	22.3
RPM=500		13	16.5	E17		E7	
E6		17.7	16.5	1.2	2.6	2	8.3
4.5	8.1	27.2	9.9	24.5	10.5	4.1	18.5
15	18.5	E2		E18		12.8	26.3
31.4	16.8	8	12.4	1	2.1		
35	12.9	16	18.6	26.8	7.4	q=6.82cc/sec.	
37	10.1					RPM=1000	
E7		q=1.717cc/sec.		Position No. 8		E3	
3.4	6.6	RPM=250				11.4	26.7
Roll No. 266		E6		Roll No. 245		8	25.3
NCL=63x10^{-3}in.		5	8.8	q=0.685cc/sec.		17.5	20.4
E11		13.8	16.1	RPM=100		E5	
13	6.9	18	22	d=22.5x10^{-3}in.		3.4	16
E12		23	16.1	E16		17.3	17.1
11.5	7.8	d=21.6x10^{-3}in.		3	15.1		
35	19.9	12	24.9	7	27	Position No. 9	
E13		NCL=32.8x10^{-3}in.		14.4	25.9		
35.2	16.8	E7		19	10.8	Roll No. 246	
47.3	11.8	6	8.1	E17		q=0.685cc/sec.	

TABLE E-1 (continued)

$X \times 10^3$ Inch	$S \times 10^3$ Inch
RPM=100	
$d=31 \times 10^{-3}$ in.	
E1	
11.6	43.2
14	43.2
15.3	43.2
21.5	35.3
24.5	23.8
E2	
7	32.4
11.4	39.6
21	37.8
q=1.717cc/sec.	
RPM=250	
E6	
4.5	21.6
16.2	40.3
21	33.1
26	22
E7	
20	36
23.2	27
q=3.42cc/sec.	
RPM=500	
E11	
1.2	9.8
28	8.1
E13	
2	9.3
22.2	30.3
E14	
6	29
15.5	40.5
3.7	22
q=6.82cc/sec.	
RPM=1000	
E17	
16.2	38.3
Position No. 10	

$X \times 10^3$ Inch	$S \times 10^3$ Inch
Roll No. 247	
q=0.685cc/sec.	
RPM=100	
$d=19.3 \times 10^{-3}$ in.	
E19	
10.8	29.6
E20	
14	26.2
E21	
8.9	34
10.3	29.6
15.2	23.2
q=1.717cc/sec.	
RPM=250	
E11	
13.8	22.2
E13	
12	28
q=3.42cc/sec.	
RPM=500	
E6	
16	12.6
E7	
14	20.6
E8	
10	32.2
12.4	19.1
E9	
13.8	22
E10	
15	10.9
q=6.82cc/sec.	
RPM=1000	
E1	
4.5	26.1
Position No. 11	
Roll No. 248	
q=0.685cc/sec.	
RPM=100	

$X \times 10^3$ Inch	$S \times 10^3$ Inch
$NCL=64 \times 10^{-3}$ in.	
E1	
2.7	9.2
5.7	9.2
14.6	9.2
40	4.8
E2	
4.4	9.2
5.3	9.2
10	9.2
34	4.5
40	4.5
45.5	4.1
q=1.717cc/sec.	
RPM=250	
E6	
2.5	9.6
4	9.6
11	9.6
19	8.1
36	6.2
42	5.2
50	3.7
E7	
1	9.7
3	9.7
17	8.7
23	8
44	4.7
53	3
q=3.42cc/sec.	
RPM=500	
E11	
0	9.8
10.5	9.5
28	6.7
E12	
0	9.6
8	9.5
13	9.5
21	8.5
38	5.9

$X \times 10^3$ Inch	$S \times 10^3$ Inch
45	4.6
q=6.82cc/sec.	
RPM=1000	
E16	
9	8.8
38	6.1
47	4.2
56	2.2
60	1.1
E17	
28	7.4
33	6.5
46	4.6
59	1.7
Position No. 12	
Roll No. 228	
q=0.685cc/sec.	
RPM=100	
$d=157.5 \times 10^{-3}$ in.	
E16	
17.6	6.98
36	11.76
39.5	12.85
42.3	12.85
76.6	15.8
E17	
41.5	13.22
58	14.7
70.4	16.52
E18	
41	13.22
44.4	13.22
61.8	16.15
E19	
17	6.24
42	13.6
63.8	15.42
74	16.52
92	16.52
97.4	15.42
138.4	8.45

TABLE E-1 (continued)

Xx10^{3} Inch	Sx10^{3} Inch	Xx10^{3} Inch	Sx10^{3} Inch	Xx10^{3} Inch	Sx10^{3} Inch	Xx10^{3} Inch	Sx10^{3} Inch
E20		90	16.1	27.7	7.35	9.4	17.8
11.5	6.24	E3		E2		E7	
15	6.24	28	10.6	5.6	9.2	24	3.68
43	13.22	139	7.1	8.2	11	E8	
66.7	15.8			12.6	12.1	10.6	18.8
80.6	16.52	Position No. 13		15.3	14.7	E9	
				18.3	13.2	4.4	11.7
q=1.717cc/sec.		Roll No. 229		22.5	11.75	7.5	16.4
RPM=250		q=0.685cc/sec.		29	4.77	14.6	16.1
E11		RPM=100		E3		22.3	3.08
21	8.1	d=25x10^{-3}in.		7.4	11		
58	15.7	E1		12.7	12.8	q=3.42cc/sec.	
71.5	16.6	7.4	16.2	14.6	14.3	RPM=500	
74	16.2	9.8	17.3	17.6	13.6	E11	
79	16.9	10.9	19.1	24.4	9.55	13.7	17.1
E12		17.8	16.2	27.5	7.35	E13	
10	4.4	20.6	8.8	E4	9.55	5.1	12.6
16	5.7	E2		3	4.5	9	16.8
19	6.6	7	15.4	9	11	NCL=32.9x10^{-3}in.	
31	10.3	13.6	19.8	14.7	12.8	E11	
		17	16.5	20.5	12.5	10.2	12.8
q=3.42cc/sec.		23.8	2.94	23.6	7.6	18.1	15.2
RPM=500		E3		25	7.6	E13	
E6		5.1	14.3	29	5.9	6.5	10.5
16.7	6.3	6.1	14.3	E5		11.4	13.8
27	9.1	13.4	18.7	3.3	5.14	E14	
33	11.8	21.1	10.3	8	11.7	27.2	6.6
E7		E4		11	13.6		
9	4.3	7	13.6	18.8	14	q=6.82cc/sec.	
23	8.8	14.8	17.6	28	6.24	RPM=1000	
29.5	10.5	21	11			d=25x10^{-3}in.	
44	13.5	E5		q=1.717cc/sec.		E16	
68	15	2.6	6.25	RPM=250		4.8	9.6
103	15.2	3.6	6.6	E6		NCL=70.8x10^{-3}in.	
124	12.2	7	14.7	6.1	7.3	8	1.6
		14.6	18.4	12	13.6	13.4	2.8
q=6.82cc/sec.		19.3	14.7	E7		20	4.8
RPM=1000		NCL=32.9x10^{-3}in.		8	9.5	38.2	7
E1		E1		29.5	2.1	57.5	4.2
19.5	7.6	5.1	8.45	E8		64.4	2.2
23	8.5	8.8	11.4	14.3	13.6	E17	
32	10.9	12	13.6	19.6	12.6	24.3	5.5
E2		14	15.1	d=25x10^{-3}in.		31	6.6
20	7.1	23.5	11	E6		40.6	6.4

TABLE E-1 (continued)

Xx10^3 Inch	Sx10^3 Inch	Xx10^3 Inch	Sx10^3 Inch	Xx10^3 Inch	Sx10^3 Inch	Xx10^3 Inch	Sx10^3 Inch
49	5.7	NCL=45.3x10^{-3}in.		39	9.9	E4	
		E11		E13		19.6	16.5
Position No. 14		6.8	11.5	27	11.8	E5	
		8.8	10.6	30	12.2	27	15.5
Roll No. 230		38	7.9			31.3	11.8
q=0.685cc/sec.		E12		q=6.82cc/sec.			
RPM=100		8	10.3	RPM=1000		q=1.717cc/sec.	
NCL=31.7x10^{-3}in.		9.7	12.5	NCL=45.3x10^{-3}in.		RPM=250	
E16		18	18.4	E1		E6	
3.2	11.4	21.5	16.3	20	16.8	11.5	12.4
10	22.4	24.4	16.2	39	4.2	18.8	18
14.4	21.7	43	3.09	40.2	2.7	E7	
19.8	20.6			E2		35.3	7.8
21.4	17.3	q=3.42cc/sec.		28	13.5	E8	
25	11.8	RPM=500		35	5.6	5	6
E17		NCL=55x10^{-3}in.		E4		13.1	12.7
3.7	9.56	E6		29.4	11.6	20.8	14.7
18.8	22.8	22	10.9			d=24x10^{-3}in.	
E18		38.4	8.6	**Position No. 15**		E8	
5	12.5	E8				2.5	11
7	18.4	9.2	8.5	Roll No. 231			
13.8	24.6	23.5	15.2	q=0.685cc/sec.		q=3.42cc/sec.	
E19		30.5	12.6	RPM=100		RPM=500	
7.4	19.1	41.6	9.3	d=24x10^{-3}in.		Roll No. 261	
10	20.6	E9		E3		NCL=42x10^{-3}in.	
11.6	23.9	5	5	10.6	27.2	E1	
28	9.2	15.6	12.3	E4		2.4	3.7
E20		25.7	12.9	10.5	26.5	10.4	11.8
5.7	16.2	37	11.8	E5		26	13.8
7.8	21	44	6.7	18.3	16.5	28.3	10.9
13	22.1	47	5	NCL=42x10^{-3}in.		34.4	7
14.8	22.8			E1		38.4	3.7
20.6	20.2	Roll No. 260		9	11.8	E2	
23	19.1	NCL=59x10^{-3}in.		10.6	12.9	24.4	12.9
24.3	17.3	E11		17.2	14.7	31.7	8.1
		22.5	9.9	20	14.3	39	2.2
q=1.717cc/sec.		29	12.2	E2			
RPM=250		50	5.9	13	14.7	q=6.82cc/sec.	
d=26x10^{-3}in.		E12		18	16.6	RPM=1000	
E11		1.8	1.18	35.2	6.62	E11	
25	7.2	19	8.9	E3		6	7
4.8	15.5	20.6	10.6	12.5	14.7	26	10.1
E14		27	12.6	20.5	17.7	33.4	6.4
8.8	27.2	36	11.5	26	14.7	E12	

TABLE E-1 (continued)

Xx10^3 Inch	Sx10^3 Inch	Xx10^3 Inch	Sx10^3 Inch	Xx10^3 Inch	Sx10^3 Inch	Xx10^3 Inch	Sx10^3 Inch
25	11.8	28	13.2			23	14.7
28	10.5	36.6	11	Position No. 17		30	8.7
E14		41.3	7.35			E7	
30.4	9.3	47	4.4	Roll No. 233		7	7.3
				q=0.685cc/sec.		10.5	10.3
Position No. 16		q=1.717cc/sec.		RPM=100		20	14.7
		RPM=250		d=19.5x10^{-3}in.		27	11
Roll No. 232		E11		E2		E8	
q=0.685cc/sec.		20	12.5	2.2	7.3	12.7	13.2
RPM=100		23.8	15.3	5.5	20.6	20	14
d=24.1x10^{-3}in.		27	14.3	11.5	22.4	25	13.2
E17		30	12.8	13.5	22	E9	
20	11.4	31.6	13.2	E4		4	7.8
21	12.1	38	9.1	15	18.4	11.8	11.7
E18		46.4	3.7	17	18.4	17.3	14.7
21.8	6.6	d=24.1x10^{-3}in.		E5		E10	
E19		E11		10	24.6	2.8	4.7
9.5	31.2	19.6	11.5	NCL=35.2x10^{-3}in.		4	6.6
15.5	24.2	E13		E1		8	8.8
21.3	9.18	17	20.6	8.8	10.6	10.8	12.2
E20		E14		23	11.7	20	12.6
16.5	19.8	18.2	12.5	26	10.6	31	4.4
NCL=52x10^{-3}in.		E15		E2		d=19.5x10^{-3}in.	
E16		15.3	23.1	4.8	6.24	E6	
29	14.7	19.8	15.7	8.5	11.4	10.8	24.2
45.3	5.5			11.8	14.3	E7	
E17		q=3.42cc/sec.		22.5	14.7	12.8	22.3
28.5	15.06	RPM=500		25.5	11	11	23.5
30.6	12.5	NCL=52x10^{-3}in.		27.4	8.45	E9	
39	8.44	E7		E3		2	11.5
45.3	5.5	16.4	13.5	29	7.3		
E18		23.5	14.5	E4		q=3.42cc/sec.	
31.3	12.8	42	5.9	23	14	RPM=500	
33	12.8	48.5	2.3	26.5	11	NCL=35.2x10^{-3}in.	
45	4.8			31	5.5	E11	
E19		q=6.82cc/sec.		E5		14.6	12.9
20	13.6	RPM=1000		10.3	14.3	16.4	12.2
22	14.3	E1		18.2	15.1	20	16.1
26	15.4	23	13.2			25	12.5
32.6	12.5	26	12	q=1.717cc/sec.		31.3	4.2
41	8.1	35	10.9	RPM=250		E12	
45.6	4.04	42	7.5	E6		8	8.6
E20		d=24.1x10^{-3}in.		15	13.2	13	11.8
14.7	13.2	15.5	22	19	15.4	16.4	14.8

TABLE E-1 (continued)

$X \times 10^3$ Inch	$S \times 10^3$ Inch	$X \times 10^3$ Inch	$S \times 10^3$ Inch	$X \times 10^3$ Inch	$S \times 10^3$ Inch	$X \times 10^3$ Inch	$S \times 10^3$ Inch
17.6	13.6			12.2	19.6		
19.2	14.3	Position No. 18		18	24.1	q=3.42cc/sec.	
22.8	12.6			22.8	24.8	RPM=500	
E13		Roll No. 234		23.8	24.8	E6	
8.4	10.9	q=0.685cc/sec.		29	21.9	23.9	14.8
13	14.5	RPM=100		32	18.9	E7	
26	9.6	d=26.6×10^{-3} in.		35.4	14.4	11.8	34.2
E15		E16		40	9.25	14.5	32.1
6.7	8.6	4.5	20.4	E20		21	22.3
30.4	5.9	E18		7.6	14.8	E8	
15.4	12.6	2.8	15.5	9.5	16.3	12.3	35.5
		8	29.6	12	18.9	NCL=45×10^{-3} in.	
q=6.82cc/sec.		13	38.2	13.5	21.1	E6	
RPM=1000		16.7	32.6	18.4	24.1	2	5
E17		21.6	20.7	20.8	24.8	20	23.6
7	8.5	E19		33	17.8	26	18.5
13.3	13.9	10.5	35.2	36.4	15.5	33	8.8
18	13.9	19	28.5			40	9.3
NCL=67×10^{-3} in.		21.4	21.8	q=1.717cc/sec.			
E16		E20		RPM=250		q=6.82cc/sec.	
14.6	5.5	5	25.9	E11		RPM=1000	
16.1	5.9	8.5	32.6	14.7	22.2	E1	
19.5	6.7	19.5	25.2	22	22.2	39	6.2
22.2	7.1	21.3	22.2	40	7.8	E2	
25.5	8.1	NCL=45×10^{-3} in.		E12		34.4	15.5
35.5	8.7	E16		13	20.7	E4	
37.5	9	7.5	12.6	16	20	21	22
61	1.7	18	23	18.5	22.2	38	9.3
E17		37	9.25	20.3	19.2	35	11.8
14.5	5.4	E17		25.5	22.2	NCL=66×10^{-3} in.	
17.2	6.2	8.8	15.5	31.2	17.8	E1	
26.4	8.8	15	20.4	37.6	9.3	25.4	14.3
34	9.3	27	20.4	d=26.6×10^{-3} in.		30	15.2
46	6.9	29.8	20	19.3	27.4	57.5	4.2
E18		31.7	15.2	23.2	15.5	E2	
45.5	8	E18		E13		50.4	9.3
E19		4.2	8.9	13	33.3	E3	
11.2	4.3	11.1	20	E14		18	14.3
20.4	7.1	17.5	21.8	11	32.6	21	16.8
50	5.9	21	24.1	15.3	31.1	28	17.2
E20		27.8	20.4	E15		30.8	16.4
34	7.8	30	18.5	4.4	18.5	47	10.8
57.4	4	37	14.8	15.4	31.1	E4	
61.4	2.6	E19		22	20.7	29	16

TABLE E-1 (continued)

Xx10^3 Inch	Sx10^3 Inch	Xx10^3 Inch	Sx10^3 Inch	Xx10^3 Inch	Sx10^3 Inch	Xx10^3 Inch	Sx10^3 Inch
7.7	6.4	26.2	11.8	RPM=500		16	15.9
50.5	8.5	29.4	12.2	E12		18	15.9
54.5	6.1	32	11.1	5	12.9	24	16.6
		36.3	8.1	8.3	16.5	28.7	13.3
Position No. 19		E3		12.5	17.2	E20	
		20.6	11.5	NCL=50x10^{-3}in.		5	6.7
Roll No. 235		31.6	10.7	10.3	8.8	29.2	11.1
q=0.685cc/sec.		39.3	7.4	16	10.9		
RPM=100		43	5.2	24	12.9	q=1.717cc/sec.	
NCL=27x10^{-3}in.		E4		27.3	11.8	RPM=250	
E1		14.4	11.1	29.5	10.9	E11	
6	15.2	25	11.5	38.5	7.5	5.6	6.7
7.5	17.7	28	12.9			17.6	14.1
11	20.4	29	12.6	q=6.82cc/sec.		24.5	14.7
16.5	22.2	36.8	8.9	RPM=1000		27.5	11.8
E2		E5		E16		31	8.6
7	14.8	23.7	14	24.4	12.3	34	5.8
17	18.5	24.8	13.3	28	10.9	36.4	3.1
E3		28	12.9	34.4	7.2		
21.3	12.6	35.3	8.9	38.7	7.1	q=3.42cc/sec.	
23	9.6	37	7.4	NCL=27x10^{-3}in.		RPM=500	
25.2	5.5	39.5	7.03	5.5	13	E6	
E4		46.5	2.22			10.3	10.9
7.5	19.2			Position No. 20		12	11.3
15.3	20.4	q=1.717cc/sec.				13.5	12.8
E5		RPM=250		Roll No. 236		15	13.7
9	18.1	E6		q=0.685cc/sec.		19	13.9
12	20.4	6.2	4.6	RPM=100		35.2	5.4
13.2	18.9	15.6	10.7	NCL=38.6x10^{-3}in.		37	3.3
15	19.6	17.2	11.1	E16			
18.5	16.6	18.8	11.1	10.5	12.9	q=6.82cc/sec.	
NCL=50x10^{-3}in.		19.6	12	17.4	15.9	RPM=1000	
E1		31.3	10.4	20.4	14.8	E1	
11.3	12.2	33	10.4	29.2	11.1	4.3	5.9
14	11.1	36.4	7.8	E17		14.7	12.9
16.7	11.1	44	4	9.6	12.9	27	9.3
20	11.5	NCL=27x10^{-3}in.		19	15.5	E2	
21.3	12.9	E8		31	8.1	4.5	6
26	12.9	3.8	10.4	E18		7	8.8
29.8	11.8	7	18.6	18	16.6	8.7	10.6
34	10	12	19.2	26.4	12.9	15	11.8
E2		24	7.1	36.1	3.3	17	11.8
13.5	9.6			E19		36.5	2.6
24.6	12.2	q=3.42cc/sec.		12	12.9		

TABLE E-1 (continued)

$Xx10^3$ Inch	$Sx10^3$ Inch
Position No. 21	
Roll No. 237	
q=0.685cc/sec.	
RPM=100	
d=$129x10^{-3}$in.	
E16	
59.8	9.2
64.2	10
68	10
70	10
81.2	9.2
85	9.2
109.5	6.7
127.2	3.3
E17	
34.4	8.1
39.2	9.2
48.3	8.9
52.4	10
55	10
57	10.3
72	10
86.5	9.2
105.8	7.4
114.3	7
E18	
30.4	8.1
35.2	9.2
58	11.5
68	10
84.5	10
E19	
41	8.9
46.2	10.3
53	10.3
58.5	10.3
76.2	10
82.5	9.2
90	8.9
94	8.1
107.8	7.4
E20	
27.3	7.4
78	10.3
85.5	10.3
95	9.2
q=1.717cc/sec.	
RPM=250	
E11	
9.2	3.1
11.8	3.7
13.4	4.7
31	7.8
35	8.4
38	8.4
41.3	9.2
47.6	9.3
67	10.1
72	9.8
87	9.6
93	9
97	8.4
109	6.7
q=3.42cc/sec.	
RPM=500	
E6	
41.2	8.9
45	9.6
53.4	9.5
66	9.9
72.3	10.1
80.3	9.1
85.5	9.3
92	8.6
98.8	7.8
107.8	6.6
111.7	6.6
q=6.82cc/sec.	
RPM=1000	
E1	
11.2	4.2
23.2	6.9
25	6.7
27.6	7.7
32.5	8
34	8.4
36.1	9
61.2	10.1
70	9.5
80.4	9.5
102	7.9
107	6.8
120.3	4.7
Position No. 22	
Roll No. 249	
q=0.685cc/sec.	
RPM=100	
NCL=$84x10^{-3}$in.	
E16	
7.2	2.22
25	8.1
39	11.1
64	14.8
84	14
E17	
44	12.2
53.8	13.7
q=1.717cc/sec.	
RPM=250	
E11	
12.5	5.5
24.7	8.9
35.6	12.3
54	9.9
65	15.2
79	16
E12	
13	5.5
22	8.9
27.4	10.2
78	15.5
82	15.7
q=3.42cc/sec.	
RPM=500	
E6	
13.2	5
19	7.2
24	9.6
44.3	14.2
53.2	14.2
66.5	15.8
81.1	17.2
E7	
25.5	9.5
78.8	16.7
84	16.5
q=6.82cc/sec.	
RPM=1000	
E3	
7	3.3
11.7	4.7
15.4	6.9
18.4	7.6
21	8.1
E4	
5.6	2.3
27.3	10.1
32.7	10.8
84	13.5
Position No. 23	
Roll No. 250	
q=0.685cc/sec.	
RPM=100	
NCL=$60x10^{-3}$in.	
E1	
8.3	11.1
26.5	25.5
31	25.1
39.4	19.6
44	16.6
56.4	4.06
E2	
29.7	24.8
37.3	22.2
39.4	21.4

TABLE E1 (continued)

Xx10^3 Inch	Sx10^3 Inch	Xx10^3 Inch	Sx10^3 Inch	Xx10^3 Inch	Sx10^3 Inch	Xx10^3 Inch	Sx10^3 Inch
50	10.7	1.5	10.7	52.4	1.7	7.4	7.3
		5.5	20.5	E12		17.2	14.7
q=1.717cc/sec.		8	23.7	21.5	6.8	20	16.2
RPM=250		10	23.2	44	4.8	21.5	16.9
E6		17	22.7	50	2.8	25.3	20.2
22	24.4	E18		E13		28.9	19.8
29	24.5	10.8	25.3	21.5	7.7	35	19.8
42	17	17	14.7	12.3	4.6	39.3	19.1
E7		NCL=59x10^{-3}in.				42	16.9
24.6	25.1	E11		q=6.82cc/sec.		49	12.8
E10		6.8	3.2	RPM=1000		52.4	9.9
14	15.2	16.2	7.7	E1		57.5	6.2
39.3	22.2	19.1	9.3	7.6	3.5	60	4.8
52.2	8.9	25	9.6	15.8	6.6		
		32.5	8.3	19.2	6.8	q=1.717cc/sec.	
q=3.42cc/sec.		41	6.4	E2		RPM=250	
RPM=500		45	4.5	6	3.1	E15	
E11		49.5	2.9	18.4	6.5	13.8	11.5
35	17.1			26.3	7.2	17.2	14.7
E12		q=1.717cc/sec.		52.5	2	19	14.7
44.4	12.2	RPM=250		E3		30.5	17.3
52	6.1	E1		6	3.1	41.5	15.4
E13		11.1	5	45	3	45.5	17
44.4	12.7	16	6.1			50	11.5
55.8	4	20.2	7.4	Position No. 25		61.5	3.2
E14		41.6	6.2			d=26.4x10^{-3}in.	
38.5	16.2	43.5	6.7	Roll No. 253		18.5	30.8
40	13.8	51.3	3.3	q=0.685cc/sec.		E16	
53	5	54	2.3	RPM=100		6.5	27.3
		d=22x10^{-3}in.		d=26.4x10^{-3}in.		20	27.2
Position No. 24		E2		E18		E17	
		0.9	7.3	7.8	34.2	6	27.2
Roll No. 252		7.2	8.3	13	39.3	15.1	38.2
q=0.685cc/sec.		E7		24.8	12.8	19.5	32.3
RPM=100		5	17.1	E19		24	13.2
d=22x10^{-3}in.		11.5	20	7	33.1		
E12				15	40.4	q=3.42cc/sec.	
7.7	24	q=3.42cc/sec.		E20		RPM=500	
13	23.7	RPM=500		8	36	E8	
E13		Roll No. 251		10.6	39.6	3.3	16.1
4.8	15.7	NCL=59x10^{-3}in.		13.2	40	5.4	23.4
9	23.5	E11		NCL=66x10^{-3}in.		E9	
11.6	22.7	21.3	7.9	E18		1.8	12.9
E14		27.5	8.6	5.4	5.5	NCL=66x10^{-3}in.	

TABLE E-1 (continued)

Xx10^3 Inch	Sx10^3 Inch	Xx10^3 Inch	Sx10^3 Inch	Xx10^3 Inch	Sx10^3 Inch	Xx10^3 Inch	Sx10^3 Inch
E8		E1		9.8	26.4	5.5	20.5
2	1.7	7.4	5.9	19.5	5.7	11.8	27.3
8.2	7.2	10.5	7.3	E11		16	18
13.5	11.8	13.4	9.9	9	26.1	E4	
27.2	19.9	29.6	13.2	E12		13.4	24.1
37	19.9	32	12.5	5.3	20.7	19.4	9.3
47.7	10.1	33.4	11	7.2	22.8	E5	
55.5	9.1	35.8	9.9	NCL=49.5x10^{-3}in.		2.6	12.6
57.3	7.6	37.6	8.4	E9		6.2	21.9
		42	5.5	2.4	2	11.1	25.4
q=6.82cc/sec.		44	4.8	10	7.7	E6	
RPM=1000		45.7	3.3	14	8.5	1.4	10
E1				22.2	12.8	12	25.9
16.5	12.3	q=1.717cc/sec.		31.4	12.3	14	21.2
32	14.3	RPM=250		37	10.1	E7	
E2		E5		46	2.3	2.3	10
1.2	3.2	11	9.8			6	21.6
8.8	9.1	15	12.9	q=6.82cc/sec.		16.3	15.4
35.5	14.3	16.8	12.9	RPM=1000		E8	
E3		20.5	12.9	E13		6	22.3
15	11.5	22.3	13.2	8.2	6.8	14.5	21.6
16.5	11.1	24	13.2	30	12.3	E9	
E4		26	13.1	E14		11	24.4
2	2.6	27.2	12.3	8.7	7.1	12.6	24.1
59.1	5	28.8	13.2	25.5	11.8	E10	
63.3	1.9	35	10.3	E15		7.2	22.6
		37.7	8.5	8	6.7	13.6	25.2
Position No. 26		40	7	28	10.9	17.2	12.6
		42	4.4	39	7.9	NCL=44.7x10^{-3}in.	
Roll No. 254		d=20x10^{-3}in.		47	2.2	E1	
q=0.685cc/sec.		5	19.1			7.8	7.2
RPM=100		7	24.2	Position No. 27		9.2	6.5
d=20x10^{-3}in.		10.5	27.9			12	9.7
E1		18	13.2	Roll No. 256		14.4	11.5
16.5	18.7	E6		q=0.685cc/sec.		17.5	11.5
E2		6	21	RPM=100		18.2	12.6
6.3	22	8	25	d=20.5x10^{-3}in.		22	14.4
9.8	28.6	12	24.2	E1		24.5	14.4
17.5	17.2	16.4	19.1	10.3	25.2	32.5	11.1
E3		18	13.2	E2		37	8.3
16.5	18.3			8.8	26.6	40	5.4
E4		q=3.42cc/sec.		11.6	27.3	43	3.6
15.2	20.9	RPM=500		19.2	6.1	E2	
NCL=49.5x10^{-3}in.		E9		E3		12.8	9.7

TABLE E-1 (continued)

Xx10^3 Inch	Sx10^3 Inch	Xx10^3 Inch	Sx10^3 Inch	Xx10^3 Inch	Sx10^3 Inch	Xx10^3 Inch	Sx10^3 Inch
13.2	10.8	6.1	5.7	E9		34	9.9
15	12.2	9.8	9	16	11.5	36.7	7.2
17.8	12.9	13.6	12.2	18.8	13.3	E13	
18.6	12.2	20.3	14.4	20.4	13.3	3.4	3
20	11.9	22	15.5	24	13.7	4.2	4.2
22.2	12.6	24.6	14.7	28.5	12.2	8.1	7.9
23	12.6	32	11.5	41.7	3.6	12.2	10.6
24.2	14.4	39.8	4.7	E10		16	13.6
27	12.6	E6		17	12.6	17	13.6
28	12.6	5	4.7	17.8	12.6	23	14.8
30	11.9	11	9	22	15.4	28.7	12.2
33.7	9.7	13.7	10.8	25	14	32.2	10.2
35	9	19.6	14	27	12.6	34.6	8.3
36.5	7.9	26.6	12.6	29.2	12.2	37	7.3
40	4.3	28.3	12.6	31	10.4	38.5	5.7
42	2.52	31.5	10.8	34.5	9.3	39.8	4.5
E3		34.5	9	35	8.3	E14	
5.2	4.7	38.5	5.7	38	6.1	7	6.5
5.5	5.4	E7				12	10.6
11	9.7	5	4.7	q=1.717cc/sec.		19	13.6
13	11.1	12.3	10.4	RPM=250		25.5	13.6
18.6	12.9	13.8	11.5	E11		30	10.8
21	13.3	15.3	12.6	3	2.59	31	10.6
24	12.9	18.1	14.7	5.7	4.5	39	4.6
25	14.4	21.5	14.7	7.5	7.2	40.5	3.6
27	12.2	26.2	13.3	9.4	6.8	E15	
29	12.6	29.7	12.2	12.5	10.3	8	7.2
32.8	10.1	30.6	11.9	14	11.9	11.2	8.6
35	9	32.5	9.3	15.8	11.8	12	9.6
36.5	7.5	35.4	7.9	19.5	13.6	14.3	11.5
41.4	3.96	E8		22	13.9	15.7	12.6
42	3.6	6	6.5	26	13.2	20.3	13.8
43	2.5	9.4	8.6	28	12.3	21.8	15.1
E4		11.6	10	29.3	12.8	22.6	13.6
14.5	11.1	13	10.8	34.5	7.9	23.7	12.9
16	11.5	17	12.6	38.6	5.6	28	11.9
19	12.9	18.5	13.7	E12		31	10.3
20	14.4	21.8	12.9	3.4	3	40	4
23.8	14.4	23	13.7	5.2	4.9	E16	
28	12.8	24.5	14.4	7	6.6	8.2	7.2
32	10.8	28.5	12.2	10	8.3	10	8.5
37.4	6.5	31.4	10.8	14.5	11.6	13	10.3
40.4	3.96	33.2	9.3	22.5	15.1	14.8	10.1
E5		35.2	9	24.3	14.4	21	12.9

TABLE E-1 (continued)

$Xx10^3$ Inch	$Sx10^3$ Inch	$Xx10^3$ Inch	$Sx10^3$ Inch	$Xx10^3$ Inch	$Sx10^3$ Inch	$Xx10^3$ Inch	$Sx10^3$ Inch
22.4	12.1	12.3	10.8			8	6.9
25.5	14.1	15	12.9	q=3.42cc/sec.		11.4	9.1
28.5	13.6	19.2	13.5	RPM=500		15.3	11.6
30.2	12.8	23	14.4	Roll No. 255		17	11.8
35.5	9.2	25	15.1	E11		19.7	12.6
41.5	4.3	29	12.2	5.8	20.3	22.3	13.9
E17		$d=20.5x10^{-3}$in.		$NCL=44.7x10^{-3}$in.		24.8	12.8
2	1.7	E11		6	6.6	34.3	10.1
4.4	4.5	2	12.9	9.5	7.8	36.5	6.2
9.1	9.9	12.7	21.6	10.3	8.5	E16	
11.4	10.2	16	15.2	12.6	11.5	7.4	5.9
23.2	15.4	18	9.3	15	13.2	9	7.4
27.8	11.4	E12		21.5	12.3	14	10.9
29.4	11.6	1	6.6	30.8	11.5	23.8	11.6
39.3	3.9	11	24.8	36	8.3	28.5	11.3
41	2.2	E13		42	3.3	36	8.6
E18		10.8	24.4	E12		43.5	2.6
1.6	0.7	E14		3	3.3	E17	
5	4.3	5	21.3	5.6	5.7	6.7	5.4
6.5	5	10	25.9	10	8.8	9	7.5
9	7.9	17.8	9.5	12	9.3	17.4	12.6
12	10.3	E15		16.5	10.9	18.4	10.8
20	11.9	3.2	13.9	28	12.2	30.6	9.8
26	16.1	9	26	32.2	10.1	38.4	6.2
32.5	10.3	E16		37	7.6	42.5	3.3
33.5	10.3	4	17	42.3	3.6	E18	
42	3	13	21.8	E13		5.6	5
E19		18	9.3	6.5	6.6	11.3	9.1
5.2	4.7	E17		10.3	8.9	15	10.1
14	12.2	3.2	18.4	13	10.9	17.2	11.8
18	13.2	5.5	19.4	21.2	13.5	23.5	12.6
20.5	14.4	9.5	23.2	25.5	14.4	38.5	6.2
23	14.4	18	7.3	33	9.3	43.4	2
25	12.9	E18		36.3	7.6	E19	
29	12.2	1.3	9.2	38.5	5.4	10	7
30.5	11.1	7	23	41.5	3	10.8	8.8
31.5	10.5	14	20.8	E14		13	10.1
35	8.9	E19		6	4.2	17	11.3
35.6	7.2	3.2	9.6	14.5	12.5	19.6	11.5
39.6	3.6	10.5	25.9	26.5	13.5	43	3.3
E20		E20		31.5	11.8	E20	
4.4	4.5	3	13.6	43.5	3.2	5	4.2
6.2	5.5	6.6	23.4	E15		6.2	5.2
7.6	7.2	10	23.7	6.4	5.4	9	7

TABLE E-1 (continued)

$Xx10^3$ Inch	$Sx10^3$ Inch	$Xx10^3$ Inch	$Sx10^3$ Inch	$Xx10^3$ Inch	$Sx10^3$ Inch	$Xx10^3$ Inch	$Sx10^3$ Inch
39	6.6	4	17.6	16	15.8	RPM=250	
		9.1	24.8	17.2	10.5	E11	
q=26.82cc/sec.		14.2	20.2	E8		8	15.4
RPM=1000		16.6	12.6	5	19.4	10	19.2
E1		E3		7.5	22.8	22.7	24
13	8.8	1.4	7.56	16.3	15.2	25.8	23.6
17	10.5	NCL=35x10^{-3}in.		NCL=35x10^{-3}in.		42	6.6
19.3	12.6	E1		E7		E12	
E2		5.8	8.3	2.5	3.7	12	18.7
4	3.1	7.3	10.8	7.7	10.1	16	18.9
40.3	4.7	9	10.8	14	13.5	19.5	19.5
43.5	2.9	11	12.6	19.5	11.8	23	21
E5		12	13.3	29	10.1	30	15.5
8	5	24	13.3	32.2	5.9	36	14.3
39	4.3	29.3	9.4			37	13.6
E6		33	2.9	q=6.82cc/sec.		40.5	6.2
10	8			RPM=1000			
40	5.4	q=1.717cc/sec.		E11		q=3.42cc/sec.	
E7		RPM=250		3	4.7	RPM=500	
6.4	4.7	E4		4.2	6.4	E6	
22.6	12.3	3.6	5.8	13.7	14	12	18.3
43	2.6	4.8	7.2	22.1	14.6	14	17.5
E8		6	7.9	25	11.8	24.4	21.6
11.4	8	7	10.1	27.2	10.1	36	18.7
43	2.8	8.5	10.7	29	6.9	E7	
E9		10.4	13			16	24.6
25.3	13.5	15	13.4	Position No. 29		22	23
E10		16.8	15.4				
11.5	9.1	21	14.8	Roll No. 223		q=6.82cc/sec.	
37	7.6	27	11.5	q=0.685cc/sec.		RPM=1000	
		29	9.2	RPM=100		E1	
Position No. 28		34	2.4	NCL=45x10^{-3}in.		18	20
		d=20.1x10^{-3}in.		E16		22.4	23.4
Roll No. 257		2.2	12.5	13	21	30	17.8
q=0.685cc/sec.		4.4	18	15	24	32.6	17.7
RPM=100		6	21.6	19	25.5	E2	
d=20.1x10^{-3}in.		9.5	25.5	23	25.8	15	18.7
E1		12	23.8	E17		22.5	26.4
0.6	3.96	16.5	15.4	7.2	13	34.5	17.1
6.4	21.2			12.8	22.5		
13.3	21.6	q=3.42cc/sec.		26	24.4	Position No.30	
17	16.2	RPM=500		30	22.2		
E2		E7				Roll No. 224	
1.8	10.4	4	16.7	q=1.717cc/sec.		q=0.685cc/sec.	

TABLE E-1 (continued)

Xx10^{3} Inch	Sx10^{3} Inch
RPM=100	
NCL=44.2x10^{-3}in.	
E1	
27	20.3
36.5	12.5
E2	
20.4	19.2
25.6	18.5
34	13.7
40.3	5.9
E3	
16.4	16.6
17.6	19.2
20.7	16.6
25	20.7
34	14.8
q=1.717cc/sec.	
RPM=250	
E6	
3.7	3.5
11.4	14.8
13	15.7
17.5	18.9
23.2	19.2
37	11.5
42	4.6
q=3.42cc/sec.	
RPM=500	
E11	
6.3	8.9
10	11.8
11.7	10.8
21	17.4
28	17.4
30	16.1
q=6.82cc/sec.	
RPM=1000	
E16	
8.5	11.8
9.5	11.4
12	12.6
13.3	14.4
14.6	12.8
32	12.3
38	6.6
Position No. 31	
Roll No. 258	
q=0.685cc/sec.	
RPM=100	
NCL=40x10^{-3}in.	
E16	
3.1	4.1
5	8.1
6.7	10.4
8.5	12.6
10.5	14.8
20.2	19.6
25	16.7
28	15
31.3	11.1
q=1.717cc/sec.	
RPM=250	
E11	
2.1	2.4
24.8	15.5
25	17
32.7	11.8
35	8.9
37.5	5.9
E12	
22	19.2
27.5	16.3
29	11.8
31	10.8
q=3.42cc/sec.	
RPM=500	
E7	
23	17.7
E8	
14.8	16.8
d=19.5x10^{-3}in.	
E6	
4.5	30.4
6.4	32.9
E7	
3.9	25.3
9	32.9
12	27.9
E8	
5.1	32.2
14	22
7.7	32.1
Roll No. 225	
NCL=62x10^{-3}in.	
E6	
5	2.6
7.7	4.2
15.8	10.1
22	12.1
45.8	9.1
E7	
16.3	9.3
26	13.2
31	14.4
49	8.5
55.4	3.9
q=6.82cc/sec.	
RPM=1000	
E1	
10.4	6.1
17.8	9.5
23	12.3
45	12.3
55	5.1
57	3.8
E2	
9.5	4.3
15	8
28.8	12.9
34.5	13.5
39	13
43.7	11.4
45.5	10.1
50.5	8
57.5	3.8
Position No. 32	
Roll No. 259	
q=0.685cc/sec.	
RPM=100	
NCL=70x10^{-3}in.	
E1	
0	7.4
18	7.4
E2	
30	6.66
E3	
24	7.4
E4	
2	9.2
8	9.2
q=1.717cc/sec.	
RPM=250	
E5	
6	9.9
49	5
E6	
5	10.4
10	9.5
19	9
30	8.4
55	3
Roll No. 226	
q=3.42cc/sec.	
RPM=500	
NCL=65.5x10^{-3}in.	
E11	
5.5	8.8
19.6	7.6
E12	
19.5	7.6
E13	
2	8.8
28.7	6.4
E15	

TABLE E-1 (continued)

$X \times 10^3$ Inch	$S \times 10^3$ Inch
5	8.8
q=6.82cc/sec.	
RPM=1000	
Roll No. 227	
E2	
1.4	9.3
E3	
19.6	7.5
25	7.2
E4	
1.5	8.1
12	8
25	7.2

TABLE E-2

STREAK LENGTH DATA OF SEPARAN

Xx10^3 Inch	Sx10^3 Inch	Xx10^3 Inch	Sx10^3 Inch	Xx10^3 Inch	Sx10^3 Inch	Xx10^3 Inch	Sx10^3 Inch
Position No. 1		102	17.8	d=20.5x10^{-3} in.		14.2	15.7
		111	13.5	E18		E18	
Roll No. 205		E17		14	28.2	21.7	13.3
NCL=118x10^{-3} in.		30	14.5	E20		E20	
q=0.685cc/sec.		55	13.9	10.4	35.6	22	10.4
RPM=100		E18					
E6		36	14.5	q=3.42cc/sec.		q=3.42cc/sec.	
39	18.3	72	17.8	RPM=500		RPM=500	
42	18.7			E1		NCL=37x10^{-3} in.	
E7		q=6.82cc/sec.		2	17.2	E1	
43	18	RPM=1000		NCL=40x10^{-3} in.		29.9	9.4
42	19.1	E11		19	24.8	E3	
85	19.1	113	9.6	E4		27.5	11.4
110	14.3	E12		21.5	25.6	E5	
113	12.8	109	11.1			19.4	16.1
E8		E13		q=6.82cc/sec.			
41	16.5	104	11.9	RPM=1000		q=6.82cc/sec.	
62	18.3	E14		E6		RPM=1000	
72	19.4	30	11.9	19	16.2	E7	
74	19.4	108	10.6	E8		10	8.5
95	15.4			29	8.5	13.5	16.1
97	16.5	Position No. 2		E10			
				26	10.5	Position No. 5	
q=1.717cc/sec.		Roll No. 206					
RPM=250		q=0.685cc/sec.		Position No. 4		Roll No. 209	
E1		RPM=100				q=0.685cc/sec.	
65	18.3	NCL=40x10^{-3} in.		Roll No. 208		RPM=100	
86	19.1	E12		q=0.685cc/sec.		NCL=58x10^{-3} in.	
E2		20.5	21.3	RPM=100		E6	
38	16.9	31.7	12.8	NCL=29.5x10^{-3} in.		41	5.9
94	17.6			E11		E7	
E3		q=1.717cc/sec.		6	11.5	31.5	7.4
30	17	RPM=250		E12		E8	
74	17.3	E16		21.3	14.8	13.4	5.5
115	13.6	11.8	19.3	E14		40.5	6.7
		E17		4	8.1	E9	
q=3.42cc/sec.		12	21.6			27	10
RPM=500		29	12.9	q=1.717cc/sec.		37.6	7.4
E16		E18		RPM=250		E10	
57	14.5	27	18.6	E16		41	6.7

TABLE E-2 (continued)

$Xx10^3$ Inch	$Sx10^3$ Inch
NCL=$44.5x10^{-3}$in.	
E7	
28	11.5
E9	
23.7	12.2
q=1.717cc/sec.	
RPM=250	
E4	
19	9.3
NCL=$58x10^{-3}$in.	
E2	
50.5	3.8
E3	
19.5	5.9
32.5	8.6
E4	
17.5	7.4
20.6	7.7
30.3	9.6
45	4.9
E5	
30	9.5
33.5	9.6
q=3.42cc/sec.	
RPM=500	
E16	
45.8	4.9
E17	
13	4.2
E20	
12.2	4.1
NCL=$44.5x10^{-3}$in.	
E17	
14	7.7
q=6.82cc/sec.	
RPM=1000	
NCL=$58x10^{-3}$in.	
E11	
20.6	6.4
37	7.1
40	5.4

$Xx10^3$ Inch	$Sx10^3$ Inch
E12	
35.5	7.3
E15	
40	6.6
Position No. 6	
Roll No. 210	
q=0.685cc/sec.	
RPM=100	
NCL=$43x10^{-3}$in.	
E11	
9	9.5
29.5	12.8
E13	
10	11
25.5	14.7
E14	
14.8	12.8
27	14.7
E15	
35.3	9.2
q=1.717cc/sec.	
RPM=250	
E16	
20.2	14.5
31.8	12.5
q=3.42cc/sec.	
RPM=500	
E1	
6.6	7.4
E2	
17	12.3
26	15.5
E4	
21.3	16.2
E5	
7	6.1
d=$26.4x10^{-3}$in.	
E4	
13.2	22.2

$Xx10^3$ Inch	$Sx10^3$ Inch
q=6.82cc/sec.	
RPM=1000	
NCL=$43x10^{-3}$in.	
E7	
24.3	16.2
32.2	10.6
E8	
5.7	5.5
E10	
11	10.2
24	11.9
Position No.7	
Roll No. 211	
q=0.685cc/sec.	
RPM=100	
d=$21.6x10^{-3}$in.	
E6	
2	6.6
3.6	14.7
10.2	23.1
E7	
10.3	23.1
E8	
4.6	16.9
E9	
3.5	14.7
16	20.2
q=1.717cc/sec.	
RPM=250	
E1	
6	16.9
E2	
3.5	15
14.5	20.7
E5	
2.3	8.8
q=3.42cc/sec.	
RPM=500	
E19	
8.5	19.2

$Xx10^3$ Inch	$Sx10^3$ Inch
q=6.82cc/sec.	
RPM=1000	
E13	
3.4	16.5
9.8	17.8
14	21.2
E15	
1.7	8.7
4	22.8
Position No. 8	
Roll No. 212	
q=0.685cc/sec.	
RPM=100	
d=$22.5x10^{-3}$in.	
E1	
3.8	12.1
9.5	22.4
E2	
4.2	14.7
17.2	16.5
E3	
14.7	18.7
E4	
11	22
E5	
16.2	14.7
q=1.717cc/sec.	
RPM=250	
E6	
17.2	12.5
E8	
9	16.4
E9	
11	16.9
E10	
10	17.6
q=3.42cc/sec.	
RPM=500	
E11	

TABLE E-2 (continued)

$Xx10^{3}$ Inch	$Sx10^{3}$ Inch
7.2	13.6
14	15.4
E12	
2	5.6
q=6.82cc/sec.	
RPM=1000	
E17	
5	17.9
Position No. 9	
Roll No. 213	
q=0.685cc/sec.	
RPM=100	
$d=26.2x10^{-3}$in.	
E17	
5	20.8
14.4	27.4
E18	
16.2	27.7
E20	
14.3	26.3
$NCL=34x10^{-3}$in.	
E17	
4.8	13.1
19	19.3
24.8	15.3
E18	
19.4	20.1
22	18.2
E19	
10.9	19
q=1.717cc/sec.	
RPM=250	
E11	
5	12.8
8.6	15.8
E12	
3	8.8
14.6	20.4
E13	
3.2	7.3
E15	
17	21.9
27	16
$d=26.2x10^{-3}$in.	
E11	
3.3	16.3
7	20.6
E12	
2.4	9.3
11.3	24
E15	
13	23.5
q=3.42cc/sec.	
RPM=500	
E6	
6	22.9
E8	
2.1	10.6
13.2	24.3
$NCL=34x10^{-3}$in.	
E6	
8	15.4
26	16.2
E8	
2	7.7
17.2	19.6
q=6.82cc/sec.	
RPM=1000	
E1	
6.5	16.2
8.2	17.2
E3	
6.1	15.2
12.8	16
29.2	10.2
E5	
18.2	18.7
$d=26.2x10^{-3}$in.	
E3	
5.8	22.2
E5	
16.4	29.8
Position No. 10	
Roll No. 214	
q=0.685cc/sec.	
RPM=100	
$NCL=51.2x10^{-3}$in.	
E1	
31.5	13.9
E2	
32	13.9
40.5	11
E3	
36	11
39	11
45.2	6.9
E4	
10	7.3
48	3.29
q=1.717cc/sec.	
RPM=250	
E6	
28.8	16.1
E7	
20	11.7
28.3	15.3
46	6.6
E10	
23	14.9
Position No. 11	
Roll No. 215	
q=0.685	
RPM=100	
$NCL=68x10^{-3}$in.	
E16	
23	7
E17	
7	8.8
E18	
6	8.8
38	6.2
E19	
7	8.4
q=1.717cc/sec.	
RPM=250	
E11	
0	8.9
14	9.1
47	5
E13	
0	10.3
E14	
20	8.2
E15	
45	4.8
q=3.42cc/sec.	
RPM=500	
E6	
0	9.4
7	9
23	7.6
E7	
15	8.7
E8	
47	4.8
E9	
52	3.9
E10	
43	4.8
q=6.82cc/sec.	
RPM=1000	
E1	
0	9.3
10	8.5
E2	
25	6.6
E4	
24	6.8
E5	
38	6.4
Position No. 12	

TABLE E-2 (continued)

Xx10^3 Inch	Sx10^3 Inch	Xx10^3 Inch	Sx10^3 Inch	Xx10^3 Inch	Sx10^3 Inch	Xx10^3 Inch	Sx10^3 Inch
		95	20	102	19.8	E6	
Roll No. 138		E14		E2		64	21.4
q=0.685cc/sec.		25.5	14.39	19	15.1	140	7.5
RPM=100		35	17.14	45	20.3	E7	
d=146x10^{-3} in.		39.5	17.6	74	22	104	19.3
E1		56	18.1	E3		E8	
15.5	12.95	104	16.2	13	11.9	38	19.8
21.5	15.13	E15		112	16.9	60	22.5
32	17.61	27.5	15.5	E4		90.5	23
34	17.9	33	16.2	133	11.5	98.5	20.9
43.5	19.04	69	19.3	Roll No. 177			
49	19.04	E16		E1		q=3.42cc/sec.	
59.5	20.1	30.5	15.8	39	19	RPM=500	
82	20.95	45	17.3	60	21	E14	
92.5	20.59	88	19.6	71	21	48	21.4
101.6	19.42	107	15.8	108	16.7	51	23.1
121.5	13.33	E17		130	10.5	E15	
E2		42	18.1	E2		79	24.4
13	13.04	75.5	20	43	19.25	E16	
16	14.1	114	14.5	74	22	21	19
28	17.13	E18		98	19.25	30	20.1
55	20.1	35	16.95	127	11.55	62	22.8
67	20.3	63	19.3	E3		E17	
94	20.77	81	20.1	28	17.1	32	20.5
115.5	15.72	95	18.6	85	19.25	34	21.8
E3		121	12.4	E4		39.5	21.9
40.5	19.23	E19		16	12.83	80	23.5
58	20.2	63	20	37	18.2	86	24.1
E4		100	17.8	72	21.4	98	22.2
7	9.33	137	2.67	E5			
19.5	14.86	E20		17	14.1	q=6.82cc/sec.	
38	19.04	26.5	15.7	41	19.24	RPM=1000	
40	19.04	28	16.2	53	21	Roll No. 177	
55	20.1	32	17.1			E16	
65	19.6	37	18.1	q=1.717cc/sec.		35	19.7
72	20.95	42.5	17.8	RPM=250		E17	
E5		64	19.5	Roll No. 139		74	26.1
11	12.76	95	19	E5		E18	
32	17.33	111.5	15.4	55	20.9	32	19.4
46.5	19.62	129	9.5	116.5	15	46	20.5
54.5	19.7	Roll No. 139		128	10.2	E19	
64	20	E1		E6		31	20.5
84	20.95	71	21.9	13	15	40	20.5
89.5	20	88	22	22	16.4	E20	

TABLE E-2 (continued)

$Xx10^3$ Inch	$Sx10^3$ Inch
43	17.2
Position No. 13	
Roll No. 140	
q=0.685cc/sec.	
RPM=100	
$d=25x10^{-3}$ in.	
E14	
20.8	11.4
Roll No. 158	
E1	
12.3	14.7
15.4	14.7
E2	
5.6	11.8
8.5	13.6
E3	
14.4	13.8
E5	
4.5	10
11.2	14.1
E6	
8.8	10.7
20.5	9.17
E7	
17.5	12.8
E8	
22	8.23
E9	
12	12.9
24.4	1.76
E10	
6	10
8.5	12.5
q=1.717cc/sec.	
RPM=250	
E15	
19	10.8
E16	
1.1	3.4
E17	
7.3	8.9

$Xx10^3$ Inch	$Sx10^3$ Inch
Roll No. 160	
E1	
7.2	12.1
20.8	7
E2	
4.4	10.6
10	14.1
14.6	14.3
q=3.42cc/sec.	
RPM=500	
Roll No. 159	
E1	
4.1	5.9
5.2	7.6
E2	
13	14.7
E5	
5.6	8
7.1	8
E6	
4.4	6.8
21	9.6
q=6.82cc/sec.	
RPM=1000	
E11	
16.8	14.4
E14	
2.5	3.9
15.4	16
E16	
6.4	10.6
E17	
7	11.1
Position No. 14	
Roll No. 161	
q=0.685cc/sec.	
RPM=100	
$NCL=30x10^{-3}$ in.	
E2	
11.3	18.6

$Xx10^3$ Inch	$Sx10^3$ Inch
18	19.1
E3	
11	17.1
23	15.9
27	5.36
E4	
7.3	16.3
22.5	17.1
E5	
6.2	12.2
E6	
12.5	17.3
21.3	16.5
E7	
18	20.3
23.4	17.1
q=1.717cc/sec.	
RPM=250	
E11	
18	20.3
E12	
6.3	12.3
17	17.4
E14	
5	8.7
E15	
24	9.4
E16	
12.5	17.1
21.8	15.4
E18	
25	11.9
q=3.42cc/sec.	
RPM=500	
Roll No. 162	
E3	
4.2	10.4
13	20.5
17	20.3
26.3	10.7
E6	
7	13

$Xx10^3$ Inch	$Sx10^3$ Inch
17.8	17.5
21	16
E7	
7.6	12.5
4	8
22	17
E8	
2	5.4
23.5	14.8
27	10.4
q=6.82cc/sec.	
RPM=1000	
E11	
18	21.4
27	4.5
E12	
4	8.8
E13	
18.2	13.4
8.8	12.3
Position No. 15	
Roll No. 165	
q=0.685cc/sec.	
RPM=100	
$d=24x10^{-3}$ in.	
E1	
10	21.5
E3	
11.5	22.2
13.5	22.2
E5	
17	22.4
E6	
18	16
20.5	14.7
E8	
20.9	11.6
5	11.2
E9	
6.8	16.9
$NCL=35x10^{-3}$in.	

TABLE E-2 (continued)

Xx10^3 Inch	Sx10^3 Inch	Xx10^3 Inch	Sx10^3 Inch	Xx10^3 Inch	Sx10^3 Inch	Xx10^3 Inch	Sx10^3 Inch
E1		10	14.3	E1		Roll No. 147	
9.5	13.7			11.6	6.6	E1	
E3		q=6.82cc/sec.		32.6	7.2	14	16
18	14.7	RPM=1000		E2		E4	
6	10.1	E7		22.5	6.7	10	19.7
E7		5.5	9.8	E3		E7	
24.5	11.8	E8		22.4	7.8	11	18.5
E8		4.8	9.1	25	7.8	E8	
3.9	8.4	8	12.5	E5		6	13
E9		E10		44	3.12	NCL=52x10^{-3}in.	
9.5	13.1	23	13.4	E7		E1	
		d=24x10^{-3}in.		40.3	4.2	21	7.6
q=1.717cc/sec.		E8		E8		E5	
RPM=250		5.5	11.6	24.5	6.96	23.6	6
E11				40.3	4.8	37	6.8
21	12.2	Position No. 16		E9		E7	
E12				38	5.4	18	7.5
23	13.5	Roll No. 146				E8	
E17		q=0.685cc/sec.		q=1.717cc/sec.		13.2	5.6
8.5	13.5	RPM=100		RPM=250		19.5	7.1
19	16	d=22x10^{-3}in.		E14			
E20		E1		5	2.1	q=6.82cc/sec.	
11	13.5	5.8	12.6	28	8.8	RPM=1000	
d=24x10^{-3}in.		E2		E15		Roll No. 167	
E12		13	18.6	3	3.2	E13	
16	19	E3		22.5	8.4	13	7.2
E18		6.3	12.7	44	1.9	35	6.4
18	16.9	13	18.6	E17		E18	
		E8		20.3	7.7	30.5	8.3
q=3.42cc/sec.		12	19.6	29	7.7	d=22x10^{-3}in.	
RPM=500		18.5	11	d=22x10^{-3}in.		E13	
Roll No. 163		E10		E11		8.8	14.5
E12		2.5	8.16	21.6	2.8	17.4	17.3
8	16.1	Roll No. 166		E12		E14	
E16		E11		13.4	18.2	13.5	21.3
7.2	18.7	2.2	7.34	E13			
NCL=35x10^{-3}in.		E20		19.5	14.4	Position No. 17	
E11		13	22.2	20	14.4		
13.5	17.2	NCL=52x10^{-3}in.		E14		Roll No. 149	
E12		E11		1.7	4.2	q=0.685cc/sec.	
7.5	12.2	4	3.14	12.9	18	RPM=100	
E15		E15				d=19.5x10^{-3}in.	
6.2	10.7	18.5	8	q=3.42cc/sec.		E12	
E16		Roll No. 146		RPM=500		12	14.4

TABLE E-2 (continued)

$X x 10^3$ Inch	$S x 10^3$ Inch	$X x 10^3$ Inch	$S x 10^3$ Inch	$X x 10^3$ Inch	$S x 10^3$ Inch	$X x 10^3$ Inch	$S x 10^3$ Inch
13.5	13.9	E7		14	6.5		
17	12.9	6	6.3	E15		q=6.82cc/sec.	
E13		7.8	7.1	29	5.3	RPM=1000	
8.5	16.1	E10		E17		E1	
E14		12.5	8.1	8	3.7	30	6.2
9	15.7	24	6.7	21	8.5	19	8.6
13	15.2	31.5	4.06	E19		17.3	8.6
E15		Roll No. 149		3	2.7	Roll No. 168	
17	13.5	E12		$d=19.5x10^{-3}$in.		E1	
E17		20	11.8	E17		19.5	12.8
16	14	E14		4	7.3	E2	
E18		17.4	10.1	Roll No. 149		2.4	4.8
13	15.7	25	9	E3		13.5	10.3
15	12.1	E15		6.5	12.4	E4	
16.4	12.4	29.5	7.1	17	10.3	19.4	10.3
Roll No. 169		E16		E6		E9	
E5		8.5	6.7	18	12.1	10	7.8
11.6	16.6	E17				$NCL=40x10^{-3}$in.	
E7		27	7.3	q=3.42cc/sec.		E1-E9	
3.9	11.4	E18		RPM=500		21	7.8
$NCL=40x10^{-3}$in.		22	10.1	Roll No. 168		23.6	7.4
E1				$NCL=40x10^{-3}$in.		3.8	3
6.5	4.06	q=1.717cc/sec.		E11		18.5	8.3
17	8.5	RPM=250		21.4	7.4	7.5	4.2
E2		E1		E12		32	5.9
12.8	6.1	20.4	10.3	30.3	6.8	6	3.8
24	8.1	23.5	8.8	E13		11.2	5.7
E3		E3		22.5	7	21.4	7.2
8.1	4.67	12	8.5	E15		6	4.1
20.7	7.1	29	7.5	12.8	5.6	10.7	5.2
26.4	6.9	E6		E16		14.3	5.8
31.6	5.7	29	7.6	12.8	6.5	20.5	8.1
38	3.04	Roll No. 169		E17		11.6	4.9
E5		E12		12.4	6.8	13.5	5.6
16.5	8.1	22.8	7.1	16	8.7	21.4	8.9
26	7.3	E14		E20		10	4.5
E6		10.3	7.3	23	6.8	11.4	5.1
17.5	9.1	32.8	2.7	$NCL=35.2x10^{-3}$in.			
E10		$NCL=40x10^{-3}$in.		E13		Position No. 18	
15.5	8.1	E12		19.5	8.4		
27	6.3	26.5	6.9	Roll No. 148		Roll No. 170	
$NCL=35.2x10^{-3}$in.		E13		E14		q=0.685cc/sec.	
E5		31	5.3	18.5	9.8	RPM=100	
20.5	8.7	E14		27	8.8	$d=26.6x10^{-3}$in.	

TABLE E-2 (continued)

Xx10^3 Inch	Sx10^3 Inch	Xx10^3 Inch	Sx10^3 Inch	Xx10^3 Inch	Sx10^3 Inch	Xx10^3 Inch	Sx10^3 Inch
E11		q=1.717cc/sec.		23	12.9	5.3	12.3
4.3	15.2	RPM=250				E12	
20.8	17.2	E14		Position No. 19		8.3	17.5
E12		22.5	14.5			16.5	14.6
10	21.2	E18		Roll No. 173		E14	
13	25.1	16.5	20.8	q=0.685cc/sec.		5	11.9
E13		Roll No. 170		RPM=100		11	19.3
13.5	24.3	E1		d=20.5x10^{-3}in.		NCL=27x10^{-3}in.	
17.7	22.1	7.8	17.1	E1		E12	
E14		E2		15.2	16.7	9.3	13.8
7	17.2	5.8	14.6	E5		E14	
9.8	19.8	E3		3	10.5	12.7	13.6
16.2	22.3	12	17.3	E7		NCL=50x10^{-3}in.	
E15		20	16.8	9.5	19.8	E12	
8.8	17.8	21.2	17	13.4	19.8	18	6.8
18.8	23.3	E4		17.3	10.5	E14	
E17		15	21.5	E9		11.6	5.2
22.4	13	13.5	19.5	2.1	7.3	22.4	6.8
E19				10	19.8		
15.7	22.5	q=3.42cc/sec.		E10		q=6.82cc/sec.	
E20		RPM=500		16.5	15.9	RPM=1000	
5.3	15	Roll No. 171		NCL=27x10^{-3}in.		E3	
8.7	19.2	E1		E9		23.5	8.1
Roll No. 150		1.3	4.8	12.2	15.9	37	6.2
E2		6.3	17.1	NCL=50x10^{-3}in.		E5	
2.5	2.8	12.6	24.8	22.5	8.8	20	8.5
14	21.3	17	23.9			d=20.5x10^{-3}in.	
17.5	21.3	E4		q=1.717cc/sec.		E1	
19	16.2	12	22.1	RPM=250		10.4	18.4
E4		E5		d=20.5x10^{-3}in.		E5	
6.1	12.3	20.3	20.4	E11		9	14.7
12	19.4			16.2	16.7	14.3	14.1
16	21.3	q=6.82cc/sec.		E12		E6	
25	8.3	RPM=1000		9.5	15.1	10.3	17.3
E7		E12		18	15.1	12.6	16.8
20	16.8	8	13.9	E13			
25.2	3.03	E13		17	12.5	Position No. 20	
E8		9	16.6	E14			
5	10.3	14	25.8	16	17.6	Roll No. 154	
22.5	13.6	E15				q=0.685cc/sec.	
E10		5.5	13.6	q=3.42cc/sec.		RPM=100	
11	16.1	E16		RPM=500		d=21.4x10^{-3}in.	
17.5	21.3	7.8	16.2	Roll No. 172		E2	
		15.5	27.9	E11		9.3	17

TABLE E-2 (continued)

$X \times 10^3$ Inch	$S \times 10^3$ Inch	$X \times 10^3$ Inch	$S \times 10^3$ Inch	$X \times 10^3$ Inch	$S \times 10^3$ Inch	$X \times 10^3$ Inch	$S \times 10^3$ Inch
8.5	18.4	25.6	8.35	11.3	5.8	53	9.4
E5		42.6	4.2	45	3.2	54.2	9.1
6.8	17					56.3	9.4
16	10.8	q=1.717cc/sec.		q=6.82cc/sec.		57.5	9.4
E7		RPM=250		RPM=1000		60.2	9.3
7	14.8	E1-E10		E11		75.4	8.8
Roll No. 174		17.5	7.6	30	9.8	85	7.6
E11		24.7	8.1	E12		94.2	7.15
12	18	34	8.4	23	8.5	E5	
E12		21	7.8	E13		27.3	7.6
1.1	2.92	17.7	6.8	14.1	10.6	58	9.4
6.6	15.9	2.5	1.67	E15		63.2	9.4
17.3	14.6	14	6.7	44.6	1.2	66.6	9.1
E14		35	8	E16		69.2	8.8
19	10.4	10.4	5.4	9	7.2	100	6.6
E15		41	4.4	27.4	9.8	105	6.2
6.8	16.7	19.8	6	40	4.2	109.5	5.3
9.8	17.7	NCL=38.6×10^{-3}in.		d=21.4×10^{-3}in.		E6	
14	16.7	E1		E12		33	8.3
E16		12.4	9.9	5.6	19.6	36	8.6
11.3	19.4	25	9.4			56	9.4
E17		E6		Position No. 21		90	7.4
11.5	17.7	25	9.2			E7	
NCL=38.6×10^{-3}in.		d=21.4×10^{-3}in.		Roll No. 157		6	3.5
E11		E1		q=0.685cc/sec.		15	5.9
20.3	11.7	7	17.4	RPM=100		40	8.8
E14		14	15.9	d=129×10^{-3}in.		61.3	8.8
32.4	6.3	E2		E1		76.6	8.7
E16		3.2	11.5	37	8.8	94	7.15
20	9.6	6	15.4	42	9.1	98	6.8
NCL=49.2×10^{-3}in.		E3		85	7.6	123	3.16
E11-E20		8.4	18.4	89	7.3	E9	
29.3	8.35			E2		17.5	6.3
38.2	6.9	q=3.42cc/sec.		30.8	7.6	87.3	7.5
5.1	3.34	RPM=500		98.3	9	96.5	7
6.6	3.76	Roll No. 175		69.5	8.4	E10	
42.4	4.6	E2		89	8.1	9.3	5.4
18.4	7.7	4	18.7	121	4.1	34.4	8.2
33	8.8	NCL=49.2×10^{-3}in.		E3		64	9
17.1	7.5	E5		37.3	8.8	67.5	9.3
30	7.7	12.5	6.8	55.8	9	90	7.6
30	8.6	35	8.5	110.8	5.5	95.2	7.15
30.6	8.35	E7		E4		98.6	6.9
15	7.3	6.4	4.8	31	8.2	Roll No. 176	

TABLE E-2 (continued)

Xx10^3 Inch	Sx10^3 Inch	Xx10^3 Inch	Sx10^3 Inch	Xx10^3 Inch	Sx10^3 Inch	Xx10^3 Inch	Sx10^3 Inch
E16		E11		37.2	18.1	E16	
29.8	7.5	8	6	49	19	30.2	10.6
32.3	7.7	10.8	6	68	19.2		
116	4.7	37	9.5			Position No. 23	
E17		64.3	9.5	q=1.717cc/sec.			
9.3	4.3	68.3	10.1	RPM=250		Roll No. 204	
27.8	6.4	69.5	9.4	E14		q=0.685cc/sec.	
86	7.7	107.7	6.9	35.3	18.1	RPM=100	
E18		E12		71	17.3	NCL=53x10^{-3} in.	
45	9.2	37	9.1	E15		E11	
83.6	7.9	78.4	8.7	43.3	17.9	32.5	27.6
91	7.5			74	17	42.7	18.5
E19		q=6.82cc/sec.		98	16.2	E12	
52	9.4	RPM=1000		E17		34.2	27.7
75.6	8.3	E1		47.5	19.1	50	6.3
82.3	8.1	59.5	9.8	E18		E14	
E20		70.5	9.7	37	18.7	7.2	15.9
60.8	9.6	82.3	8.3			51.7	5.2
66	9	89	8.7	q=3.42cc/sec.			
92.4	7.5	90.2	8.9	RPM=500		q=1.717cc/sec.	
112	5.35	100	7.9	Roll No. 178		RPM=250	
		E2		E1		E16	
q=1.717cc/sec.		61.8	9	46	17.9	9.4	18
RPM=250		83.7	9	65.5	17.9	48	11.8
Roll No. 157		92.3	8.5	94.5	19.9	E17	
E11				E2		11.4	22.2
69	8.9	Position No. 22		37	14.6	E18	
70	8.9			41	15.3	1.5	2.2
78.5	8.3	Roll No. 179		E3		19.5	23.6
113.2	5.6	q=0.685cc/sec.		12.5	10.3	24	22.9
121.8	3.8	RPM=100		28	14.3	33.5	25.4
E12		NCL=100.5x10^{-3} in.		52.3	16.2	44.3	17.7
37.5	8.5	E1		72	14.9		
43.5	9.1	5.8	6.6			q=3.42cc/sec.	
50	9.4	79.4	19	q=6.82cc/sec.		RPM=500	
52.3	9.8	E2		RPM=1000		Roll No. 181	
69.4	9.1	23.6	14.3	E11		E2	
74	8.8	47	21.3	32.5	13.8	13.6	14.5
87	8	64.5	18.1	80.6	16.4	E5	
91.5	7.8	81.8	17.5	E12		44	11.4
		E3		36	13.4	E8	
q=3.42cc/sec.		28	16.6	69	12.4	37.8	19.4
RPM=500		E4		E15			
Roll No. 156		19	14.9	20	12.9	q=6.82cc/sec.	

TABLE E-2 (continued)

Xx10^3 Inch	Sx10^3 Inch
RPM=1000	
E15	
35.4	22
Position No. 24	
Roll No. 183	
q=0.685cc/sec.	
RPM=100	
d=22x10^{-3}in.	
E1	
8.1	19.8
14	24.1
E2	
10.8	17.3
16	15.8
E4	
9	16.9
15.3	16.2
E9	
14	19.8
NCL=59x10^{-3}in.	
E1	
26.5	7.2
E9	
34.4	7.2
q=1.717cc/sec.	
RPM=250	
d=22x10^{-3}in.	
E14	
20	3.2
E15	
7	13.7
E16	
11	23.3
5.4	13.4
E17	
13	20.9
E18	
14.8	12.2
E19	
2.8	4
18	4.6
E20	
10	20.9
q=3.42cc/sec.	
RPM=500	
Roll No. 182	
E17	
12	21.2
Roll No. 203	
NCL=59x10^{-3}in.	
E15	
36.6	6.8
Position No. 25	
Roll No. 185	
q=0.685cc/sec.	
RPM=100	
d=26.4x10^{-3}in.	
E1	
3.6	14.4
13.3	23.8
E2	
10.5	20.2
21.8	16.9
E3	
11	22
16.3	23.4
E4	
2.7	10.8
22	16.2
E5	
12.2	22.7
E6	
8.3	19.8
21	19.4
NCL=66x10^{-3}in.	
E3	
24.4	9
27.8	9
38	9
E6	
39	8.6
E8	
19	9
35	9
45	9
E9	
10	5.4
15	7.9
17.7	7.9
25.5	9
28.5	9
q=1.717cc/sec.	
RPM=250	
E11	
19.5	10.1
31.3	10.1
E12	
23.5	9.4
E13	
43	7.8
55	5
29	9.4
d=26.4x10^{-3}in.	
E11	
8	20.2
13.7	23.8
E12	
10	19
11.3	20.9
13.5	21.6
E13	
12	22.2
14.3	23.6
17.4	25
22	15.8
q=3.42cc/sec.	
RPM=500	
Roll No. 186	
E1	
10.9	18.4
12.2	21.2
18	25
E2	
10.7	18.4
24.8	6.5
E3	
2.5	9.4
18.3	25.8
22.8	13.8
NCL=66x10^{-3}in.	
E1	
27.2	9.9
42	9.1
E4	
31.2	10.1
51	6.5
E5	
15	7.6
q=6.82cc/sec.	
RPM=1000	
E11	
54	6
E12	
31	8.3
E14	
16	7.4
E16	
19	8.7
E19	
30.8	9.1
36	9.6
d=26.4x10^{-3}in.	
E14	
7.2	19.3
9	20.4
11.5	17.4
E15	
4.1	16.5
6.8	22.5
9.5	19.3
17.5	20.2
E17	
15	23.9
12.5	24.8
E19	
4.8	18.4
14	21.6

TABLE E-2 (continued)

Xx10^3 Inch	Sx10^3 Inch	Xx10^3 Inch	Sx10^3 Inch	Xx10^3 Inch	Sx10^3 Inch	Xx10^3 Inch	Sx10^3 Inch
17.3	18.4	Roll No. 187				8.4	17.3
		E11		Roll No. 189		11.4	17.7
Position No. 26		17	5.4	q=0.685cc/sec.		E2	
		E13		RPM=100		17	14.4
Roll No. 188		2.4	9.1	d=22.3x10^{-3}in.		E3	
q=0.685cc/sec.		E16		E13		8.5	17.6
RPM=100		10	21.5	19.5	12.6	E5	
d=20x10^{-3}in.		E18		E14		4	15.3
E1		8	18.2	14	17.3	E6	
2	8.6	15	17	E16		9.1	17.1
13	18	NCL=46.4x10^{-3}in.		18.8	13	E7	
E2		E11		E17		21.2	5.3
10.2	18	42	2.6	8.3	16.9	E8	
E7		E13		E20		12.5	19.2
4.3	11.5	4.6	3.7	9.6	18.7		
E9		E14		NCL=44.6x10^{-3}in.		q=3.42cc/sec.	
13.8	17.3	27.8	8.3	E16		RPM=500	
NCL=46.4x10^{-3}in.		40	5.5	22	10.1	Roll No. 190	
29.5	7.2	E15		38	5.4	E5	
30.8	7.2	10	5.4	E17		9.9	17.6
32.7	7.2	24	8.3	14.6	8.3	18	13.4
				E20		E6	
q=1.717cc/sec.		q=6.82cc/sec.		19	9	5.4	17.6
RPM=250		RPM=1000				18.4	13.4
E11		E1		q=1.717cc/sec.		E8	
23	7.2	10.5	5.2	RPM=250		14	18.2
E14		E2		E1		E9	
19.3	7.6	16.4	7.4	11.8	7.2	9.5	18
E15		E3		17	9.4	NCL=44.6x10^{-3}in.	
23.5	7.2	27	7.4	22.6	10.1	E2	
E16		E4		E2		23.5	9.6
17	6.9	19.8	7.4	35	6.9	E3	
E17		d=20x10^{-3}in.		E3		15.2	7.7
28.7	6.6	E1		21	8.6	23.2	7.7
E18		4.6	14.4	E5		E5	
25	8.5	E2		8.8	6.5	7.8	6.4
d=20x10^{-3}in.		7.8	13.7	E6		18.9	7.7
E14		E4		19.5	8.2	35.5	5.2
10	18.1	5.3	12.2	E7		38.5	4.5
E18		9	14.3	28.4	9.1	E6	
11.1	18.1	E10		E8		10.5	8
		11.5	19.7	24.5	8.8	21.8	9.3
q=3.42cc/sec.				d=22.3x10^{-3}in.		33	8.3
RPM=500		Position No. 27		E1		37	6.8

TABLE E-2 (continued)

$Xx10^3$ Inch	$Sx10^3$ Inch
E7	
34.2	6.8
E8	
20.4	9.5
23.5	8.9
30.6	8.6
E9	
19	9.5
q=6.82cc/sec.	
RPM=1000	
E11	
22.6	10.1
E12	
8.1	7.6
E13	
23	8.5
35.2	6.1
E14	
14	9.3
34	6.8
E15	
34.8	7.7
E16	
30.6	7.7
40	4.2
24.3	8.6
E17	
12.5	8.8
21.5	9.8
24.5	9
35	9.8
40	4.2
E18	
4	3.3
14.5	9.5
32.5	9.5
E19	
4.2	3.9
E20	
15.3	8.6
$d=22.3x10^{-3}$in.	
E12	
6.5	22.3

$Xx10^3$ Inch	$Sx10^3$ Inch
E18	
16	15.8
Position No. 28	
Roll No. 192	
q=0.685cc/sec.	
RPM=100	
$d=20.1x10^{-3}$in.	
E1	
6.4	16.5
14.8	15.4
E2	
13.5	17.2
E3	
9.8	18.3
12	19.1
E5	
10.4	18.3
E7	
10.4	18
5	14.7
15.8	14.3
$NCL=35x10^{-3}$in.	
E8	
14	8.4
E9	
11.2	7.7
q=1.717cc/sec.	
RPM=250	
E14	
25.4	8.2
$d=20.1x10^{-3}$in.	
E11	
12	17
E12	
2	6.5
4	12.2
10.8	17.6
14	16.6
17	10.3
E13	
11	16.9

$Xx10^3$ Inch	$Sx10^3$ Inch
18	6.3
q=3.42cc/sec.	
RPM=500	
Roll No. 191	
E12	
1.5	5.7
8.5	18.3
E13	
8.8	19.7
13.6	18.5
18.3	6.8
E14	
13.2	18.5
E15	
13	19.5
q=6.82cc/sec.	
RPM=1000	
E2	
11	22.6
E3	
11	22.3
14	16.7
E4	
15.7	13.4
E5	
14.3	21.2
E6	
16	17.2
E7	
5.2	12.8
10.8	19.7
Position No. 29	
Roll No. 193	
q=0.685cc/sec.	
RPM=100	
$d=26.6x10^{-3}$in.	
E14	
15.2	20.3
E15	
22.5	14.5

$Xx10^3$ Inch	$SxI0^3$ Inch
E16	
9.4	21.8
1.5	6.5
E20	
13	21.8
q=1.717cc/sec.	
RPM=250	
E3	
16.1	21
19.5	16.8
E4	
20.6	14.5
E9	
10.5	23.8
q=3.42cc/sec.	
RPM=500	
Roll No. 202	
E1	
8.8	21.4
17.3	23.6
E5	
22.8	11.3
q=6.82cc/sec.	
RPM=1000	
E20	
13.4	14.4
Roll No. 194	
E5	
4.1	17.3
Position No. 30	
Roll No. 196	
q=0.685cc/sec.	
RPM=100	
$d=21.5x10^{-3}$in.	
E1	
18.5	14
E3	
12	25.9
E4	

TABLE E-2 (continued)

Xx10^3 Inch	Sx10^3 Inch	Xx10^3 Inch	Sx10^3 Inch	Xx10^3 Inch	Sx10^3 Inch	Xx10^3 Inch	Sx10^3 Inch
6	19.8	3	13.7	E14		E20	
E5		16.3	19.4	15	15.1	35.2	7.1
4.5	16.2	E4		23.3	14.4	27.4	16.1
8.2	19.1	10.4	24.9	E15			
17.4	18	NCL=44.2x10^{-3}in.		14.5	18.3	q=6.82cc/sec.	
NCL=44.2x10^{-3}in.		E2		E16		RPM=1000	
E1		17.4	10.9	19	19.8	E1	
37.8	6.5	22.6	12	E17		12.5	13.5
E3		E3		6	12.6	22.7	12.9
23	12.6	7.3	6.8	19.5	19.4	20.5	13.5
E4		34	9.5	32	14.4	E2	
13.3	10.1	E4		E18		7.5	11.8
E5		18	11.8	12	14.4	12.5	15.2
10.3	10.1	E5		36	8.3	20	14.7
34.3	9	10	7			E4	
E6				q=1.717cc/sec.		7	10.9
35	7.2	q=6.82cc/sec.		RPM=250		20.5	16.1
		RPM=1000		E5			
q=1.717cc/sec.		E11		11	19.4	Position No. 32	
RPM=250		8.5	6	E6			
Roll No. 197		17.5	10.2	26	18.7	Roll No. 199	
E2		E17		E7		q=0.685cc/sec.	
10	7.5	19.2	11.1	34.5	9.4	RPM=100	
16.4	10.1	E18		E8		NCL=70x10^{-3}in.	
E4		32	10.9	22	19.4	E1	
21.2	10.4	d=21.5x10^{-3}in.		E10		8	7.7
d=21.5x10^{-3}in.		E12		3	6.8	33	7.7
E2		5.4	12.4	16.5	18	E2	
4.5	15.8	8	17.2	28.5	15.1	0	7.7
8	21.6	E18				20	7.3
E3		14.5	19.7	q=3.42cc/sec.		27	7.3
6.3	16.6	E20		RPM=500		34	7.7
14.3	22.6	5.4	14.2	Roll No. 201		E3	
E4				E13		6	7
10.5	21.6	Position No. 31		38	6.7	34	7.3
				E14		E4	
q=3.42cc/sec.		Roll No. 197		30	15.2	30	6.6
RPM=500		q=0.685cc/sec.		E15		40	7.3
Roll No. 195		RPM=100		17	17.7	E5	
E1		NCL=40x10^{-3}in.		32.5	10.1	0	7.3
2	11.5	E13		E17		3.5	7.3
E2		12	17.6	7.8	11.8	9	7.3
9	23.6	24.3	18	E18		14.5	7.7
E3		29	18	26.2	16.2	26	7.3

TABLE E-2 (continued)

Xx10^3 Inch	Sx10^3 Inch	Xx10^3 Inch	Sx10^3 Inch
40	6.6	q=6.82cc/sec.	
45	6.6	RPM=1000	
52	5.1	E11	
		11	7.5
q=1.717cc/sec.		21	7.5
RPM=250		50	4.8
E11		58	4.8
2	7.5	62	3.3
5	7.5	E12	
16	7.5	49	5.5
22	7.5	55	5.1
26	7.5	E13	
53	6.6	10	7
57	5.9	19	7
E12		37	6.4
0	7.3	39	6.4
4	7.3	55	5.4
13	7.3	59	4.2
25	7.3	E14	
27	7.3	5	7.5
35	7.3	9	7.5
56	5.9	23	7.5
		58	5.7
q=3.42cc/sec.			
RPM=500			
Roll No. 200			
E1			
5	8.1		
10	8.1		
15	8.1		
28	8.1		
53.5	5.2		
64	3		
E2			
22	6.9		
27	6.9		
41	6.7		
57	4.9		
E3			
21	7		
39	7		
57	4.7		
60	4.2		